

# **Large Eddy Simulation and Analysis of Truck Generated Droplet Spray Transport at Bridges**

---

Nuclear Science and Engineering Division

## **About Argonne National Laboratory**

Argonne is a U.S. Department of Energy laboratory managed by UChicago Argonne, LLC under contract DE-AC02-06CH11357. The Laboratory's main facility is outside Chicago, at 9700 South Cass Avenue, Argonne, Illinois 60439. For information about Argonne and its pioneering science and technology programs, see [www.anl.gov](http://www.anl.gov).

## **DOCUMENT AVAILABILITY**

**Online Access:** U.S. Department of Energy (DOE) reports produced after 1991 and a growing number of pre-1991 documents are available free at OSTI.GOV (<http://www.osti.gov/>), a service of the U.S. Dept. of Energy's Office of Scientific and Technical Information

### **Reports not in digital format may be purchased by the public from the National Technical Information Service (NTIS):**

U.S. Department of Commerce  
National Technical Information Service  
5301 Shawnee Rd  
Alexandria, VA 22312  
**www.ntis.gov**  
Phone: (800) 553-NTIS (6847) or (703) 605-6000  
Fax: (703) 605-6900  
Email: **orders@ntis.gov**

### **Reports not in digital format are available to DOE and DOE contractors from the Office of Scientific and Technical Information (OSTI):**

U.S. Department of Energy  
Office of Scientific and Technical Information  
P.O. Box 62  
Oak Ridge, TN 37831-0062  
**www.osti.gov**  
Phone: (865) 576-8401  
Fax: (865) 576-5728  
Email: **reports@osti.gov**

## **Disclaimer**

This report was prepared as an account of work sponsored by an agency of the United States Government. Neither the United States Government nor any agency thereof, nor UChicago Argonne, LLC, nor any of their employees or officers, makes any warranty, express or implied, or assumes any legal liability or responsibility for the accuracy, completeness, or usefulness of any information, apparatus, product, or process disclosed, or represents that its use would not infringe privately owned rights. Reference herein to any specific commercial product, process, or service by trade name, trademark, manufacturer, or otherwise, does not necessarily constitute or imply its endorsement, recommendation, or favoring by the United States Government or any agency thereof. The views and opinions of document authors expressed herein do not necessarily state or reflect those of the United States Government or any agency thereof, Argonne National Laboratory, or UChicago Argonne, LLC.

# **Large Eddy Simulation and Analysis of Truck Generated Droplet Spray Transport at Bridges**

---

prepared by  
S.A. Lottes and M.A. Sitek

Nuclear Science and Engineering Division, Argonne National Laboratory

April 2024

# Table of Contents

1	Introduction .....	2
1.1	The Tunnel Effect.....	2
1.2	Objectives.....	4
2	Computational Model Geometry.....	5
3	CFD Modeling Methodology .....	7
3.1	Spray Droplets .....	7
3.2	Turbulence Model and Management of Computer Resources.....	12
3.3	Time Needed to Reach Maximum Droplet Accumulation on Girders .....	14
3.4	Effects of Vehicle Starting Position .....	16
4	Governing Equations.....	18
4.1	Navier-Stokes Equations Governing the Air Flow.....	18
4.2	Droplet Equations of Motion.....	19
5	Base Case and Test Matrix for Parametric Study.....	21
6	Results and Discussion.....	23
6.1	Base Case .....	23
6.2	Varying Number of Girders with Constant Deck Width.....	32
6.3	Varying Underclearance .....	35
6.4	Varying Truck Speed.....	38
6.5	Varying Height of Girders.....	41
6.6	Varying Width of Overhang.....	42
6.7	Vertical Abutment versus Sloped Embankment.....	43
6.8	Varying Wind Speed at Zero Angle of Attack .....	47
6.9	Varying Wind Angle of Attack .....	51
6.10	Constant Wind versus Wind Gust.....	53
7	Conclusions .....	56
8	Acknowledgements.....	59
9	References .....	59

## List of Figures

Figure 1-1: (Photo). Grade separation between 8 Mile Road and Interstate 75.....	3
Figure 1-2 Illustration. Tunnel scenario from FHWA Technical Advisory.....	3
Figure 2-1: Bridge and abutment geometries.....	5
Figure 2-2: Bridge domain enclosing sliding truck domain.....	6
Figure 3-1: Droplets coming off truck cab tires and in the near wake colored by droplet height..	8
Figure 3-2: Example plot of water droplet mass suspended in the domain vs time. ....	9
Figure 3-3: Size distribution of droplets leaving truck tire surface.....	10
Figure 3-4: Settling time from 5-foot elevation for droplets from 1 to 1000 $\mu\text{m}$ .....	10
Figure 3-5: Normal size distribution of droplets leaving wheel well.....	11
Figure 3-6: Spray droplet parcels versus height above roadway for 50 $\mu\text{m}$ mono size droplets and a normal distribution of droplets.....	11
Figure 3-7: Droplet distribution at a moment in time for simulations of truck passage past a bridge using both URANS and LES equations to solve for the air flow field. ....	13
Figure 3-8: Comparison of droplet suspended mass for a truck passing through a domain. ....	14
Figure 3-9: Accumulated droplet mass on girders 1 through 4 (G1, G2, G3, G4) for base case truck passage event.....	15
Figure 3-10: Reduced domain for calculation of droplet deposition on girders faster and with less computer resources after truck has passed.....	15
Figure 3-11: Mass of saltwater droplets suspended in the air at various heights.....	16
Figure 3-12: Top view of truck wake with spray showing that the distance between large eddies is about 10 meters.....	17
Figure 3-13: Droplet mass of the base case for truck starting position varied from 0 m to -7.5 m and calculated with the reduced domain.....	17
Figure 6-1: Droplet laden truck wake during afternoon rain on I70 in Utah, upper frame, droplet laden truck wake visualization of truck geometry used in simulations, lower frame. ....	24
Figure 6-2: Truck transit under bridge showing droplet transport in wake colored by droplet elevation.....	25
Figure 6-3: Droplet flow between and under girders and over bridge deck at increasing times with cone glyphs showing velocity direction, colored with velocity magnitude.....	28
Figure 6-4: Droplets carried by eddies into space between girders for first seven seconds after truck passage. The truck motion is right to left; upper part of trailer is grey box in upper left	

frame. Arrows show droplets initially following a clockwise induced cavity flow motion in the space between girders..... 29

Figure 6-5: Visualization accumulated droplet distribution on the girders showing the leading side on top, and trailing side on bottom. Droplets size is scaled up to make them visible. .... 30

Figure 6-6: Droplet accumulation on leading and trailing sides of girders. .... 31

Figure 6-7: Percentage of droplet accumulation on bottom flange..... 31

Figure 6-8: Schematic showing varying range of number of girders. .... 32

Figure 6-9: Variation of accumulated mass of droplets with number of girders. .... 32

Figure 6-10: Droplet accumulation by girder number for varying number of girders. .... 33

Figure 6-11: Droplet accumulation on leading and trailing sides of girders for varying numbers of girders. .... 35

Figure 6-12: Plan view of bridge deck ..... 36

Figure 6-13: Droplet accumulation on girders of base case for underclearance from 15 to 40 ft. .... 36

Figure 6-14 Percentage of droplet accumulation on lower flange for base case underclearance and large underclearance of 40 ft. .... 37

Figure 6-15: Droplet accumulation on girders of base case for truck speeds of 30, 45, and 60 mph and underclearance in the range of 15 to 40 ft. .... 39

Figure 6-16: Droplet accumulation of girders as a function of truck speed for various underclearances from 16 ft to 30 ft. .... 39

Figure 6-17 Percentage lower flange droplet deposition for various truck speeds of 30, 45, and 60 mph..... 40

Figure 6-18: Schematic for test of smaller girder height..... 41

Figure 6-19: Droplet accumulation for 54-inch and 30-inch girder heights. .... 41

Figure 6-20: Droplet accumulation on leading vs trailing sides of girders..... 42

Figure 6-21: Schematic of 2 tested bridge deck overhangs..... 42

Figure 6-22: Droplet accumulation on girders for two deck overhangs..... 43

Figure 6-23: Droplet accumulation on girders showing leading and trailing side amounts..... 43

Figure 6-24: Vertical wall abutment (top) versus sloped embankment (bottom). .... 44

Figure 6-25: Droplet accumulation for vertical wall abutment vs sloped embankment..... 45

Figure 6-26: Droplet accumulation on leading and trailing sides of girders compared for sloped embankment and vertical abutment..... 46

Figure 6-27: Schematic showing bridge with truck and wind direction. .... 47

Figure 6-28: Visualization of droplet accumulation on girders for 25 MPH headwind..... 48

Figure 6-29: Droplet accumulation of leading and trailing sides of girders for 25 MPH headwind and no headwind..... 49

Figure 6-30: Percentage of droplet deposition on bottom flange by girder and side for 25-mph headwind..... 50

Figure 6-31: Variation of droplet accumulation of girders with wind speed for head wind. .... 50

Figure 6-32: Percentage of droplet mass depositing on lower flange as a function of headwind speed. .... 51

Figure 6-33: Diagram showing wind directions. .... 52

Figure 6-34: Per girder and total droplet accumulation on girders for wind directions between 0 and 180 degrees at a wind speed of 25 mph..... 52

Figure 6-35: Percent of droplet deposition on lower flange as a function of wind angle for wind speeds of 2 mph and 25 mph. .... 53

Figure 6-36: Suspended droplet mass between girders as a function of time for headwind and tailwind cases at a wind speed of 25 mph..... 53

Figure 6-37: Diagram for cases of constant 2 mph wind versus 2 mph wind gusts at 45 and 135 degrees with respect to the front of the truck starting at 8 seconds..... 54

Figure 6-38: Droplet deposition for a 2-mph wind gust at an angle of attack of 45- and 135- degrees in (b) compared to no wind also in (b) and constant 2 mph wind in (a). .... 55

## List of Tables

Table 1: Base Case with List of Varied Parameter Values for the Case Set .....	21
Table 2: Truck Reynolds Number .....	22

## Nomenclature

Symbol	Physical quantity
$A_p$	Droplet projected area [m <sup>2</sup> ]
$D_d$	Droplet diameter [m]
$C_d$	Droplet drag coefficient
$f_b$	Body force per unit volume vector acting on air [N/m <sup>3</sup> ]
$F_b$	Resultant body force acting on a droplet [N]
$F_d$	Drag force on droplet [N]
$F_p$	Pressure gradient or buoyancy force on droplet [N]
$F_s$	Resultant surface force on a droplet [N]
$g$	Acceleration of gravity vector [m/s <sup>2</sup> ]
$m_d$	Mass of a droplet [kg]
$\dot{m}_p$	Mass rate of tire spray droplet parcels [kg/s]
$\dot{n}_p$	Parcel injection rate [# /s]
$n_d$	Number of spray droplets in a tracked parcel of droplets
$p$	Filtered air pressure [Pa]
$p_{static}$	Static air pressure [Pa]
$r_d$	Droplet position vector [m]
$Re_p$	Droplet Reynolds number
$Re_t$	Truck Reynolds number
$S$	Strain rate tensor [s <sup>-1</sup> ]
$t$	Time [s]
$T$	Filtered stress tensor [Pa]
$T_{SGS}$	Subgrid scale turbulent stress tensor [Pa]
$u$	Filtered vector velocity of air [m/s]
$u_d$	Droplet velocity vector [m/s]
$u_s$	Slip velocity vector between the air and droplet velocity [m/s]
$V_d$	Volume of droplet [m <sup>3</sup> ]
$\mu$	Material dynamic viscosity of air [Pa-s]
$\mu_t$	Subgrid scale turbulent viscosity [Pa-s]
$\rho$	Density of air [kg/m <sup>3</sup> ]
$\rho_w$	Density of water [kg/m <sup>3</sup> ]

# 1 Introduction

Weathering steel is a particular type of steel that develops a higher level of atmospheric corrosion protection than non-weathering grades of steel. While uncoated weathering steels have the appearance of being “rusted”, there are many forms of ferric oxyhydroxides (aka. rust) that can form on steel. The predominant ferric oxyhydroxide that gives uncoated weathering steel its tightly adherent patina is goethite. The atmospheric corrosion protection comes from alloying, primarily with a copper composition greater than 0.20 percent and also small amounts of chrome, nickel, and silicon. Bare atmospheric corrosion resistant steels have been recognized as far back as 1905 with very early editions of the American Society for Testing and Materials (ASTM) A 7 “Standard Specification for Steel for Bridges and Buildings” [1]. Uncoated weathering steel (UWS) is the lowest cost corrosion protection system possible for a steel bridge based on the first cost. Provided the UWS is used in an optimal environment that allows the protective patina to form, UWS also provides the lowest life cycle cost. The protective patina on UWS does not form or degrades in continuously damp conditions, forming a higher proportion of lepidocrocite, or in the presence of a concentration of chlorine ions that is too high, forming a higher proportion of akageneite.

The use of UWS for bridges began in the mid-1960’s. The steels were first marketed under proprietary names falling under the ASTM A 242 specification (first published in 1941) [2], and by 1968 they fell under the ASTM A 588 specification [3]. The first uncoated weathering steel bridge was built over the New Jersey Turnpike in 1964 [4]. Shortly thereafter, Michigan began wide use of the product due to the potential advantage of much lower maintenance and life cycle costs compared to using steel in bridges that requires periodic painting. Between 1964 and 1980, Michigan built 513 uncoated weathering steel bridges, with an additional 100 bridges built by counties [5]. One of these was the Eight Mile Road Bridge in Detroit, Michigan. A portion of this bridge interchange was a depressed roadway with a low, 14’7” clearance and vertical retaining walls very near the shoulder. After an eight-year exposure study, it was found the corrosion rate never tapered off and in general their overall experience with uncoated weathering steel was poor [6]. This led the Michigan DOT to issue a total moratorium on uncoated weathering steel in 1980, leading other states to also question their use of uncoated weathering steel. To facilitate a national discussion on the performance and use of UWS, the Federal Highway Administration (FHWA) held a forum of 131 participants comprised of federal, state, and industry representatives in July 1988 [5]. An outgrowth of this forum was Technical Advisory (TA) 5140.22, to provide recommendations to bridge owners and designers on conditions and locations that appeared to be associated with increased corrosion risk for existing bridges and to identify situations in which the use of uncoated weathering steel should be avoided for new designs [7]. In particular, the TA advised against using UWS in grade separations, “produced by the combination of narrow depressed roadway sections between vertical retaining walls, narrow shoulders, bridges with minimum vertical clearances and deep abutments adjacent to the shoulders.” This particular part of the TA became known as the “tunnel effect.”

## 1.1 The Tunnel Effect

A structural geometry created by a grade separation between two intersecting roadways with a bridge structure is referred to as a “tunnel” where the overhead spanning bridge forms the ceiling of the “tunnel.” The grade separation between 8 Mile Road and Interstate 75 on the north side of Detroit, MI is shown in Figure 1-1. It is believed this particular bridge geometry was the genesis of the tunnel scenario illustration shown in Figure 1-2 taken from TA5140.22 which illustrates where UWS “...should be avoided where winter deicing salt use is significant.” The specific concern is that the spray coming off vehicle tires driving on wet pavement beneath the bridge will

transport water and deicing chemicals up to the overhead girders, and thus expose them to higher times of wetness and expose them to chloride ions.



Source: © 2021 Google®

Figure 1-1: (Photo). Grade separation between 8 Mile Road and Interstate 75.



Source: FHWA

Figure 1-2 Illustration. Tunnel scenario from FHWA Technical Advisory.

Figure 1-2 is a source of debate because it provides no specific details to define the geometry that makes a grade separated bridge a “tunnel,” it merely provides a simple illustration. Consequently, the advisory led to many questions regarding its application. Among them, the following questions have been asked:

- Are there minimum or maximum values of underclearance that are most concerning?
- Is the tunnel effect influenced by just truck traffic, or all traffic?
- Does girder spacing influence the tunnel effect?
- Does girder depth influence the tunnel effect?

- Does the deck overhang influence the tunnel effect?
- Does the width of the roadway carried by the grade separated structure have an influence?
- Is it only a concern with vertical wall bridge abutments?
- Does the posted speed limit have an effect?
- How much deicing chemical has to be used before it is “significant”?

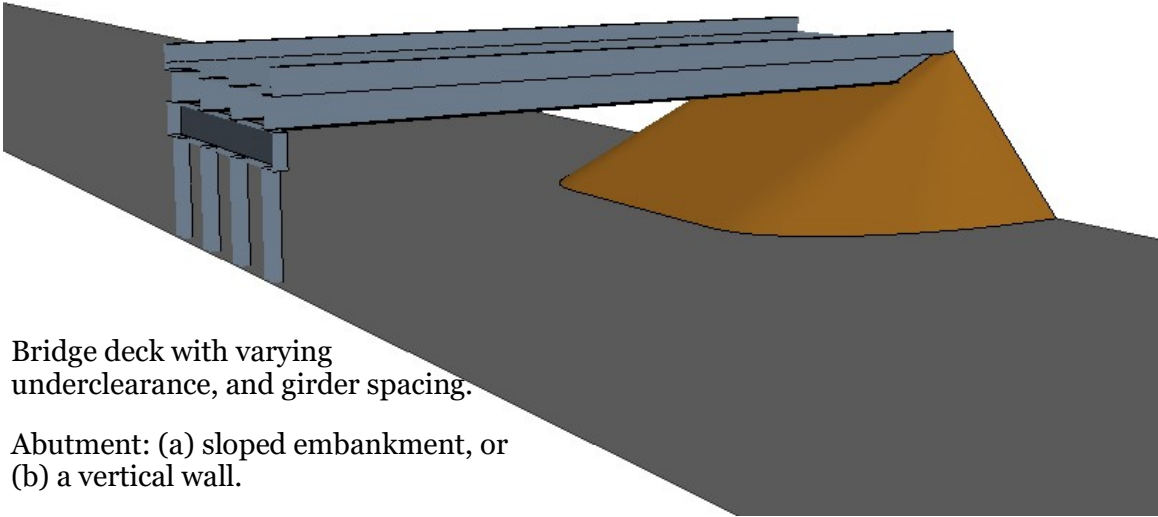
Based on the list of questions above, there has been a need to explore the variable space to better understand what defines a “tunnel” and what are the major variables that contribute to deicing chemical deposition on bridge girders. Two approaches to investigating and answering these questions are: (1) measure the conditions at uncoated weathering steel bridges and correlate with the condition of the bridge, and (2) investigate the transport of deicing chemical spray from tires up into and deposition on the uncoated weathering steel bridge girders using computational fluid dynamics (CFD). This report documents the results of a study employing approach (2), the use of CFD to study transport of droplet spray from tires up to the bridge girders and deposition on the girders.

## **1.2 Objectives**

The FHWA has undertaken a multi-year project to update the 1989 TA to make it more quantitative in lieu of its current qualitative form. The CFD part of the project is covered in two reports [8] and this report. The CFD analysis models how vehicular tire spray can be transported from a roadway up to an overhead bridge structure using a model comprised of two rigid bodies (the bridge with surroundings and the vehicle) in a fluid domain, with the vehicle moving through the fluid domain at a specified speed. The efficacy of this approach was first explored in 2011-2013, [8]. The current effort explores the effect of underclearance, girder spacing, girder height, deck overhang distance, and vehicle speed on the deposition of truck tire spray from wet roads on overhead bridge girders. The study also included a small set of cases with wind to test the sensitivity of results to the presence of wind.

## 2 Computational Model Geometry

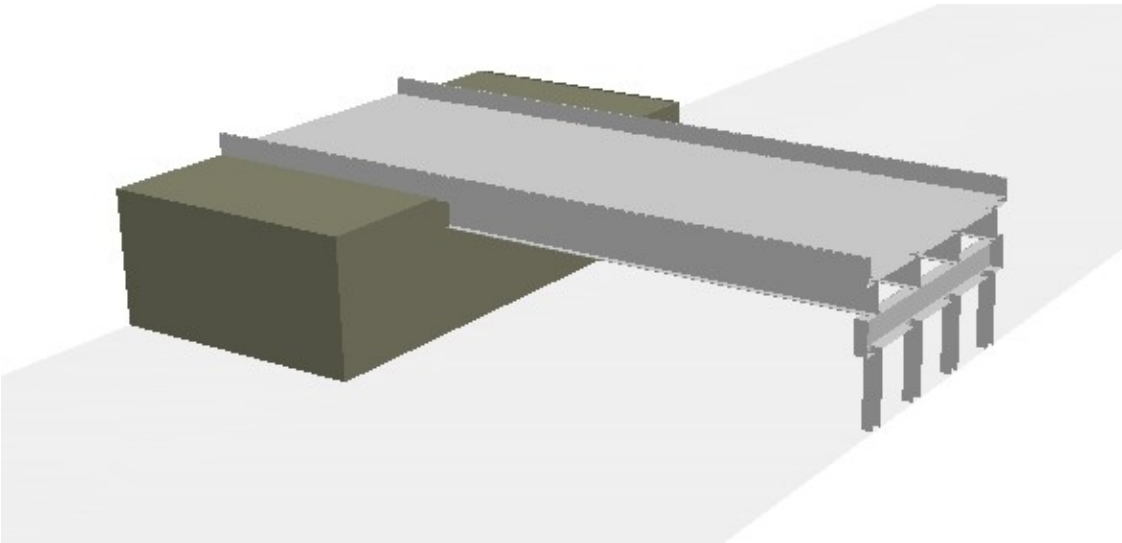
The geometry of the model consists of a symmetric half domain with stationary bridge and abutment in two configurations, one with sloped embankment and the other with a vertical wall as shown in Figure 2-1. The model also includes a truck that moves through the domain relative to the bridge as shown in Figure 2-2. The motion of the truck with respect to the bridge requires some special handling. The domain with the bridge contains an empty rectangular tunnel through which a second domain containing the truck slides, as shown in Figure 2-2. Variable values such as air speed and droplet tracks are interpolated across the interface between the bridge and truck subdomain as the truck subdomain slides through the bridge domain.



Bridge deck with varying underclearance, and girder spacing.

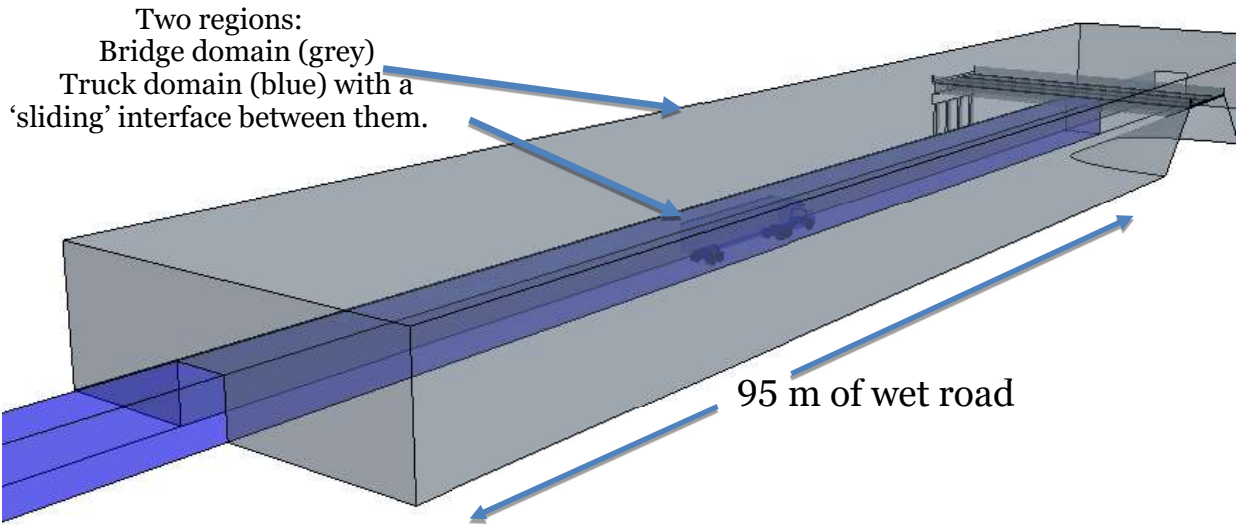
Abutment: (a) sloped embankment, or (b) a vertical wall.

(a) Bridge with sloped abutment

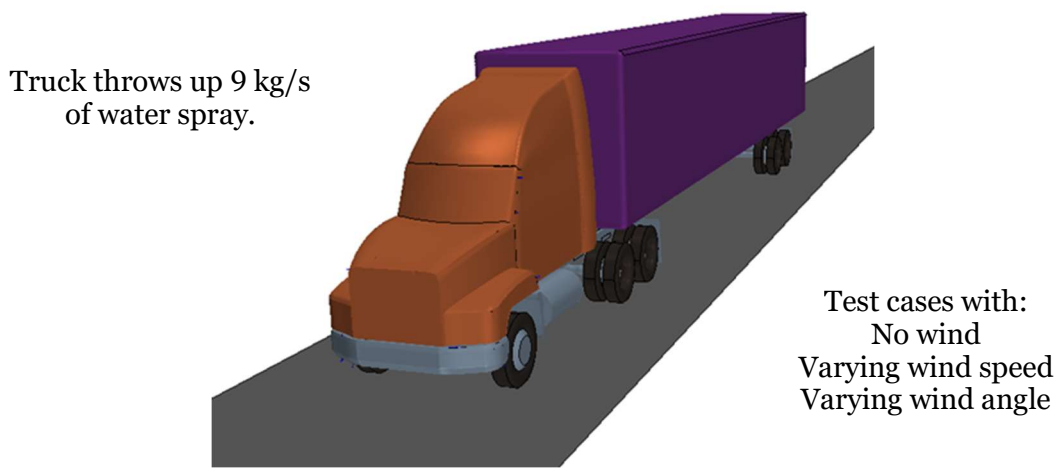


(b) Bridge with vertical wall abutment

Figure 2-1: Bridge and abutment geometries.



(a) Truck domain in blue slides through larger bridge domain in grey at the speed of the truck



(b) Truck domain may have 1 truck, 2 trucks, or a truck and a passenger vehicle

Figure 2-2: Bridge domain enclosing sliding truck domain.

### 3 CFD Modeling Methodology

The truck-spray-bridge system has many different elements that need to be included in a CFD model, and these put significant demand on computer resources. The major model elements are multiphase flow consisting of air and water droplets, turbulent transport of droplets in the truck wake, parametric geometry variation of the bridge, and the relative motion of truck and bridge. In order to include all of the needed elements and to be able to finish the computation of a case within a few days on 128 cores, approaches to and simplifications of the included models that provide good engineering results while still being sufficiently computationally efficient are needed. The following sections cover the important model elements, such as turbulence model and droplet spray model, with the important features that need to be included and the modeling options that were chosen with background and reasons for the modeling choices.

#### 3.1 Spray Droplets

The droplet spray coming off of the truck tires can be modeled either using an Eulerian or a Lagrangian approach. The Eulerian approach treats the droplet distribution as a continuous distribution of number density or volume fraction and is very computationally efficient for a mono-size distribution of droplets, involving only one scalar material conservation and one vector momentum conservation partial differential equation (PDE) to solve. The Lagrangian approach tracks individual droplets by solving Newton's law of motion embodied in an ordinary differential equation (ODE) for each droplet of a statistically significant number of droplets to determine the distribution and droplet paths of an entire spray or set of sprays that may contain several orders of magnitude more droplets than those that are tracked. With current computer clusters and CFD software several hundred thousand droplets can be tracked in a typical computation. While the Eulerian approach to solving for the droplet distribution and paths using PDEs is very computationally efficient, current CFD software does not account well for interaction of droplets with larger scale turbulent eddies, see Section 3.2, and therefore Lagrangian particle tracking was chosen to determine the transport of droplets up to the bridge girders.

Based on the literature and previous work [8], droplets are injected from tire surfaces at a mass rate of 0.5 kg/s from each wheel at a spray angle of 7.5 degrees from the tangent line with the tire tread. Each injected and tracked droplet is referred to as a droplet parcel because it represents many droplets that follow the same statistical path. The mass injection rate from a wheel,  $\dot{m}_p = 0.5$  kg/s, parcel injection rate,  $\dot{n}_p$ , mass of a single droplet,  $m_d$ , and number of droplets per parcel,  $n_d$ , are related by:

$$\dot{m}_p = m_d n_d \dot{n}_p \quad (1)$$

and therefore, the number of droplets in a parcel is:

$$n_d = \dot{m}_p / (m_d \dot{n}_p) \quad (2)$$

Figure 3-1 shows droplets coming off the cab tires in the near wake colored by the height above the pavement and rendered with a larger size to make them visible. Two options for modeling droplet interactions at solid surfaces are used. At the bridge girders, droplets colliding with a girder surface stick to the surface and accumulate, with the software keeping track of how much is present. For all other solid surfaces, when droplets intersect the surface, they pass through the surface and are removed from the simulation. Allowing droplets to leave the domain and simulation when they intersect a non-girder surface saves the computational effort needed to keep

track of them when they leave the domain and helps to maintain a statistically significant number of actively moving droplets in the system near the maximum that can be tracked.

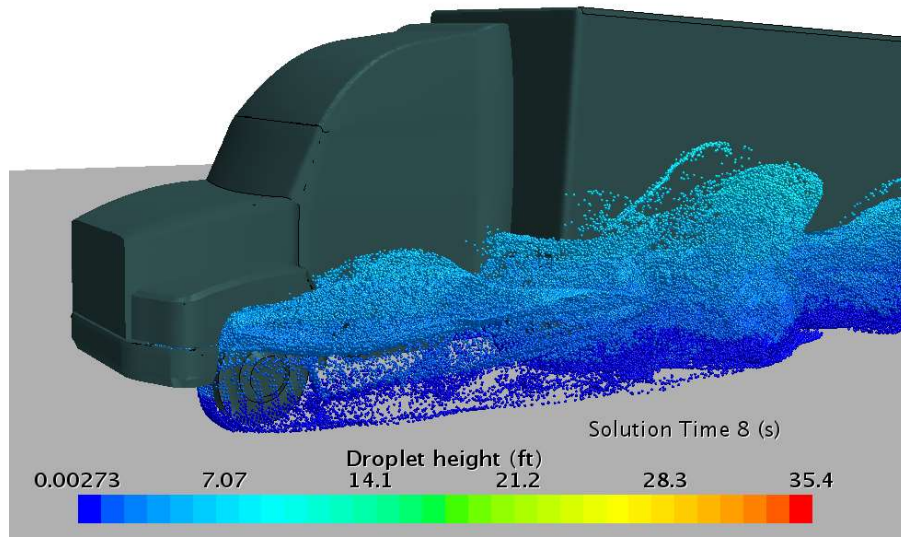


Figure 3-1: Droplets coming off truck cab tires and in the near wake colored by droplet height.

The amount of injected and suspended droplet mass from the truck tires for a typical case is plotted versus time in Figure 3-2. The steady increase of injected mass stops and remains constant at a little over 4 seconds when the truck leaves the domain. Most of the injected droplet mass is close to the roadway surface and settles fairly quickly back onto the roadway and out of the domain. This phenomenon can be seen in the blue line that is determined by summing up the droplet mass over the volume of the domain to get the suspended droplet mass remaining in the domain at a particular point in time. This line also increases at a constant rate while the truck is in the domain throwing off water spray from the tires but is considerably less than the injected water mass because it does not include the mass of droplets that have collided with surfaces under the truck or settled back onto the roadway. Once the truck has left the domain, the remaining droplet mass is that of droplets that may have been lofted up pretty high by turbulent eddies in the wake and may remain lofted up until the turbulent eddies have dissipated and the droplets settle back down onto the roadway under the influence of gravity. The blue line also stops growing at a little over 4 seconds when the truck leaves the domain, and then begins to slowly decrease as the eddies dissipate and droplets settle out of the flow. The peak suspended droplet mass is about 9 kg for this case. For 50  $\mu\text{m}$  diameter droplets, this is about 140 billion droplets in the domain. The software tracks a maximum of about 300,000 droplet parcels efficiently, and that means that a droplet parcel represents about half a million droplets.

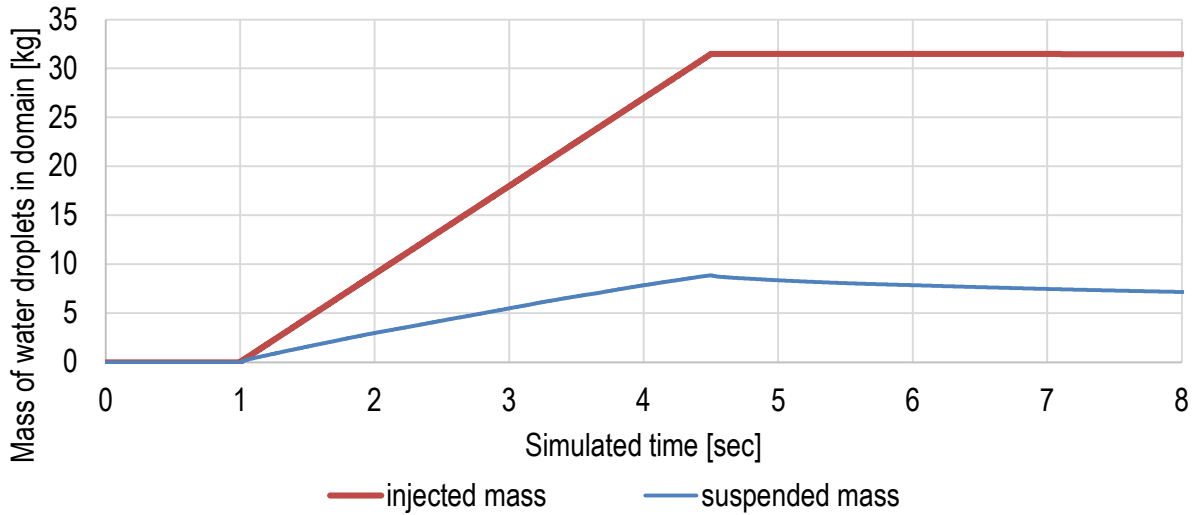


Figure 3-2: Example plot of water droplet mass suspended in the domain vs time.

The droplet spray coming off the truck tires has a size distribution, and previous work [8] has shown that spray droplets escaping the wheel well or mud flaps and undercarriage are in a size range of 0 to 100  $\mu\text{m}$  because larger droplets have too much inertia to make the turn from wheel well or truck trailer under carriage out into the truck wake without hitting surfaces of the wheel well or under carriage. The droplet size range is divided into categories in Figure 3-3. Small droplets up to a diameter of about 10  $\mu\text{m}$  respond very rapidly to changes in velocity of surrounding air and can be treated as a dissolved component of the air mixture. Under wet conditions, droplets in the aerosol size range up to 10  $\mu\text{m}$ , are a very small fraction of the mass of droplets in a truck wake because mass scales with the cube of the diameter. Therefore, droplets less than 10  $\mu\text{m}$  in diameter are not a significant fraction of the droplet mass that is deposited on bridge girders due to the passage of a truck. When a dry salt film remains on the roadway after a snow event, however, resuspension of aerosol size salt dust by passing vehicles over a period of weeks might contribute to the accumulation of salt on bridge girders, and that possibility is beyond the scope of this study. A few simulations were done to test transport of aerosol salt dust up to girder level in the previous report [8] for several wind conditions and under some assumptions of salt dust resuspension by solving the Reynolds Averaged Navier-Stokes equations for the salt dust transport. Concentrations in the range of 0.5 to 2 ppm were found at the girder level. This study did not model deposition under dry conditions, which would be primarily due to salt dust settling on the top surfaces of girder flanges.

As noted, previous work determined that droplets larger than about 100  $\mu\text{m}$  are unlikely to enter the truck wake due to collisions with truck surfaces, wheel well, or truck trailer undercarriage after being shed from truck tires. The size range of interest is therefore 10 to 100  $\mu\text{m}$ . Figure 3-4 shows droplet settling times in still air from 5 feet, approximately the top of wheel well height, with the size range of interest highlighted in green. The settling times in still air in the size range of interest range from 5 seconds for 100  $\mu\text{m}$  droplets up to 8 minutes for 10  $\mu\text{m}$  droplets.

### Model treatment of particle size:

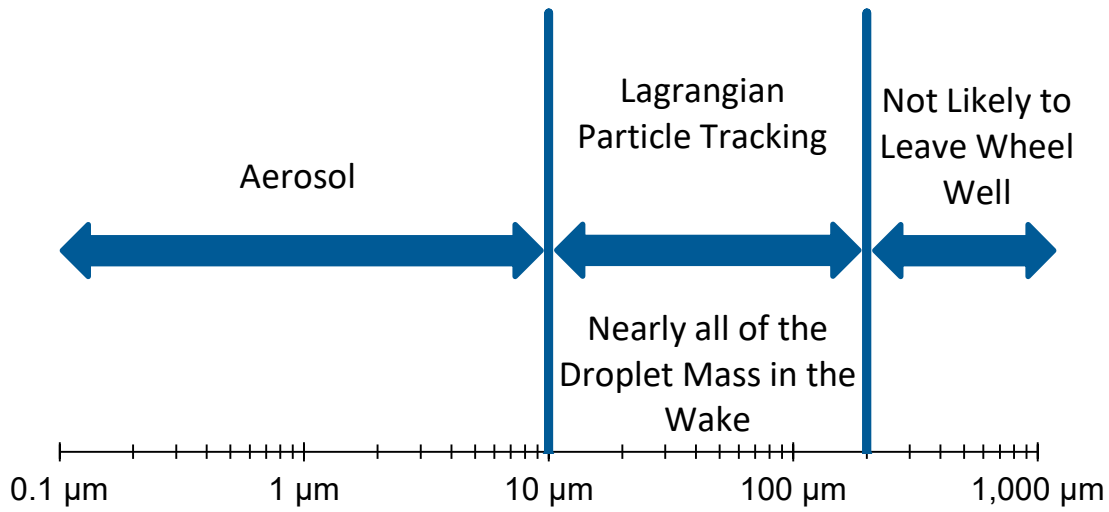


Figure 3-3: Size distribution of droplets leaving truck tire surface.

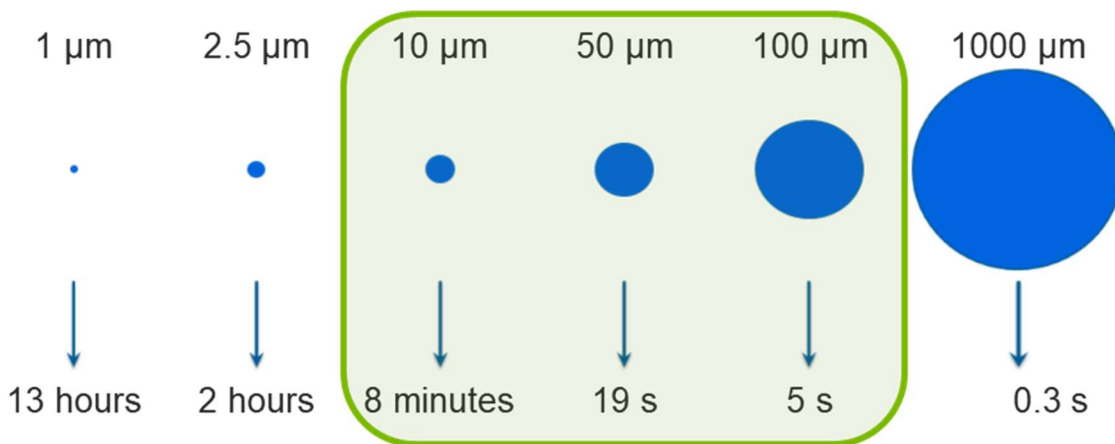


Figure 3-4: Settling time from 5-foot elevation for droplets from 1 to 1000 μm.

Solving for the transport of a mixture of droplets with a size distribution is possible with current CFD software, but doing so either greatly increases the computational resources and effort needed or greatly reduces the number of droplets of any single size that can be tracked. Some initial testing with a base case was done to determine if using a mean droplet size of 50 μm could be used to save on computational resources and maintain an adequate population of droplets at the girder level to compute deposition patterns on the girders. A normal distribution of droplets with a mean diameter of 50 μm is shown in Figure 3-5. Simulations were done using the additional computer resources to track droplets over the entire size distribution and a reduced computer resource simulation tracking mono-sized droplets injected at the mean diameter. The amount of droplet mass reaching girder height with these two approaches was nearly the same as shown in Figure 3-6. Therefore, because these simulations are very computationally expensive, the use of mono-sized droplets at a mean diameter of 50 μm was chosen for running the parametric test set of simulations.

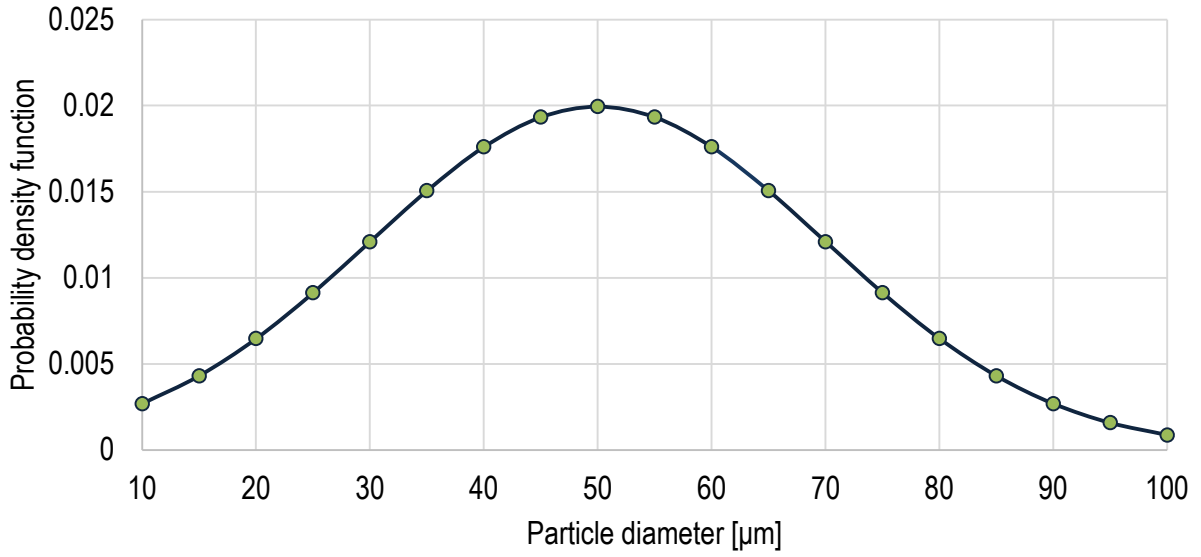


Figure 3-5: Normal size distribution of droplets leaving wheel well.

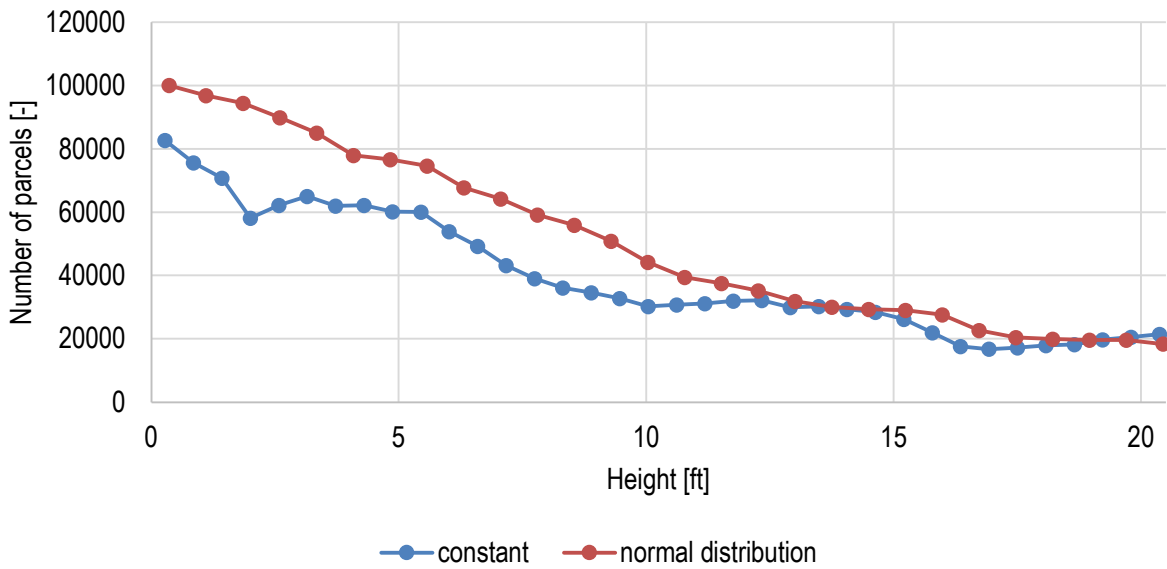


Figure 3-6: Spray droplet parcels versus height above roadway for 50 μm mono size droplets and a normal distribution of droplets.

## 3.2 Turbulence Model and Management of Computer Resources

Previous work [8] employed a k-epsilon turbulence model using the unsteady Reynolds averaged Navier-Stokes (URANS) equations to solve for the air flow and wake generated by the truck passage. Lagrangian particle tracking was used to solve for the paths of a statistically significant number of droplets shed from the truck tires. Solving the URANS equations for the air flow yields a mean flow field that does not contain the large turbulent eddies shed from the truck and other structures. The droplet tracking in this case is limited to capturing the effects of the mean flow field on the transport of droplets shed from the truck tires and fails to capture transport of droplets within large eddies, which is important in this application. The large eddy simulation (LES) turbulence model solves the unaveraged Navier-Stokes equations for the air flow over the range of length scales that can be resolved in the computational grid and uses a sub grid model to solve for effects of air turbulence at smaller scales. Use of LES captures the generation and flow of large eddies that contain most of the turbulent energy. These large eddies have sufficient translational and rotational energy to exert enough drag force on droplets within them to cause the droplets to remain within the eddies and closely match their motion, except in tight turns around structures. In those tight turns near structures, the drag exerted by the air on droplets may not be sufficient to overcome the inertia of a droplet, and the droplet may collide with the structure. The capability to model these physics interactions between air flow and droplets in a truck wake makes use of the LES turbulence model and is an excellent approach for determining the droplet transport in vehicle wakes with droplet deposition on bridge girders. Previously however, the use of LES to run a large parametric matrix of cases was not feasible because using LES requires about an order of magnitude more computer resources than solving the URANS equations for the air flow. In 2012 and 2013 when the first effort to model truck tire spray droplet transport was done, the high-performance computer (HPC) cluster that was available for the work was not capable of running the planned number of cases within a reasonable time using LES. In this second phase of truck spray modeling, however, employing LES for the planned case matrix became feasible on an upgraded HPC cluster with careful design of the model domain and the method of running cases. Techniques that could reduce computer resource usage were applied to complete the test case set in a reasonable time. These are covered in the following paragraphs.

Figure 3-7 shows the droplet distribution in the truck wake after the truck has passed under a bridge but before it leaves the domain. The figure compares the use of a URANS k-epsilon turbulence model to determine droplet transport in the wake generated by the motion of the truck to using a much more computationally expensive LES turbulence model. The simulation using the URANS model averages out most of the air eddy motion in the truck wake. Droplets in the size range less than 100  $\mu\text{m}$  follow air motion in the wake very closely, and therefore the motion of droplets is limited to be close to the boundary of the wake. The wake in the URANS simulation shown in top of Figure 3-7 does reach the bridge girders, but it barely does so, and no droplets are carried above the level of the bridge deck. In contrast, the lower half of Figure 3-7 shows the droplet distribution around the bridge after truck passage using the LES turbulence model. The large eddies generated by the truck passage billow up above bridge deck height, and those eddies carry droplets with them. This additional droplet transport in large eddies to greater heights is not captured in the URANS turbulence model simulation. For this reason, the LES turbulence model appears to be the best choice for investigating droplet transport up to bridge girders and droplet interaction with bridge girders.

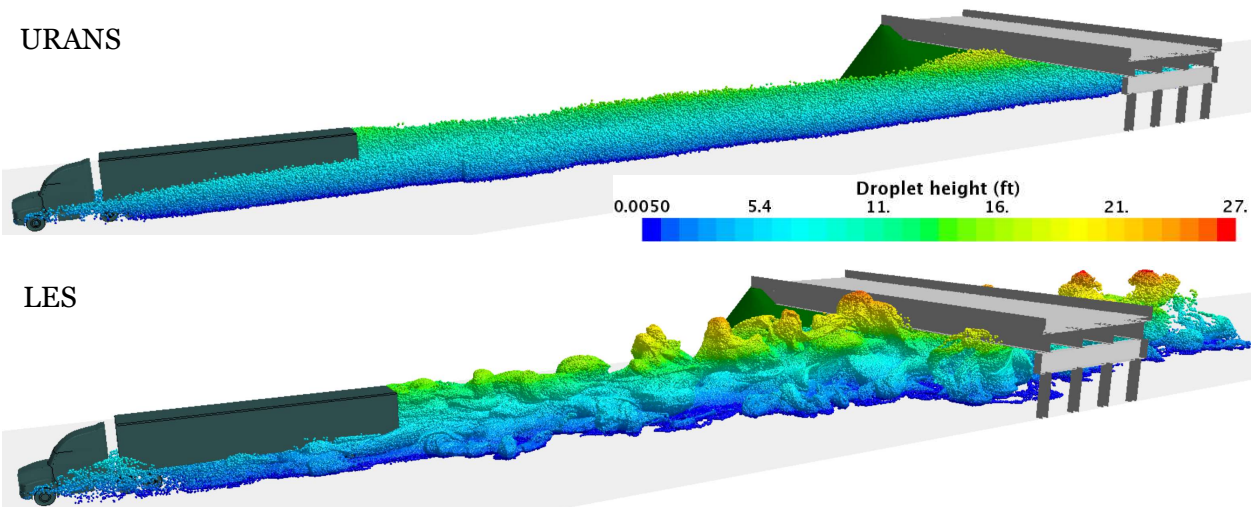


Figure 3-7: Droplet distribution at a moment in time for simulations of truck passage past a bridge using both URANS and LES equations to solve for the air flow field.

Droplets are injected from the truck tires into the system from the time the truck enters the domain until the truck emerges from the other side of the bridge, at about 4.5 seconds of simulated time. Droplets are not injected after that time because droplets injected into the system after the truck emerges out from under the bridge has no chance of reaching bridge girders. Therefore, there is no need to expend computational time and resources tracking those droplets. Figure 3-8 shows the suspended droplet mass for both a large eddy simulation, LES, and an unsteady Reynold's averaged Navier-Stokes turbulence model, URANS. Most of the large eddy transport of droplets is averaged out in the URANS simulation, including a significant amount of vertical transport to higher elevations, which results in droplets that are closer to the ground and settle out faster as a result. A considerably larger droplet suspended mass is visible in Figure 3-8 for the LES simulation compared to the URANS simulation. By the time injection from the truck stops when the truck emerges out from under the bridge at about 4.5 s, the droplet suspended mass that has not settled out or collided with a surface in the LES simulation is over 2 times the suspended mass of the URANS simulation. After 4.5 s, the droplets in the LES simulation have to settle from greater heights, which will take longer, making LES simulation very important in capturing the amount of droplet mass transport in the truck wake. Therefore, achieving a more accurate estimation of the amount of droplet mass transported up to bridge girders and deposited on them using LES was judged to be worth the large increase in computer resources to use the LES turbulence model, and it was chosen for running the study case set.

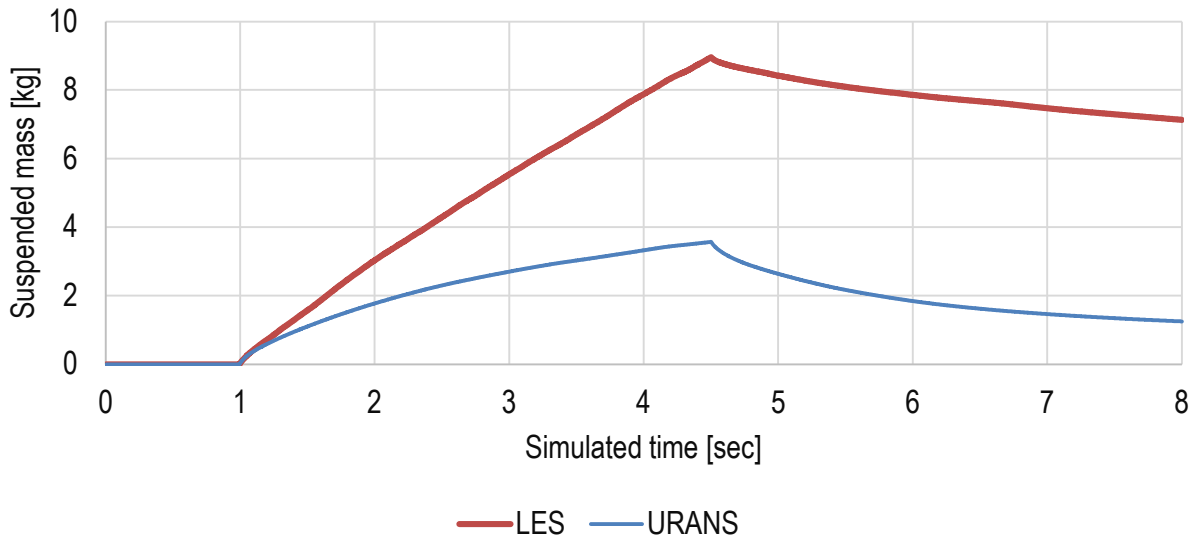


Figure 3-8: Comparison of droplet suspended mass for a truck passing through a domain.

### 3.3 Time Needed to Reach Maximum Droplet Accumulation on Girders

The base case simulation, see Section 5, was run until no further changes were noticeable in the mass of saltwater accumulated on girders, which occurred between 120 and 140 seconds, as shown in Figure 3-9. The truck transit time through the domain was about eight seconds at 60 mph. The mass of droplets being transported upward via turbulent eddies in the wake and continuing to flow under the bridge due to the wake longitudinal flow induced by the truck continues to build up between the girders until about thirteen seconds has elapsed, as shown in Figure 3-11. After that, droplets collide with the girders or settle out of the flow, and the suspended mass between girders decays for approximately the next 100 seconds.

With the full computational domain, these cases require about 1.1 hours of wall time to run 1 second of simulated time on 128 computer cores, or about 4.5 days to complete a simulation run out to 120 seconds. The test case matrix consists of about 100 cases. At a completion rate of 4.5 days per case, it would have taken about 1.3 years of wall time running cases continuously 24 hours per day, 7 days per week. An alternative approach was sought to completing the computationally expensive large eddy simulation runs that would still yield the same high-quality results but would not take so much computer and wall clock time. A close examination of the base case run revealed that once the truck has passed out of the domain and the mass of droplets circulating between girders has reached its peak, further evolution of the air and droplet flow system is a consequence of the slow dissipation of the induced eddy flow between girders and the coincident deposition of droplets from those eddies on the girders.

To see if simulations could be sped up, a copy of the domain was greatly reduced in size, putting the roadway normal boundaries close to the bridge, as shown in Figure 3-10, was created. Figure 3-11 shows a plot of the mass of saltwater droplets suspended in the air at various heights during a simulation. At the maximum of suspended droplet mass between girders, occurring at about 13 seconds simulated time, all of the field variables including pressure, air and droplet velocities, droplet positions, etc., were mapped onto corresponding locations in the reduced domain, and the computation was continued on the smaller domain from the simulation time of 13 seconds

out to a simulation time between 120 and 140 seconds when droplet mass accumulation on girders had reached a nearly constant value. Droplet accumulation and distribution on the girders was the same using these two approaches, complete simulation on full domain and only simulation of truck passage and droplet lofting between girders on the full domain, followed by simulation on a reduced domain around the bridge until droplet accumulation on girders ceased. Using the reduced domain approach after the truck has passed, also reduced the wall time needed for a case from about 5 days down to 1 day, a remarkable speedup by about a factor of five, making completion of the case matrix well within a year possible.

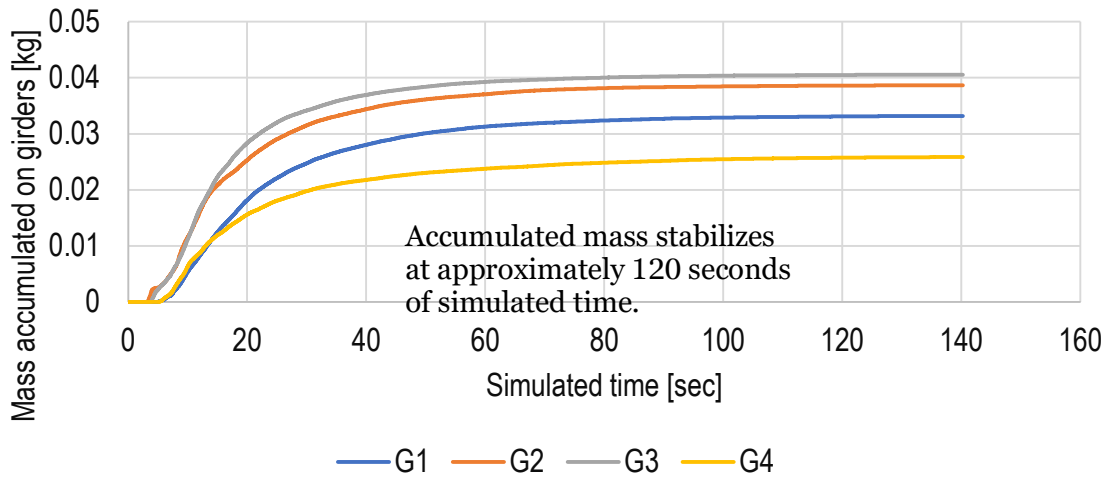


Figure 3-9: Accumulated droplet mass on girders 1 through 4 (G1, G2, G3, G4) for base case truck passage event.

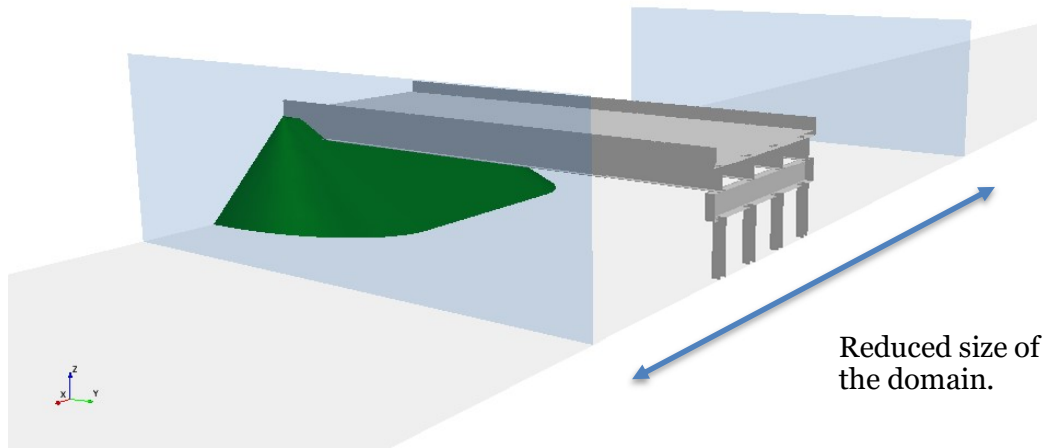


Figure 3-10: Reduced domain for calculation of droplet deposition on girders faster and with less computer resources after the truck has passed.

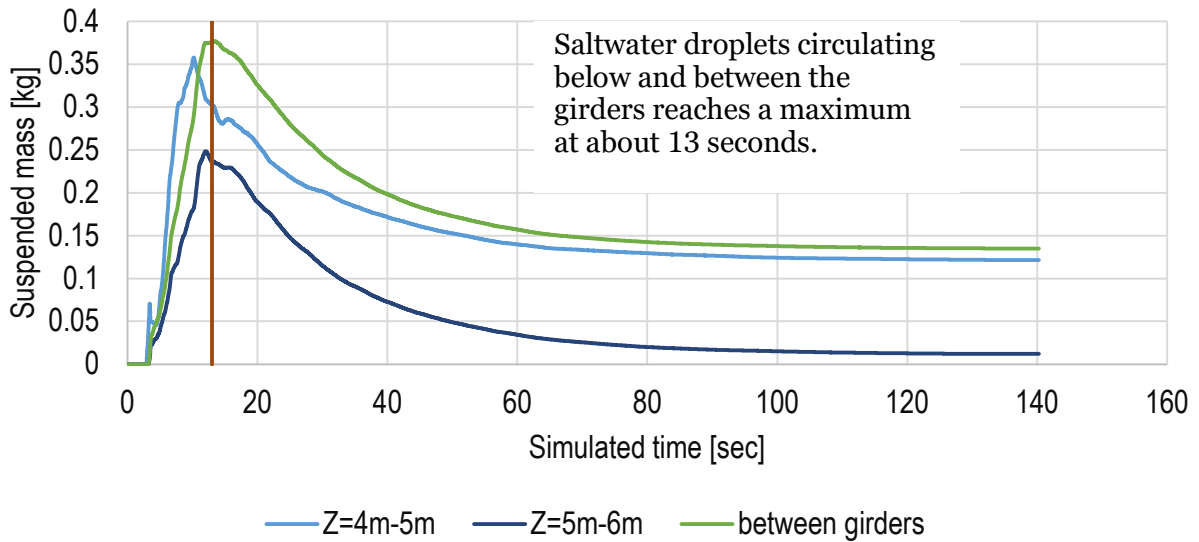


Figure 3-11: Mass of saltwater droplets suspended in the air at various heights.

### 3.4 Effects of Vehicle Starting Position

The starting position of the truck may affect results because large eddy shedding events may be at different stages of completion when the truck enters the space under the bridge deck. Large eddies are shed from the truck with a length between large eddy groups of about 10 m. This length is the same length scale as the girder spacing, and consequently the position of these groups interacting with the bridge may vary depending on the location where the first one is generated. To check for the effect of the starting position of the truck on the droplet mass accumulated on girders, tests were run using the base case with the truck starting position offset backward by 2.5, 5.0, and 7.5 m (8.2, 16.4, and 24.6 ft) from the base case starting position at 0 m. The plot of droplet mass accumulation on the bridge girders for these tests, shown in Figure 3-13, indicates that droplet deposition on the girders may vary by 25% for a single truck passage event depending on the synchronization between eddy shedding and the bridge girder position. Over a large number of passing trucks the total accumulation should be close to the number of passing trucks times the mean of the variation caused by starting position.

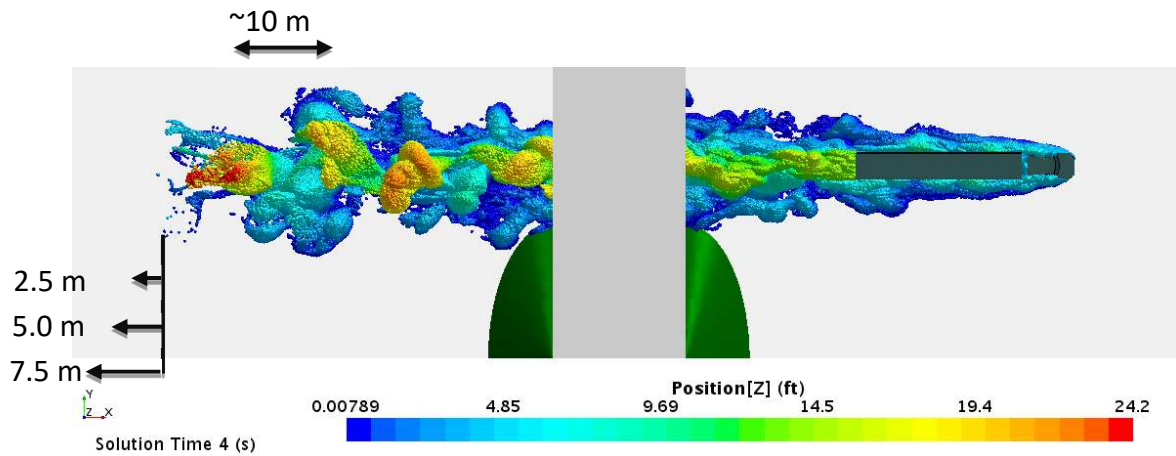


Figure 3-12: Top view of truck wake with spray showing that the distance between large eddies is about 10 meters.

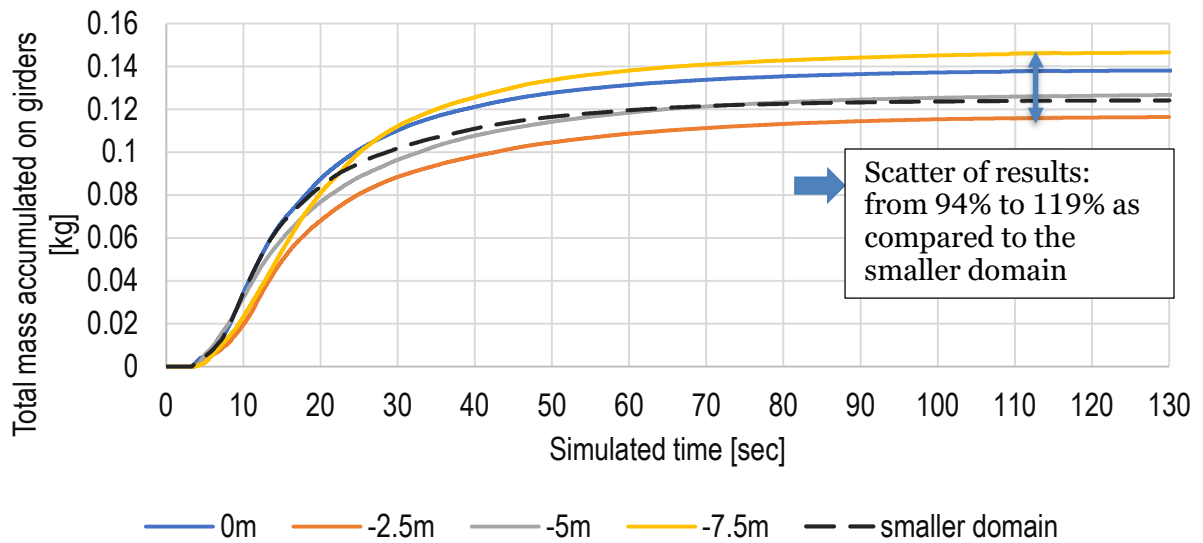


Figure 3-13: Droplet mass of the base case for truck starting position varied from 0 m to -7.5 m and calculated with the reduced domain.

## 4 Governing Equations

When droplets are thrown off the tires, they enter the air flow in the wheel wells and the undercarriage of the trailer. The droplets that do not collide with a wheel well or the truck trailer undercarriage surfaces or do not fall back on the roadway, enter the truck wake and tend to travel with the turbulent eddies in the wake. The turbulent wake starts at the front of the truck and extends far beyond the back of the trailer. This turbulent air flow that is transporting the droplets of interest, is a two-phase flow, with a continuous medium, the air, and a discrete distribution of water droplets. The motion of droplets is determined by two forces, gravity and drag. The air flow influences the droplet flow through drag force and consequent momentum exchange between the moving air and droplets. The air flow is governed by the Navier-Stokes partial differential equations with sink terms in the momentum equation accounting for the effects of droplet drag on the airflow. Newton's laws of motion, expressed as ordinary differential equations, govern the motion of droplets through the air under the influence of the two forces of air drag and gravity. The governing equations for the air and droplets are solved iteratively until the solution converges at each time step. Time steps are solved until a final distribution of the droplets on surfaces is determined.

### 4.1 Navier-Stokes Equations Governing the Air Flow

The continuous fluid phase of air flow is determined by solving the transient Navier-Stokes equations over large eddy length scales that can be resolved in the computational grid. The influence of eddies smaller than the computational grid cell spacing is determined using a subgrid scale turbulence model that provides the contribution to the fluid stress from the subgrid scale. This approach is referred to as large eddy simulation (LES).

The Navier-Stokes equations for conservation of mass and momentum, respectively, for air flow in the form used in LES are:

$$\frac{\partial \rho}{\partial t} + \nabla \cdot (\rho \mathbf{u}) = 0 \quad (3)$$

$$\frac{\partial (\rho \mathbf{u})}{\partial t} + \nabla \cdot (\rho \mathbf{u} \otimes \mathbf{u}) = -\nabla \cdot p \mathbf{I} + \nabla \cdot (\mathbf{T} + \mathbf{T}_{SGS}) + \mathbf{f}_b \quad (4)$$

where  $\rho$  is the air density,  $\mathbf{u}$  is the filtered velocity,  $p$  is the filtered pressure,  $\mathbf{I}$  is the identity tensor,  $\mathbf{T}$  is the filtered stress tensor,  $\mathbf{T}_{SGS}$  is the turbulent stress tensor modeling the subgrid scale stresses, and  $\mathbf{f}_b$  is the sum of body forces, such as gravity and centrifugal force.

The subgrid scale stress tensor is given by:

$$\mathbf{T}_{SGS} = 2\mu_t \mathbf{S} - \frac{2}{3}(\mu_t \nabla \cdot \mathbf{u}) \mathbf{I} \quad (5)$$

where  $\mu_t$  is the subgrid scale turbulent viscosity, and  $\mathbf{S}$  is the strain rate tensor given by

$$\mathbf{S} = \frac{1}{2}(\nabla \mathbf{u} + \nabla \mathbf{u})^T \quad (6)$$

and

$$\mu_t = \rho \Delta^2 S, \quad S = \sqrt{2\mathbf{S}:\mathbf{S}} \quad (7)$$

Additional details for the LES air flow model equations can be found in the STAR-CCM+ user guide [9].

## 4.2 Droplet Equations of Motion

A Lagrangian approach is used to solve for the motion of the droplets coming off of the truck tires. In the Lagrangian approach, the motion of each droplet through the air is traced by solving the ordinary differential equation governing its conservation of momentum at each time step. The number of droplets thrown off of the truck tires is overwhelmingly huge, making it impossible to compute droplet paths for all individual droplets. The computer cluster used for this study can solve for the paths of several hundred thousand droplets in the system at one time. This number of droplets is considered statistically significant and the droplets that are tracked are referred to as packets, each packet representing the mass of a large number of droplets that would share similar paths. The total droplet mass associated with an injected packet is tracked along with the information on the position and velocity of the droplet at each time step. The equation governing the conservation of momentum of a droplet is:

$$m_d \frac{d\mathbf{u}_d}{dt} = \mathbf{F}_s + \mathbf{F}_b \quad (8)$$

where  $m_d$  is the mass of the droplet,  $\mathbf{u}_d$  is the velocity vector of the droplet,  $\mathbf{F}_s$ , is the resultant sum of surface forces acting on the droplet, and  $\mathbf{F}_b$  is the resultant sum of body forces acting on the droplet. The body force on a droplet is:

$$\mathbf{F}_b = m_d \mathbf{g} = \rho_w V_d \mathbf{g} \quad (9)$$

where  $\rho_w$  is the saltwater density,  $\mathbf{g}$  is the gravity vector, and  $V_d$  is the droplet volume.

In the truck-bridge system, there are two surface forces acting on droplets, drag,  $\mathbf{F}_d$ , and the pressure gradient or buoyancy force,  $\mathbf{F}_p$ :

$$\mathbf{F}_s = \mathbf{F}_d + \mathbf{F}_p \quad (10)$$

the pressure gradient or buoyancy force is given by:

$$\mathbf{F}_p = -V_d \nabla p_{static} = -V_d \rho \mathbf{g} \quad (11)$$

where  $p_{static}$  is the static pressure. The gravity and buoyancy forces on a droplet combine as

$$\mathbf{F}_b + \mathbf{F}_p = (\rho_w - \rho) V_d \mathbf{g} \quad (12)$$

Because the saltwater density,  $\rho_w$ , is around 1000 kg/m<sup>3</sup> and the density of air is three orders of magnitude smaller,  $\rho = 1.2$  kg/m<sup>3</sup>, the buoyancy force of the droplets in air has little effect on the results.

The drag force of the air on droplets in the tire spray is given by:

$$\mathbf{F}_d = \frac{1}{2} C_d \rho A_p |\mathbf{u}_s| \mathbf{u}_s \quad (12)$$

where  $A_p = \pi D_d^2/4$  is the projected droplet area,  $D_d$  is the droplet diameter, and  $C_d$  is the drag coefficient given by the Schiller-Naumann correlation,

$$C_d = \begin{cases} \frac{24}{Re_p} (1 + 0.15 Re_p^{0.687}) & Re_p \leq 1000 \\ 0.44 & Re_p > 1000 \end{cases} \quad (13)$$

where  $Re_p$  is the droplet Reynolds number:

$$Re_p = \frac{\rho |\mathbf{u}_s| D_d}{\mu} \quad (14)$$

and where  $\mathbf{u}_s = \mathbf{u} - \mathbf{u}_d$  is the slip velocity vector between the air and droplet velocity, and  $\mu$  is the dynamic viscosity of air.

The state of the droplet field is evolved by holding the air velocity field fixed, and solving Eqn. (8) for each droplet packet velocity, and then changing its position according to

$$\Delta \mathbf{r}_d = \mathbf{u}_d \Delta t, \quad (15)$$

where  $\Delta \mathbf{r}_d$  is the change in a droplet position vector,  $\mathbf{r}_d$ , for time step  $\Delta t$ .

## 5 Base Case and Test Matrix for Parametric Study

Large eddy simulation uses a large amount of computer resources and takes a long time to complete compared to using URANS with the k-epsilon turbulence model. The heavy computer resource usage of LES limits the number of cases that can be run in a parametric study. To investigate the effects of variation of as many parameters as possible, a base case was chosen, and the parameters of interest were varied one at a time while the others remained constant at the base case values. The base case for the study is defined in Table 1 with the parameters of interest listed in the first column, the base case values of these parameters listed in the second column and the values of the varied parameters listed in the third column for the case set of simulations.

Table 1: Base Case with List of Varied Parameter Values for the Case Set

Parameter	Base Case	Modified Values
<b>Type of embankment</b>	Sloped	Sloped or Vertical wall
<b>Under clearance</b>	16 ft (4.9 m)	15, 17, 18, 19, 20, 22, 24, 30, 35, and 40 ft (4.6, 5.2, 5.5, 5.8, 6.1, 6.7, 7.3, 9.1, 10.7, and 12.2 m)
<b>Number of girders</b>	4	5, 6, 7
<b>Girder height</b>	54 inch (137 cm)	30 inch (76 cm)
<b>Parapet height</b>	3 ft (0.91 m)	NA
<b>Deck overhang</b>	3 ft (0.91 m)	5 ft (1.5 m)
<b>Number of vehicles</b>	1	2, trailing vehicle: truck or passenger vehicle
<b>Vehicle speed</b>	60 mph (96.6 kph)	30, 45 mph (48.3, 72.4 kph)
<b>Wind angle</b>	No wind	0, 45, 90, 135, 180 degrees
<b>Wind speed</b>	No wind	2, 10, and 25 mph (3.2, 16.1, and 40.2 kph)

Most of the test cases use the truck speed of the base case of 60 mph (96.6 kph) because 60 mph is a common speed, especially on interstate highways in cities. In addition, 60 mph was chosen for the base case because, being the highest tested speed, it was also expected to produce the most droplet deposition on bridge girders among the tested speeds. Table 2 shows the truck speeds tested and the Reynolds numbers,  $Re_t$ , for air flow past the truck that characterize the flow regime.

For flow past bluff bodies at high Reynolds numbers, as in these cases with Reynolds numbers all greater than about 3 million, and where the bluff body is not highly streamlined, the wake is broad and characterized by the shedding of large turbulent eddies that grow and spread out as the distance between a wake cross section and the bluff body grows.

Table 2: Truck Reynolds Number

Truck Speed mph	Truck Speed m/s	Reynolds Number	Wake Type
<b>60</b>	27	$5.5 \times 10^6$	Fully Turbulent
<b>45</b>	20	$4.1 \times 10^6$	Fully Turbulent
<b>30</b>	13	$2.7 \times 10^6$	Fully Turbulent

The base case was a real bridge crossing over I-77 near Beckley, WV, thus it represents a valid structural design. For this work, the bridge is merely a rigid volume within a fluid and does not have structural properties. Some of the base case modified values, such as number of girders, girder height, and deck overhang may not result in a valid structural design, they were created merely to understand the effect of that variable on the droplet distribution that occurs when a truck passes under the bridge with spray coming off the tires.

## 6 Results and Discussion

The number of cases in the case matrix covering parameter variations of interest is limited because large eddy simulation requires a large amount of computer resources and time to complete analysis of one case compared to using a turbulence model, such as a k-epsilon turbulence model, with the unsteady Reynolds averaged Navier-Stokes governing equations. The approach to investigating all of the parameters of interest in this study was to define a base case that had geometry and conditions close to those that could lead to a buildup of salt from evaporated droplets deposited on bridge girders with a large number of truck passage events, and then to run variations of the base case varying one parameter at a time to investigate the effects of variation of each parameter on amount and location of droplet deposition on the bridge girders. The following sections present the results of the analysis of the base case followed by sections covering variation of each of the parameters in the case matrix.

### 6.1 Base Case

The base case used an 18-wheel semitruck with trailer passing under a bridge at 60 mph (97 kph). The truck trailer was 8.5 ft (2.6 m) wide by 14 ft (4.3 m) high giving a projected frontal area of 119 ft<sup>2</sup> (11.1 m<sup>2</sup>) and a hydraulic diameter of 10.6 ft (3.2 m). Taking properties at an air temperature of 25 °C (77 °F) gives an air density of 1.18 kg/m<sup>3</sup> and viscosity of  $1.84 \times 10^{-5}$  kg/m-s. At 60 mph, the Reynolds number for the moving truck is  $5.7 \times 10^6$ . At this Reynolds number, the truck wake is fully turbulent, wide, and expanding. The bridge had four 54-inch-high (137 cm) girders with a 24-inch wide by 1.5-inch thick (61 cm by 3.8 cm) bottom flange. Although the girder height was changed to 30 inches (76 cm) for one case, the flange width was not changed. The base case has an abutment with a sloped embankment and an underclearance of 16 ft (4.9 m). The parapet height was 3 feet (0.9 m), and the deck overhang was 5 ft (1.5 m). As seen in Figure 6-2 the truck wake is characterized by large turbulent eddies carrying droplets shed from truck tires outward and upward from the centerline of the wake past the trailer. The droplet packets used to track a statistically significant number of droplets are visualized with balls that are much larger than the 50 μm droplets themselves in order to make them visible. In reality a droplet laden truck wake appears as a fine mist as shown in the upper frame of Figure 6-1, while the lower frame of Figure 6-1 shows the visualization of the droplet laden wake of a similar truck, that was used in the simulations of this study. In the visualization, the rising droplets in the eddies in the wake behind the trailer are clearly visible, while in the photo of the truck in rain, the droplets in the rising eddies in the wake behind the trailer tend to washout and just add blur to the landscape behind the truck because the droplets are small and spread out as the wake width increases with distance from the truck. The droplets in the eddies respond very quickly to the motion of the air in the eddies and are therefore easily carried with the eddies. The visualization of the droplets also provides a good visualization of the boundaries of the eddies themselves.

The frames in Figure 6-2 show that for an observer traveling with the truck, droplets in the immediate downstream of the trailer do not extend significantly above the trailer height. However, for an observer on the ground by the bridge, the wake grows in both width and height downstream of the truck with eddies swirling outward from the truck centerline. As a consequence, droplets are carried in the eddies up between the girders and also well above the height of the bridge deck as seen in the lower frame of Figure 6-2. The air in the truck wake is being dragged along with the truck, which is moving at 60 mph (97 kph). Very close to the truck surface boundaries, the air speed is 60 mph and decreases with distance from the truck as it interacts with the surrounding air. Because the wake is moving in the direction of the truck, more droplets move under the bridge and up into the girders as time passes. This continues until enough time has passed for the energy of the eddies in the wake to dissipate and the droplets either collide with surfaces or settle out onto horizontal surfaces under the force of gravity.

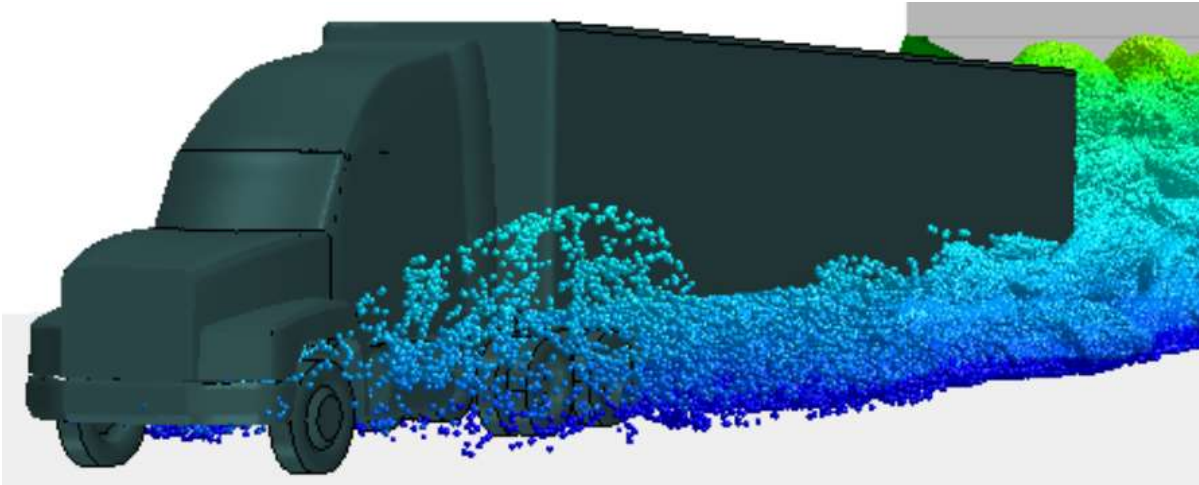


Figure 6-1: Droplet laden truck wake during afternoon rain on I70 in Utah, upper frame, droplet laden truck wake visualization of truck geometry used in simulations, lower frame.

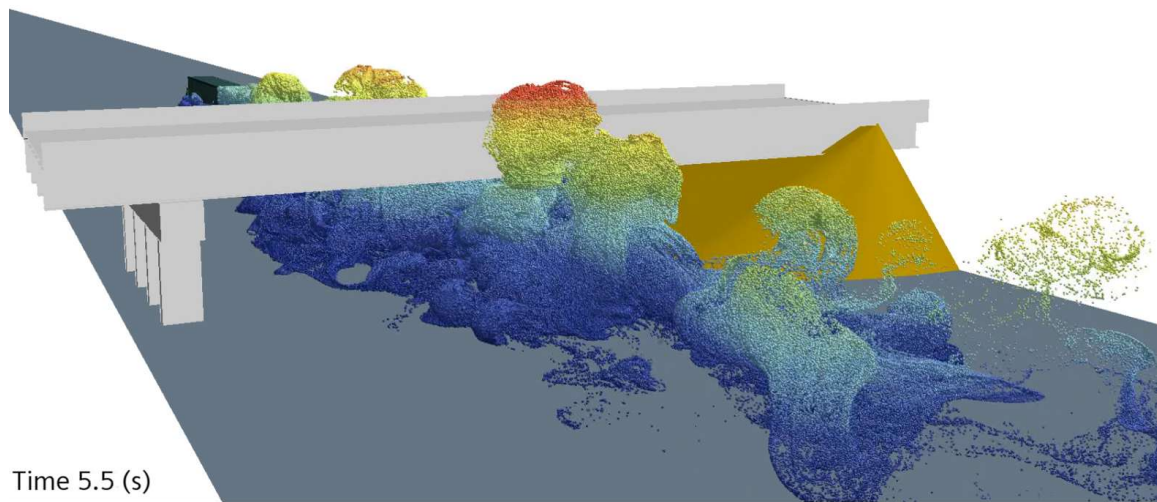
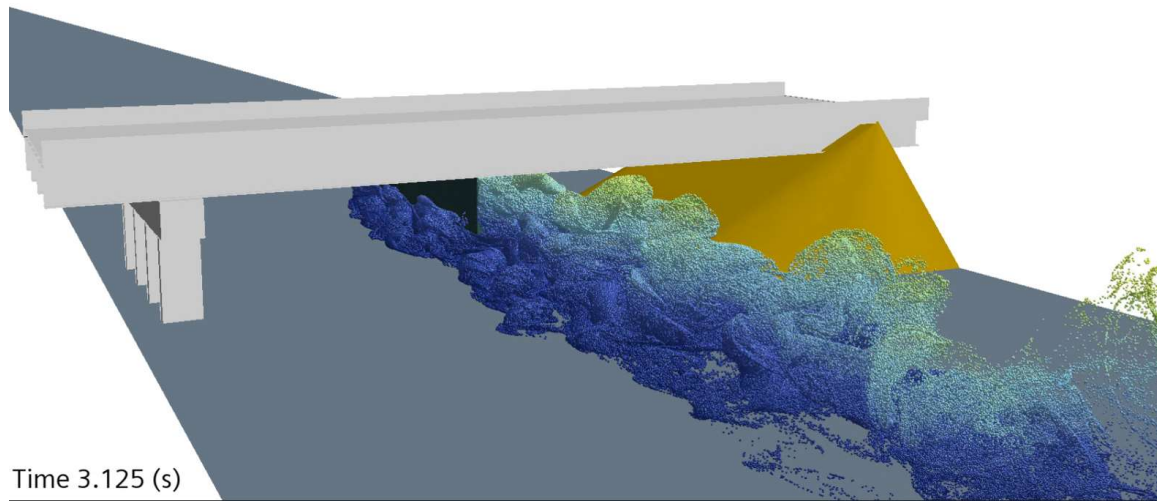
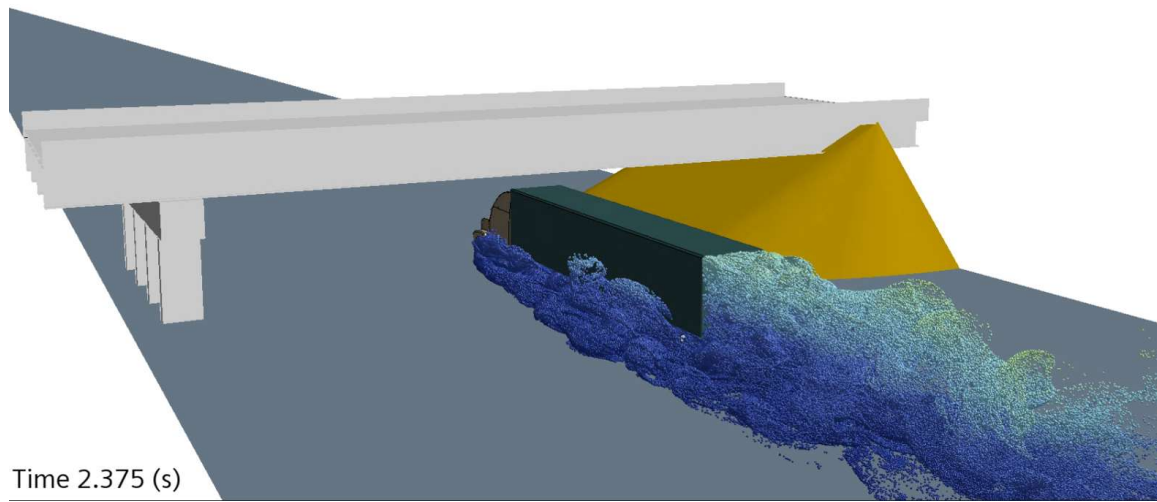
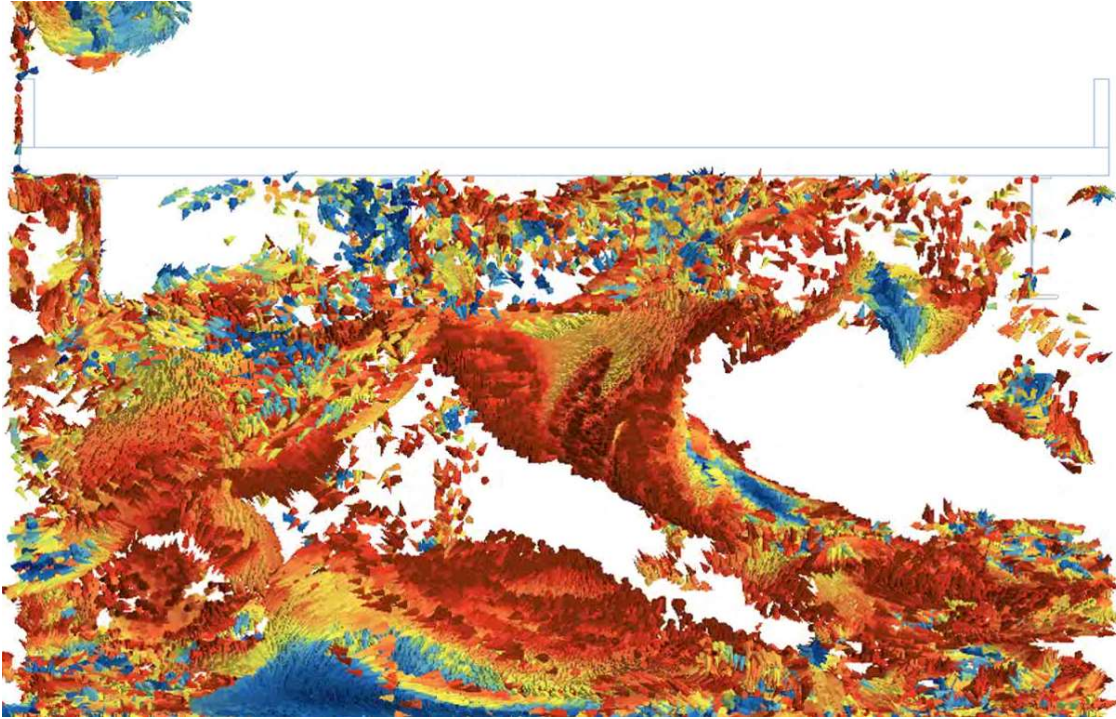


Figure 6-2: Truck transit under bridge showing droplet transport in wake colored by droplet elevation.

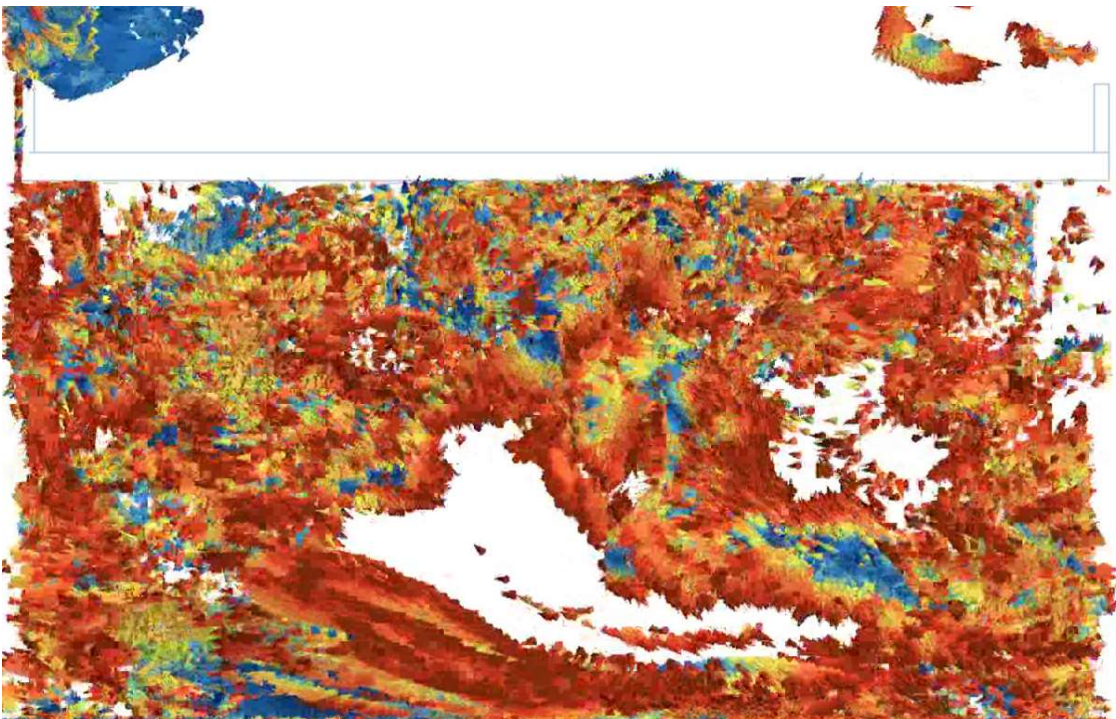
Droplet motion between and interaction with bridge girders is shown for four different times in Figure 6-3 and Figure 6-4. In Figure 6-3 the droplets are rendered with cone glyphs that point in the direction of droplet motion. The cones are colored with the magnitude of the droplet velocity. The droplet motion at the instants of time shown is chaotic but swirls are visible with brighter colored circular paths surrounding empty or darker colored cores. If the truck were moving slow enough to have a laminar flow in the wake, the flat surface of the top of the trailer would induce a cavity flow circulating in the direction of truck motion on the open side of the cavity space between girders. The chaotic motion of turbulent eddies breaks up the simple motion of circulating cavity flow for the most part and depending on the time of a snapshot and position of eddies from the truck, the air rotation in the cavities between girders may even be counter to what would be expected from the direction of motion of the truck. If droplets have a trajectory toward a girder surface and their velocity is fast enough, then even though the air always turns to follow the boundaries of the confinement, the inertia of some of the droplets may be too great and they may fail to turn, and in that case, they collide with one of the girder surfaces. The software keeps track of the number of droplet packets that hit girders and the droplet mass that accumulates on girder surfaces through collisions. It also keeps track of droplet packets that settle onto the horizontal surfaces of girder flanges through the action of gravity.

Figure 6-4 shows droplets rising up between girders just after the truck passes under the bridge. The grey top end of the truck trailer is still visible in the frame on the upper right. The flow between girders induced by the flat surface of the top of the trailer is strongest during and just after the truck passes. In this time period, an eddy full of droplets can be seen rising up into the space between girders 2 and 3 in the center of the bridge width. The arrows show the direction of the induced flow. Following the development of the droplet flow in this space, droplets are seen to be turned and flow up the girder on the left side of the cavity, then across the bottom of the bridge deck, and finally just reaching the girder on the right where they either collide or are turned down toward the flange. Note that for droplets on the right side of the cavity the momentum of droplets will be down toward the flange and this momentum is augmented by gravity force also pulling droplets down toward the trailing flange. This combination appears to make it more likely for droplets to deposit on the trailing flange when a cavity flow between girders satisfies these conditions.

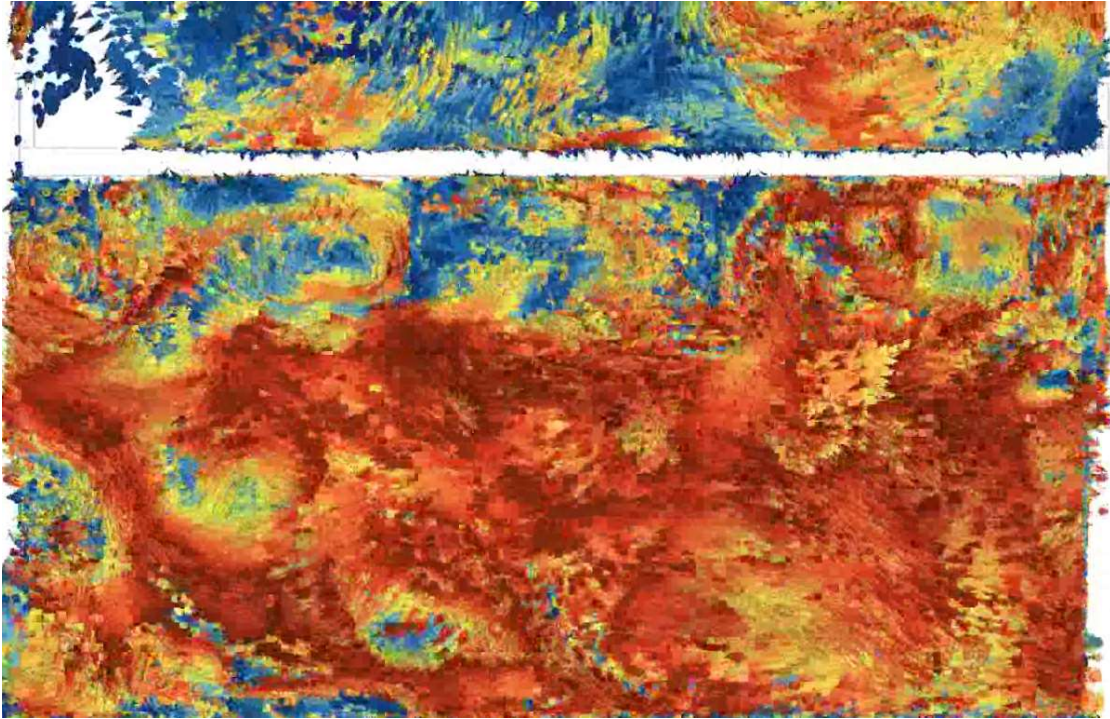
Figure 6-5 provides a visualization of the droplet distribution pattern on the girders with views from front and back with respect to the travel direction of the truck, which is indicated with an arrow in the figure. The pattern on the webs appears to have a concentration over the top of the truck path but the pattern still appears to be fairly random, which is expected because the motion of the eddies carrying the droplets is very chaotic. The bottom flanges, especially the trailing flanges, appear to have a very high accumulation of droplets.



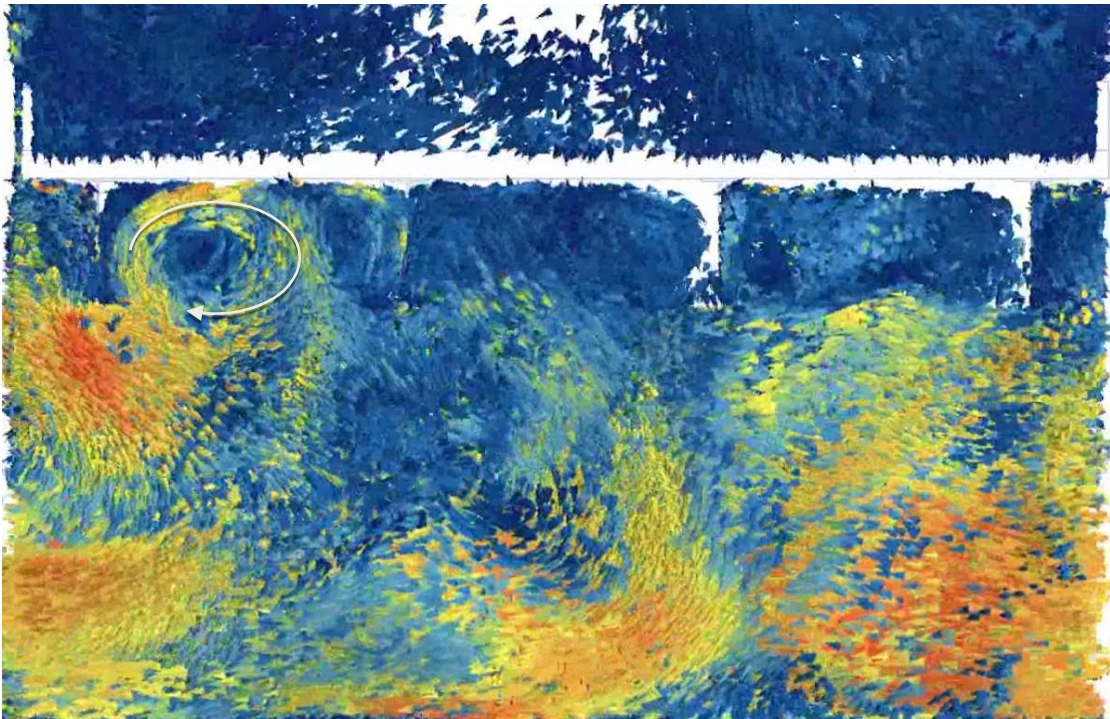
(a) Start of cavities between girders filling with droplets



(b) Continued filling of cavities between girders filling with droplets



(c) near peak of droplet velocity with truck passage,



(d) droplets slowing down after truck passage

Figure 6-3: Droplet flow between and under girders and over bridge deck at increasing times with cone glyphs showing velocity direction, colored with velocity magnitude.

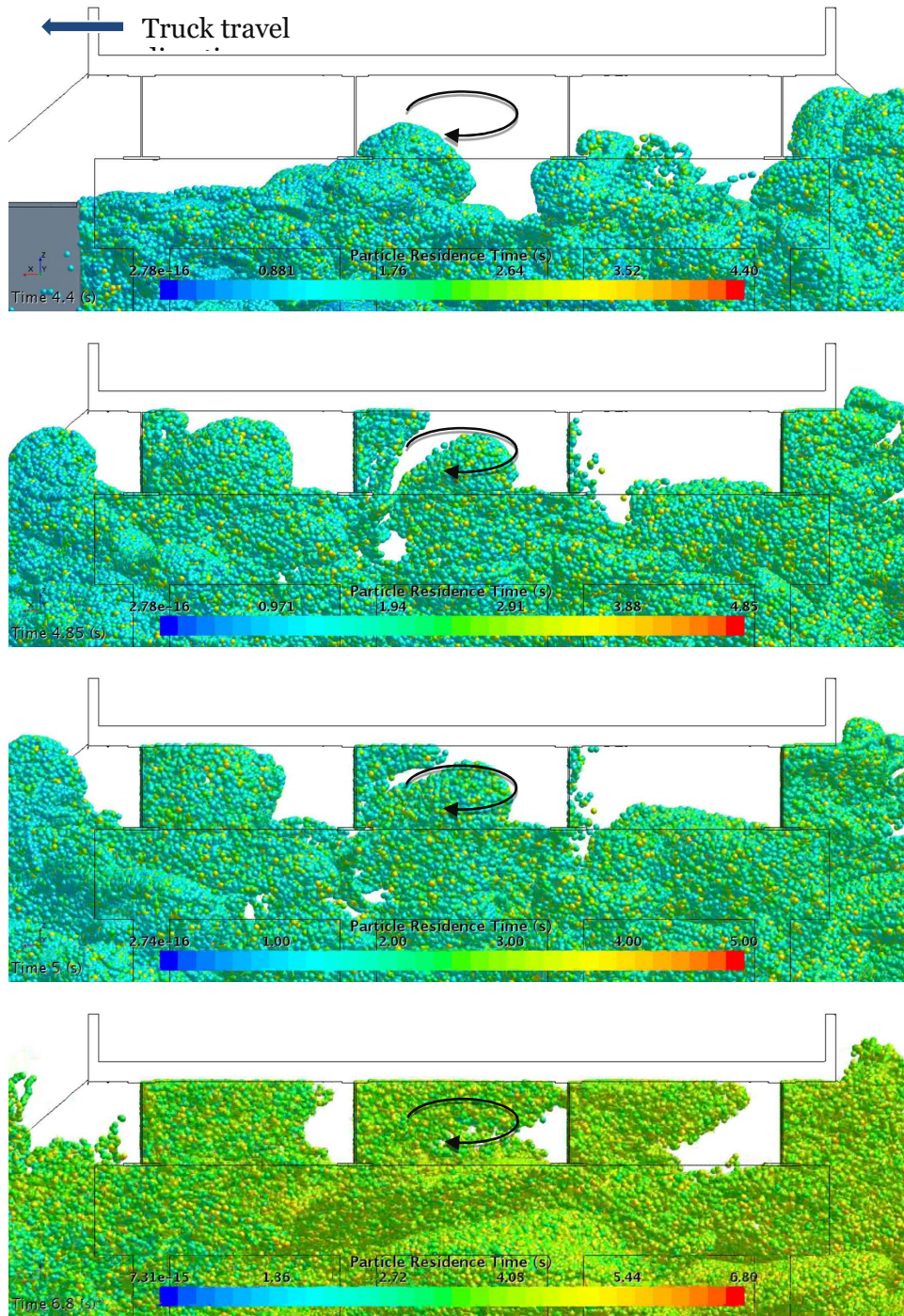


Figure 6-4: Droplets carried by eddies into space between girders for first seven seconds after truck passage. The truck motion is right to left; upper part of trailer is grey box in upper left frame. Arrows show droplets initially following a clockwise induced cavity flow motion in the space between girders.

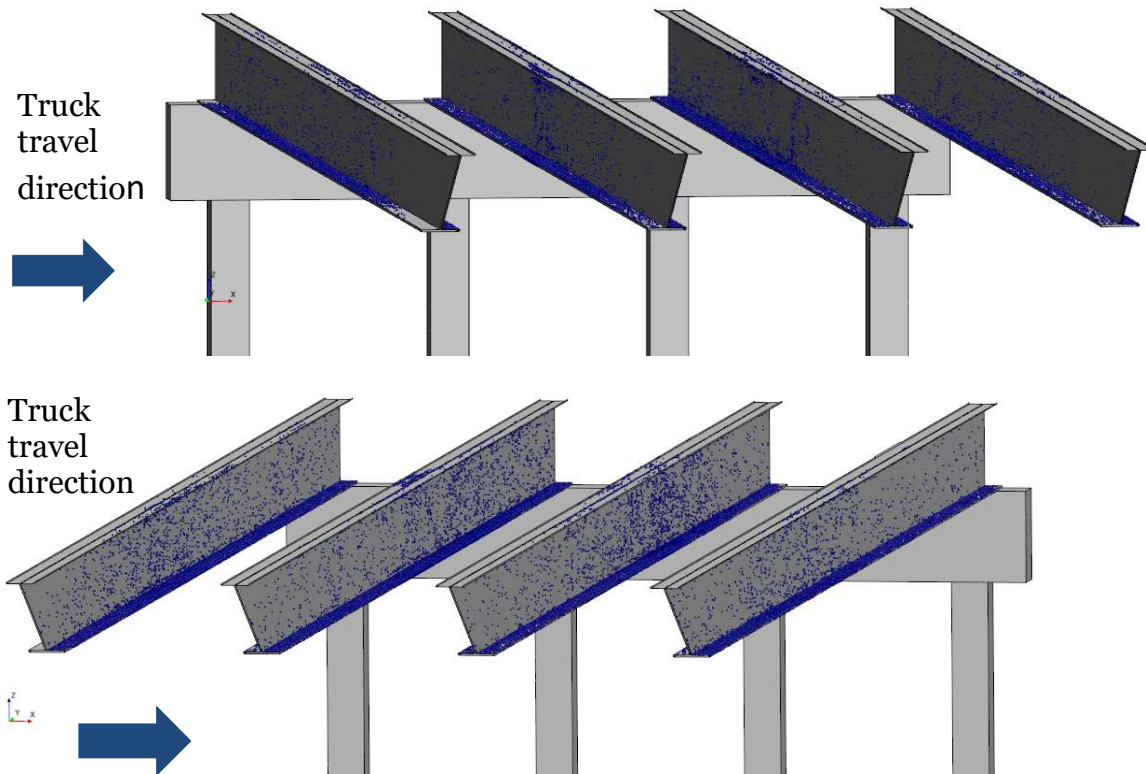


Figure 6-5: Visualization accumulated droplet distribution on the girders showing the leading side on top, and trailing side on bottom. Droplets size is scaled up to make them visible.

Figure 6-6 shows the amount of droplet accumulation on the leading and trailing sides of the girders in a bar graph. The leading side is the side that faces the approaching truck. Droplet accumulation is the greatest on the trailing side of the girders in all cases, and the difference is the greatest on the first couple of girders that the truck passes beneath. The 2<sup>nd</sup> girder in the base case is the one with the most accumulation and it has the greatest difference between leading and trailing sides. Figure 6-7 shows the percentages of droplet deposition on the bottom flange and the rest of the surfaces, the web and upper flange, again separated by leading and trailing sides. This graph shows that between 80 and 90 percent of the droplet deposition is on the bottom flanges. Combining information from Figure 6-6 showing largest accumulation on the trailing side of the girders, by more than a factor of two on girders G1, G2, and G4, and the large percentage accumulating on the lower flange, leads to the conclusion that the largest accumulation of droplets is on the trailing bottom flanges. Considering the induced cavity flow in the bottom right frame of Figure 6-4, the cavity flow direction next to the trailing web is down toward the bottom flange and considering that flow momentum is combined with the acceleration of gravity also pulling droplets in the flow down toward the bottom trailing flange, the heavy droplet accumulation on the trailing bottom flange makes sense. Those two conditions do not occur for the leading flange where the cavity flow is up and away from the flange or for the top flanges where gravity force opposes droplet travel into the upper flange. Having both flow and gravity favor droplet deposition on the trailing bottom flange appears to account for the large fraction of accumulation there. Noting that the turbulent eddies in the truck wake are very chaotic and rotating in many directions, other surfaces do experience droplet accumulation, especially the leading bottom flange in cases where eddy motion is carrying droplets toward that flange. Gravity also adds to the

force favoring deposition on the leading bottom flange when compared to the web or upper flanges.

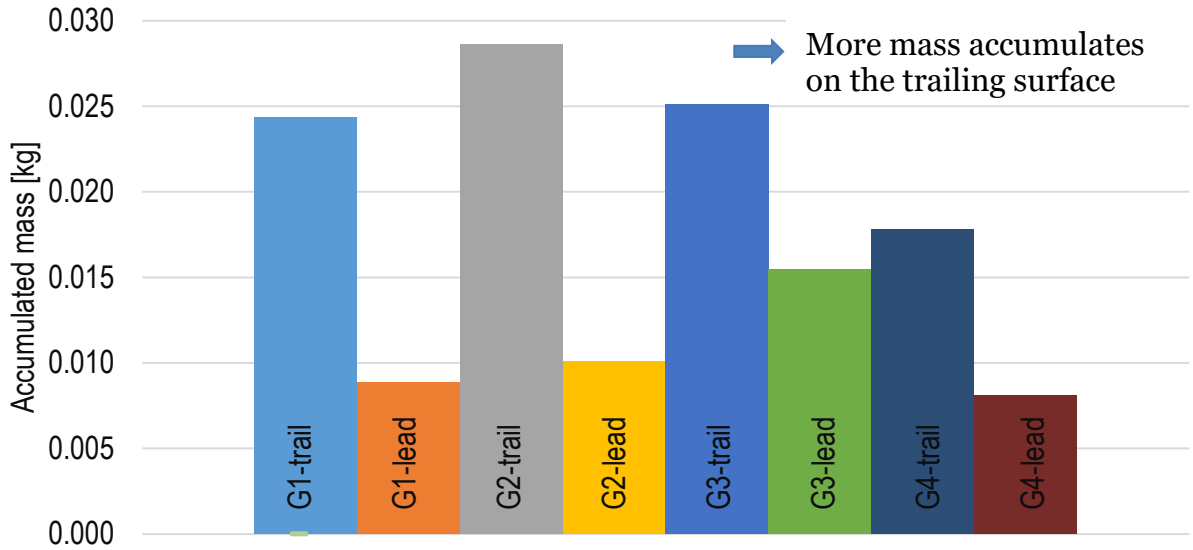
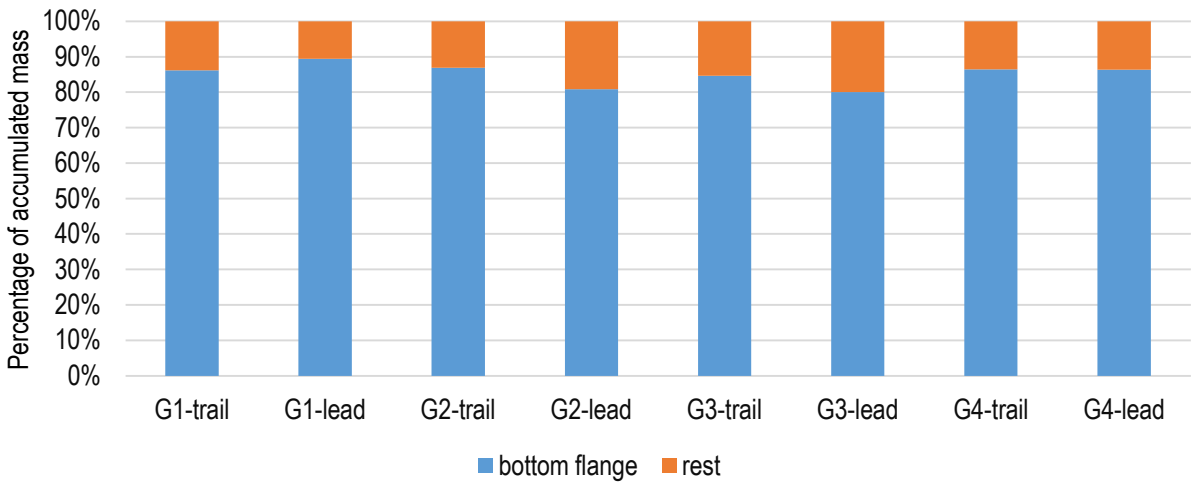


Figure 6-6: Droplet accumulation on leading and trailing sides of girders.



➡ Significantly more saltwater accumulates on the bottom flange.

Figure 6-7: Percentage of droplet accumulation on bottom flange.

## 6.2 Varying Number of Girders with Constant Deck Width

The number of girders was varied from four to seven using the base case geometry. As girders were added, the width of the bridge deck was held constant, the height of the girders remained constant, and spacing between girders was equidistant. Therefore, as girders were added, the distance between them decreased and the total surface area of all girders increased. Figure 6-8 is a schematic showing the girder layout for the ends of the range with the minimum of 4 girders on the left and the maximum of 7 on the right. The variation of the total accumulation of droplet mass on the girders is shown in Figure 6-9. The total accumulation of droplets from the passage of a truck increases with increasing number of girders up to a factor of 1.3 with 6 girders compared to 4, probably due to increasing girder surface area as the number of girders increases from 4 to 6, but then the accumulation decreases back to approximately the deposition with 4 girders when there are 7 girders, which may be due to weaker induced cavity flow between the girders due to the reduced spacing.

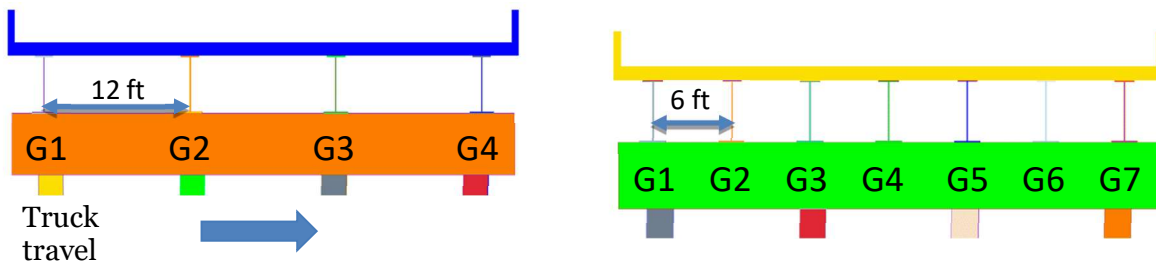


Figure 6-8: Schematic showing varying range of number of girders.

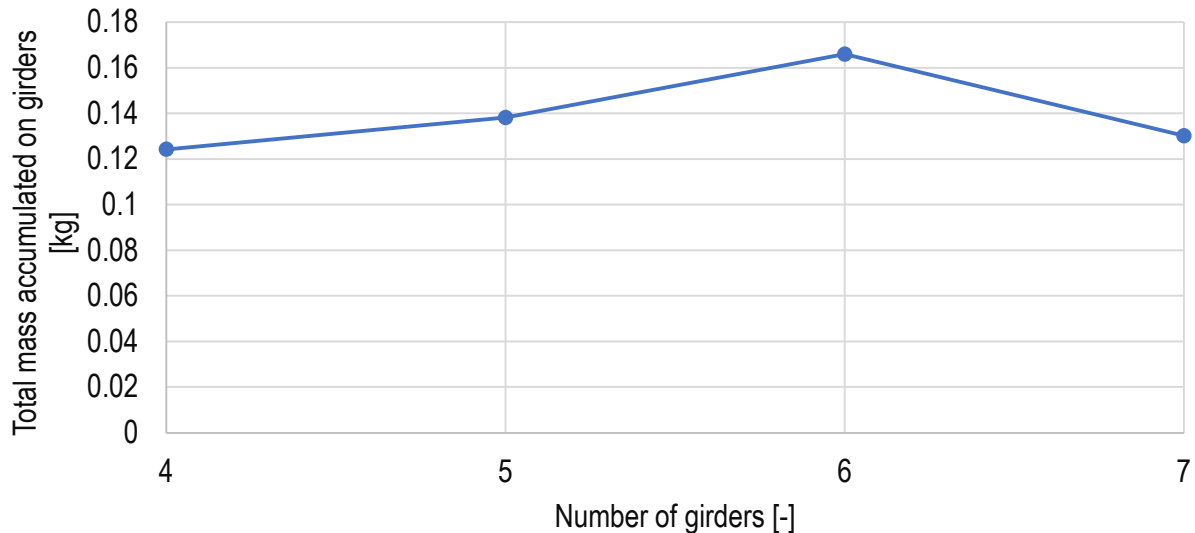


Figure 6-9: Variation of accumulated mass of droplets with number of girders.

Figure 6-10 shows the droplet accumulation on the individual girders for the cases. Highest accumulations tend to be on 2<sup>nd</sup> and 3<sup>rd</sup> girders. Recall that interaction of eddies with girders is somewhat sensitive to truck starting position due to the periodicity of eddies spinning up from

the truck wake. Therefore, some of the variation in accumulation of droplet mass as girders are added may be due to the changes in girder position with respect to the truck starting position.

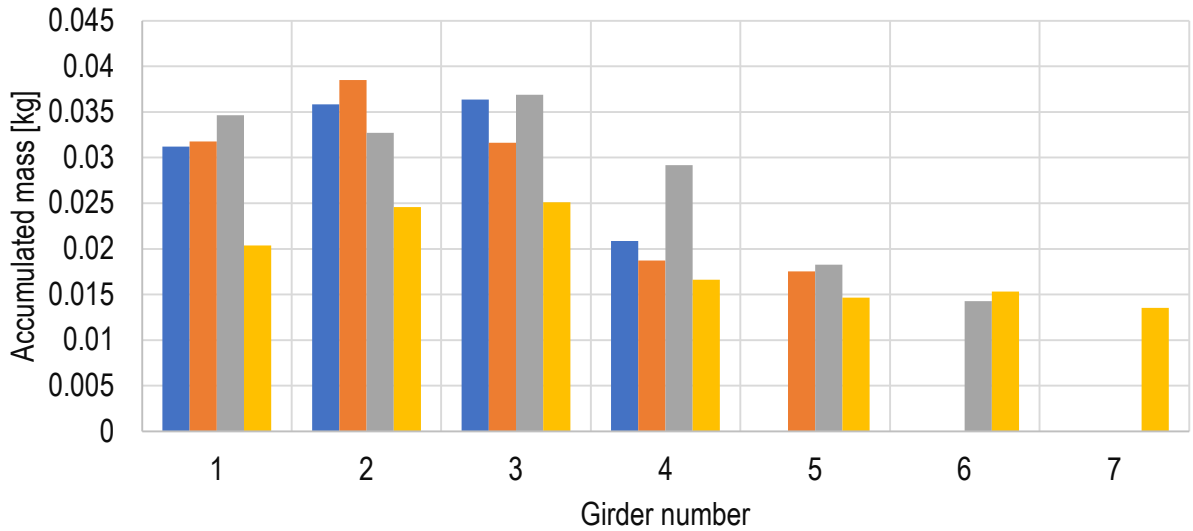
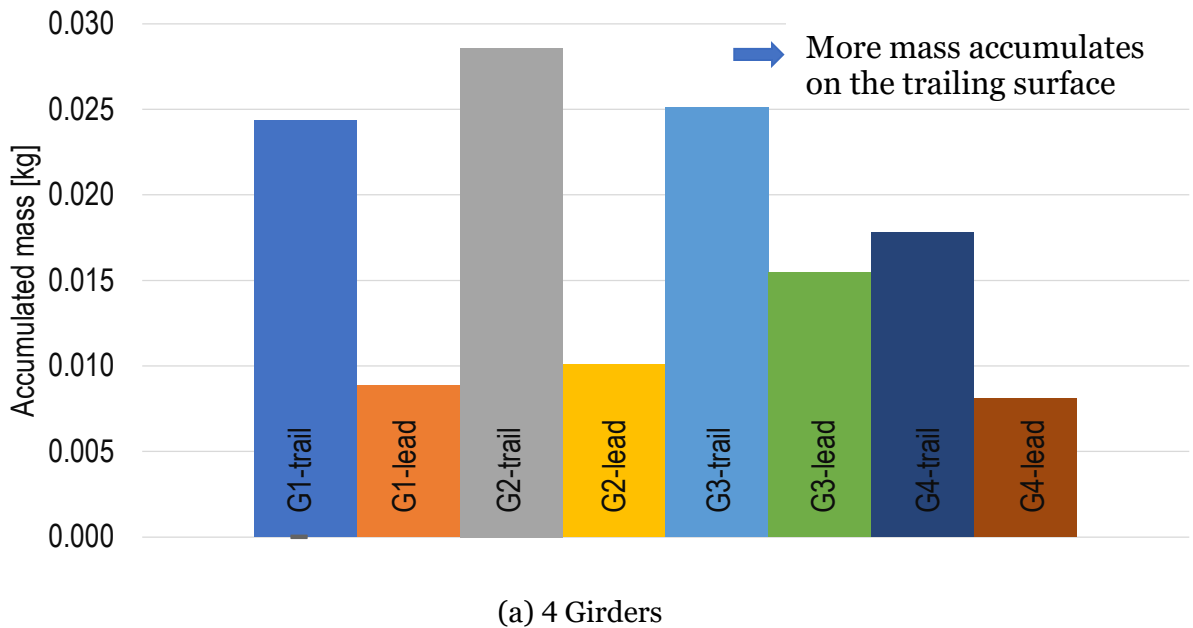
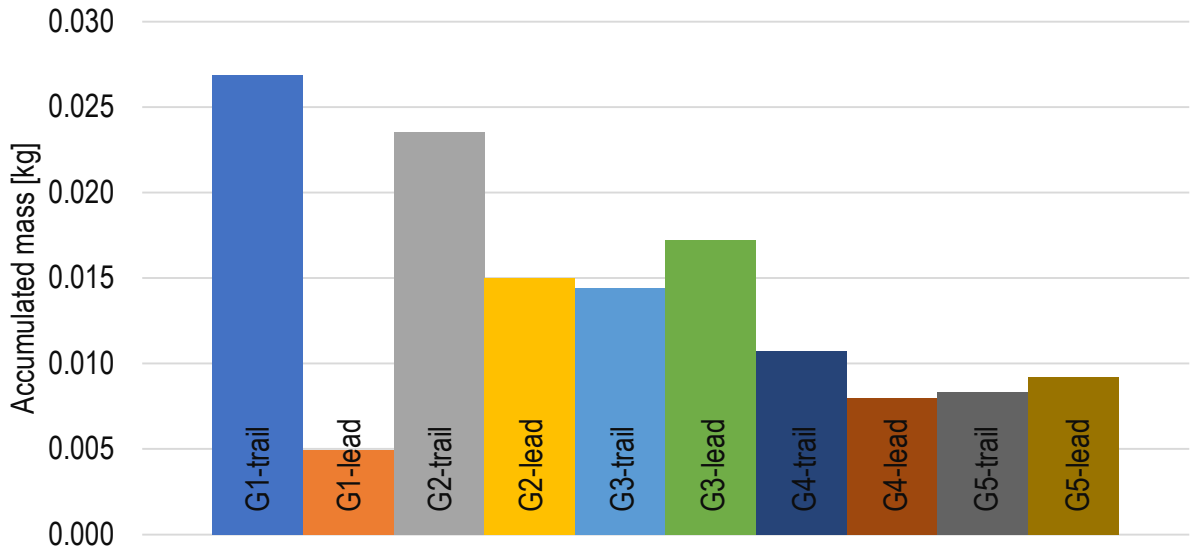


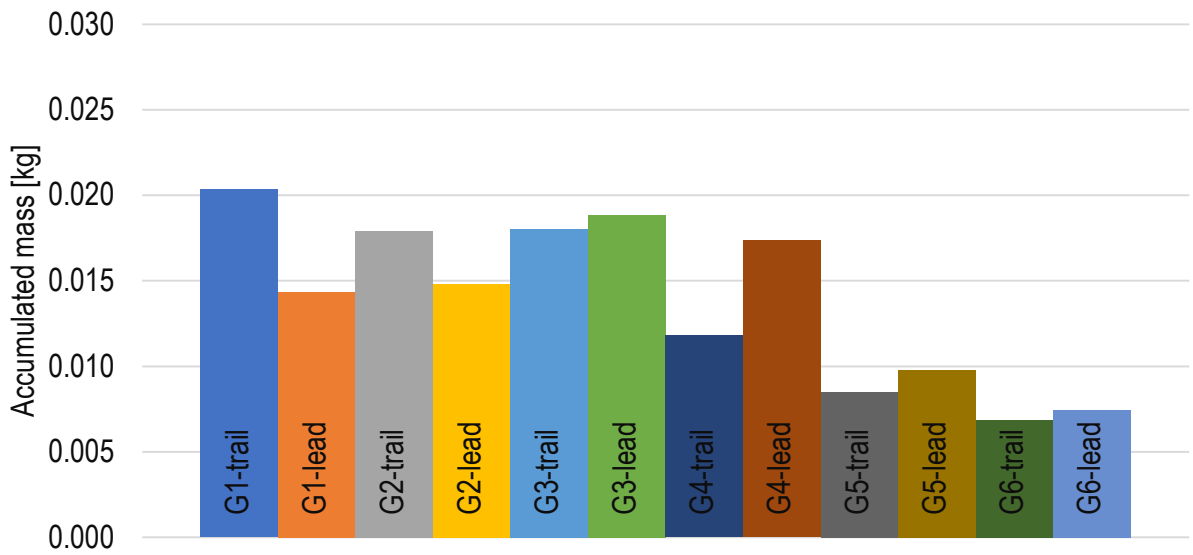
Figure 6-10: Droplet accumulation by girder number for varying number of girders.

Accumulation on the leading and trailing side of girders for the varying number of girders is shown in Figure 6-11. In general, more droplets accumulate on the trailing side of girders due to the induced direction of the cavity flow between girders. Note, however, that the leading side of girder 3 accumulates more than the trailing side when there are 5 and 6 girders, and for cases with 5 through 7 girders, there is more accumulation of droplets on the leading side of the last girder than on the trailing side. For the last girder, there is no cavity on the trailing side.

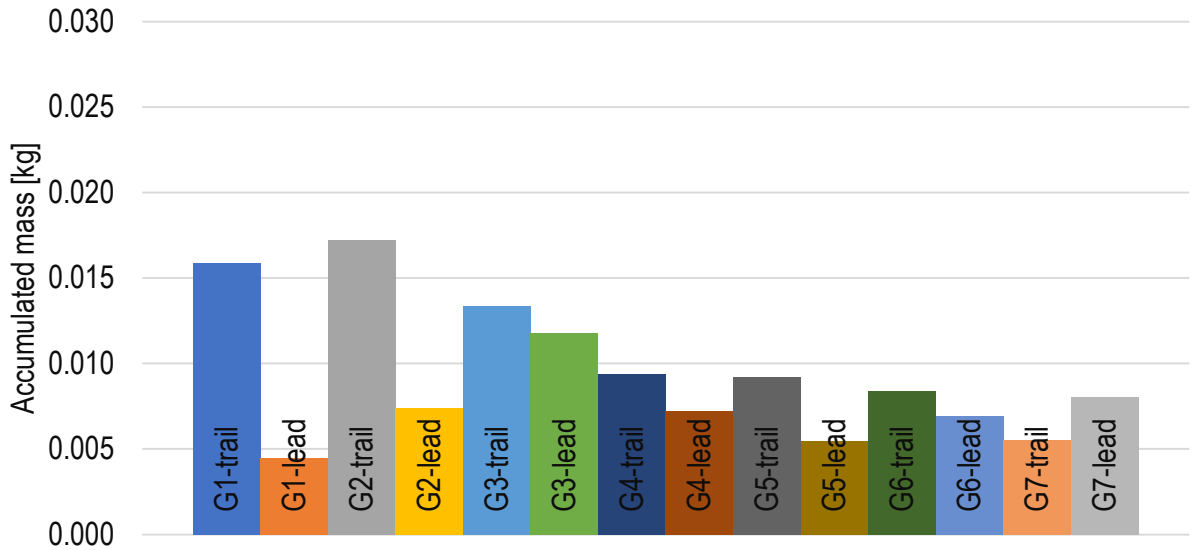




(b) 5 Girders



(c) 6 Girders



(d) 7 Girders

Figure 6-11: Droplet accumulation on leading and trailing sides of girders for varying numbers of girders.

### 6.3 Varying Underclearance

Droplet concentration in the wake of a truck decreases with height above the pavement as shown in Figure 3-6, when the truck is out in the open. That relation indicates that droplet deposition on bridge girders might decrease with increasing underclearance, and if so, risk of excessive corrosion on uncoated weathering steel bridges might be reduced to acceptable levels by increasing the underclearance. Test cases were run with an underclearance height that ranged from 15 ft (4.6 m) to 40 ft (12 m) with a truck trailer that was 14 ft (4.3 m) height as shown in Figure 6-12. An initial set of varied test cases up to 24 ft (7.3 m) of underclearance at 60 mph (97 kph) truck speed did not show a clear pattern between 15 ft (4.6 m) and about 22 ft (6.7 m) of underclearance. Smaller clearances appear to cut off a lot of the large droplet laden eddies in the truck wake, helping to limit deposition. However, the induced cavity flow in the space between girders should be stronger when the clearance between the bottom of the girders and the top of the truck trailer is smaller. Finally, as previously noted, droplet concentration in the truck wake decreases with height, so with sufficiently high underclearance, the droplet deposition on girders should decrease with increasing underclearance. Cases at 30, 35, and 40 ft (9.1, 10.7, and 12.2 m) of underclearance were added to the case matrix to check the downward trend of droplet deposition for clearances higher than 24 feet (7.3 m). The results of all of the 60 mph (97 kph) cases with varied underclearance are plotted in Figure 6-13. Droplet deposition at underclearance greater than 22 ft (6.7 m) does continue to drop with height, however, even at 40 ft (12 m) of underclearance, it has not yet dropped an order of magnitude below the deposition at 20 ft (6 m). Apparently, the large eddies in the truck wake billow up quite high and those eddies are able to transport droplets with them.



Figure 6-12: Plan view of bridge deck

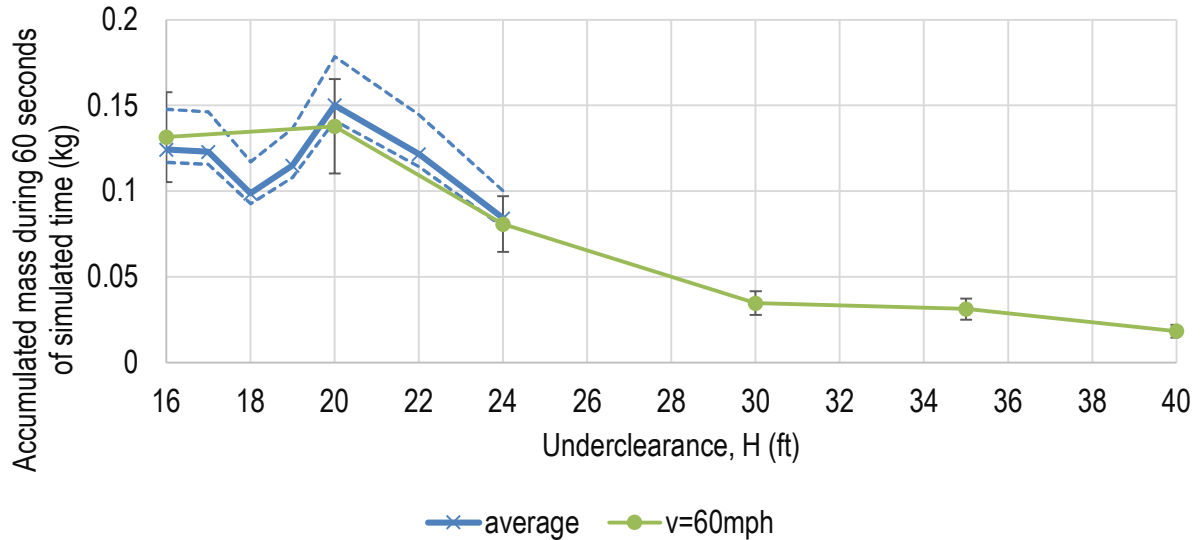
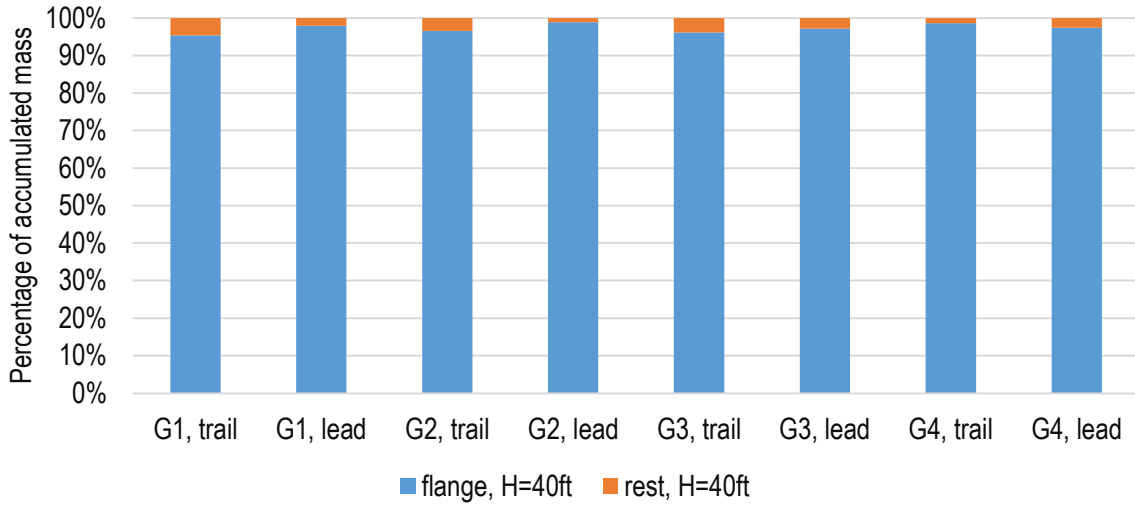
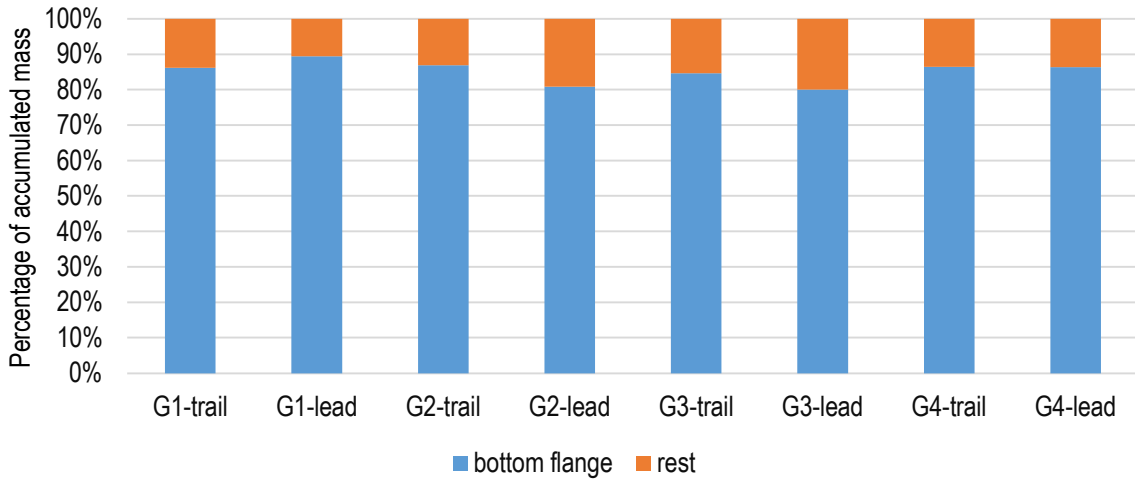


Figure 6-13: Droplet accumulation on girders of base case for underclearance from 15 to 40 ft.

Figure 6-14 compares the percentage of droplet accumulation on the lower flange for two cases, the base case and the extreme case of very large underclearance of 40 ft. In the case of very large underclearance, the percentage of droplet accumulation on the lower flange is much greater than in the 16 ft underclearance base case. As the distance between girders and truck increases, the induced strength of the cavity flow between girders decreases and the droplet velocities decrease between the girders. As a consequence, a larger fraction of the droplet accumulation that does occur happens through settling of droplets on the lower flange instead of droplet collision with the web or upper flange.



(a) Percentage of droplet mass on lower flange for 60 mph truck with 40 ft underclearance



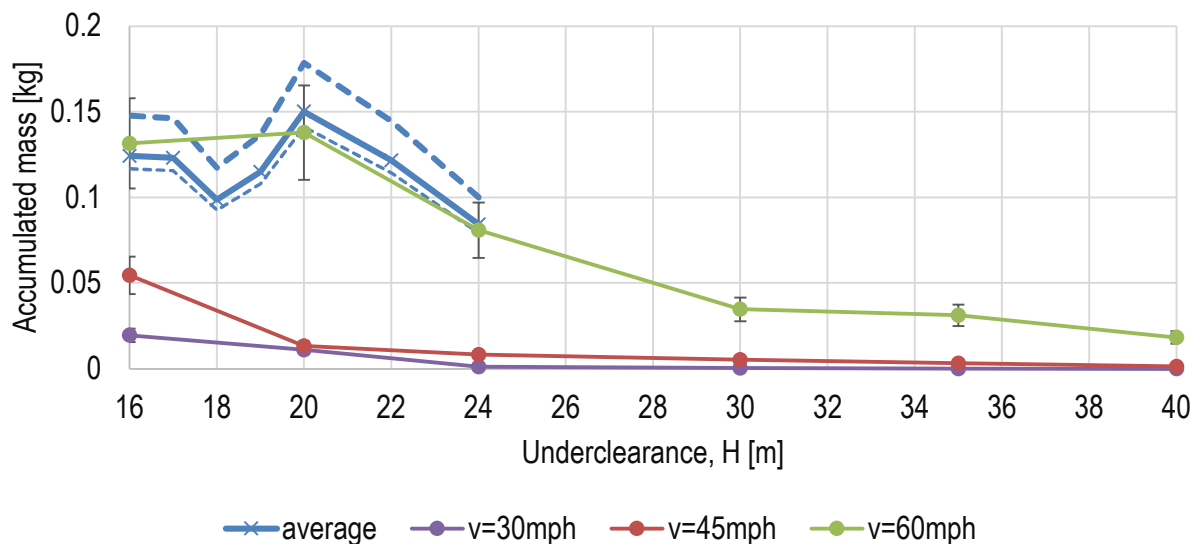
(b) Percentage of droplet mass on lower flange for 60 mph truck with 16 ft underclearance

Figure 6-14: Percentage of droplet accumulation on lower flange for base case underclearance and large underclearance of 40 ft.

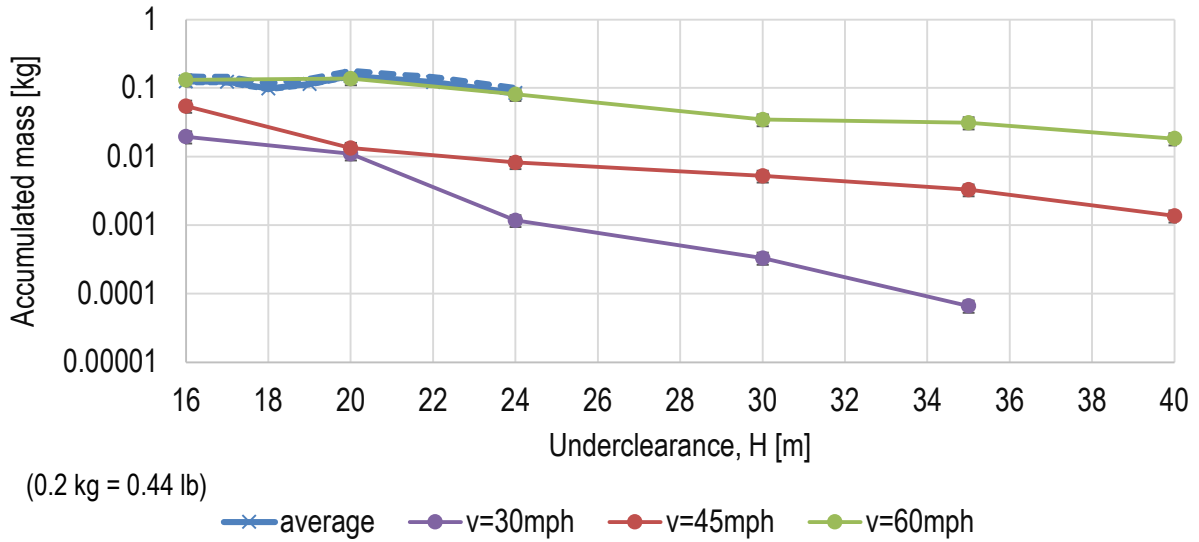
## 6.4 Varying Truck Speed

The combined effects of truck speed and underclearance were investigated. Cases at underclearances up to 40 ft (12 m) were run for trucks moving with the lower speeds of 30 and 45 mph (48 and 72 kph). The drag force on the truck is proportional to the square of the truck speed, and the energy required to overcome drag is drag force times distance. Much of the energy going into overcoming drag on the truck ends up in the wake momentum and turbulent eddies of the truck wake, which is consequently proportional to the velocity squared. At lower truck speeds, the energy in wake momentum and eddies transporting droplets from tires drops off dramatically, and as a result, droplet deposition on girders also drops off dramatically. At 45 mph (72 kph) and 16 ft (4.9 m) of underclearance, deposition is less than half that at 60 mph (97 kph) and 16 ft (4.9 m) underclearance. At 30 mph (48 kph), deposition drops to less than 1/6 of the amount at 60 mph at 16 ft (4.9 m) of underclearance. Droplet deposition also decreases monotonically and nearly exponentially with increasing underclearance height as shown in Figure 6-15 in the lower pane with the log scale on the vertical axis.

Droplet accumulation on girders as a function of truck speed is plotted in Figure 6-16 for underclearance heights from 16 to 30 ft (5.3 to 9.1 m). The plots show clearly that the increase in deposition of droplets on girders with truck speed is rapid and nonlinear. The interaction of eddies carrying droplets with girders is complex and chaotic and therefore, any single test point may vary a fair amount from a smooth relation. For example, the points at 20 and 24 ft (6 and 7.3 m) underclearance appear low at 45 mph (72 kph), but then rebound at 60 mph. Because truck drag is proportional to truck speed squared, droplet deposition may be close to a quadratic function of truck speed.



(a) Droplet accumulation on girders as a function of underclearance for various truck speeds shown with linear scale on vertical axis.



(b) Droplet accumulation on girders as a function of underclearance for various truck speeds shown with log scale on vertical axis

Figure 6-15: Droplet accumulation on girders of base case for truck speeds of 30, 45, and 60 mph and underclearance in the range of 15 to 40 ft.

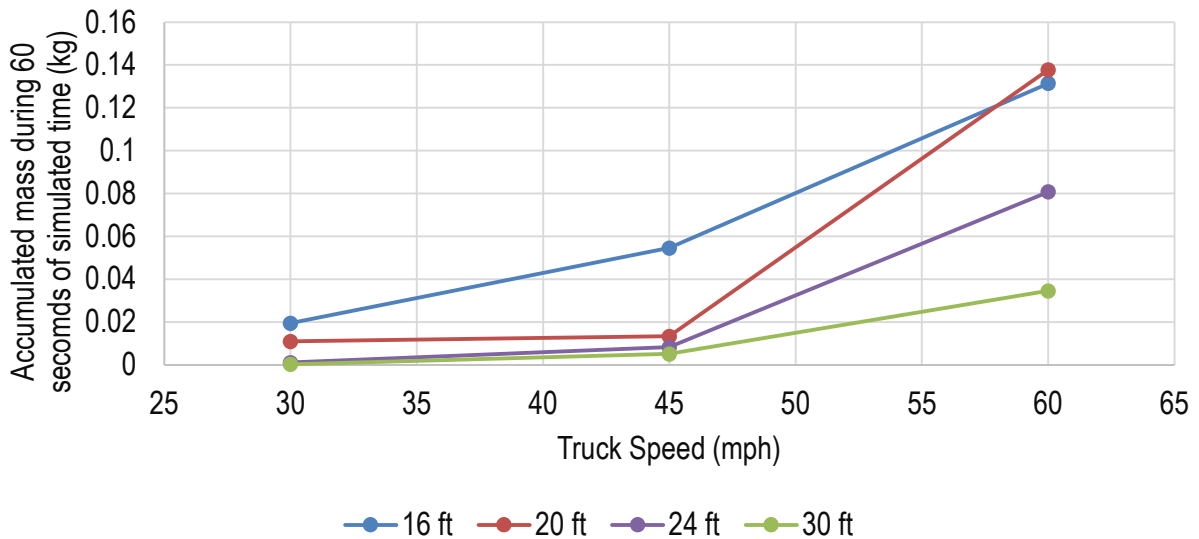


Figure 6-16: Droplet accumulation of girders as a function of truck speed for various underclearances from 16 ft to 30 ft.

Figure 6-17 compares the percentage of girder droplet deposition on the lower flange for three truck speeds of 30, 45, and 60 mph. As the truck speed decreases, the speed of droplets in the eddies also decreases and the strength of cavity flow induced by the top of the trailer passing the bottom of girder cavities also decreases. Lower droplet speeds and weaker cavity circular flow between the girders leads to a greater percentage of droplets that make it up to girder height

settling out on to the lower flange under the influence of gravity as opposed to colliding with and adhering to the web and upper flange.

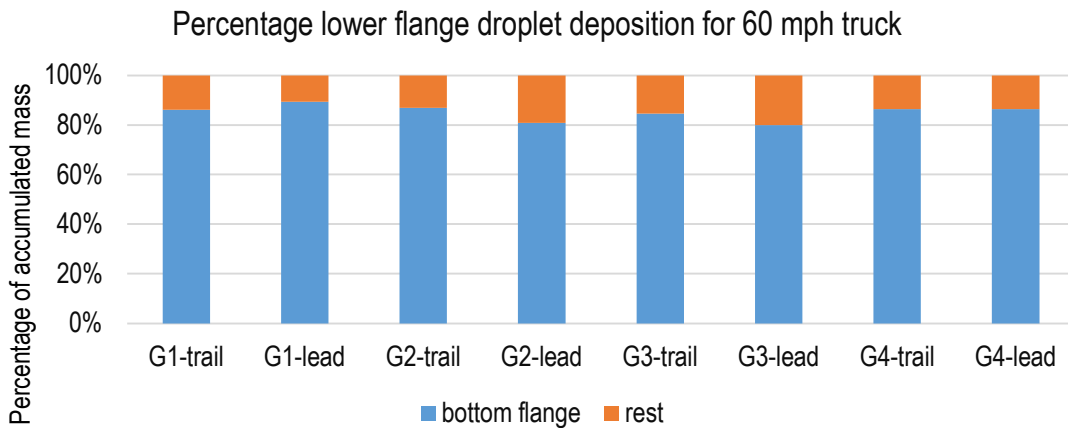
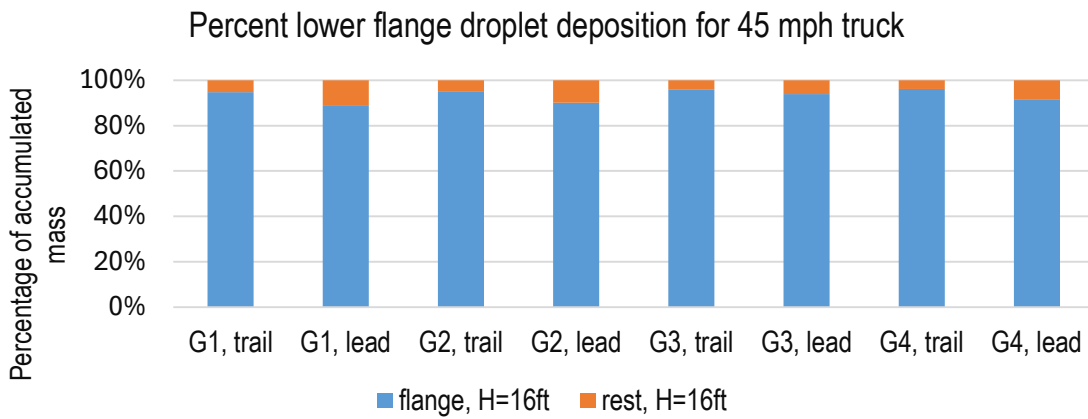
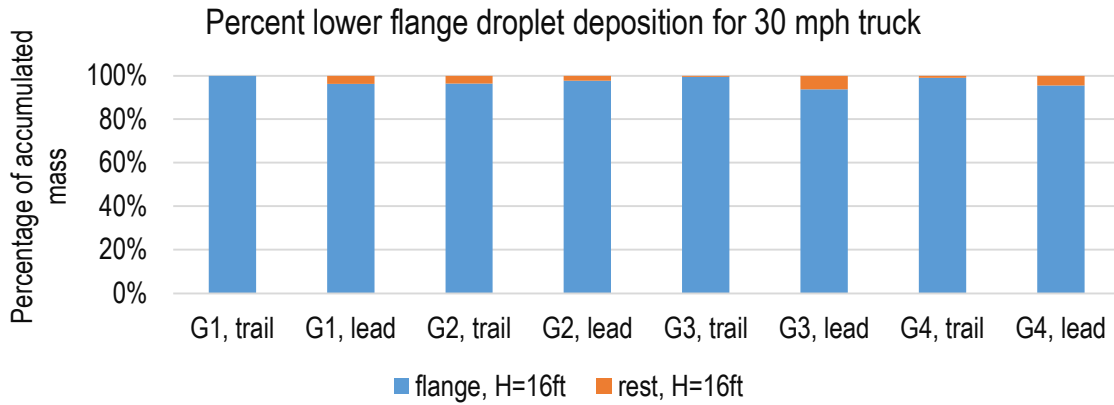


Figure 6-17: Percentage lower flange droplet deposition for various truck speeds of 30, 45, and 60 mph.

## 6.5 Varying Height of Girders

One case with a smaller girder height of 30 inches (76 cm) was run, compared to the girder height in base case of 54 inches (137 cm). All of the other geometry dimensions remained the same as in the base case, and the case was not expected to correspond to a realistic geometry or to be structurally sound, but rather it was created to test the effect of varying the girder height parameter by itself. Only the web height was changed; the flange dimensions remained the same. Figure 6-18 shows a schematic of the girder height geometry difference between the two cases. Figure 6-19 shows that reducing the girder height from 54 inches to 30 inches resulted in a decrease in droplet accumulation on the girders of approximately 57%. In other terms, when the girder height is reduced by a factor of 1.8 by reducing just the web height, the deposition was reduced by a factor of 2.4. Reducing the web height reduces the volume of droplets circulating in the space between girders and would account for most of the reduction in deposition. The reduction in deposition exceeds the reduction in volume, however, and the additional reduction in deposition is likely due to reduced strength of circulation in the smaller space.

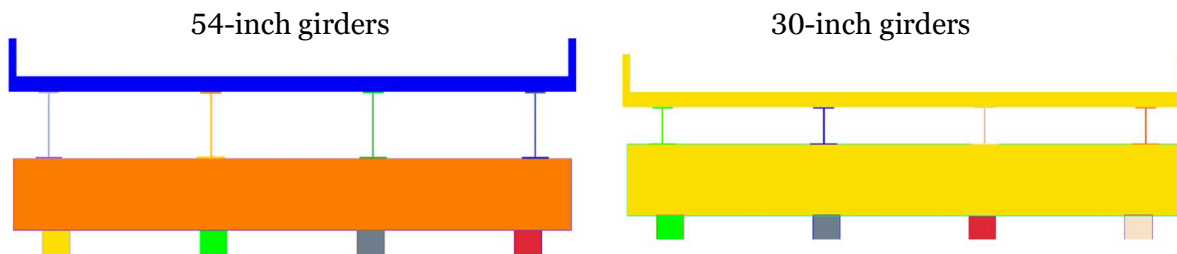


Figure 6-18: Schematic for test of smaller girder height.

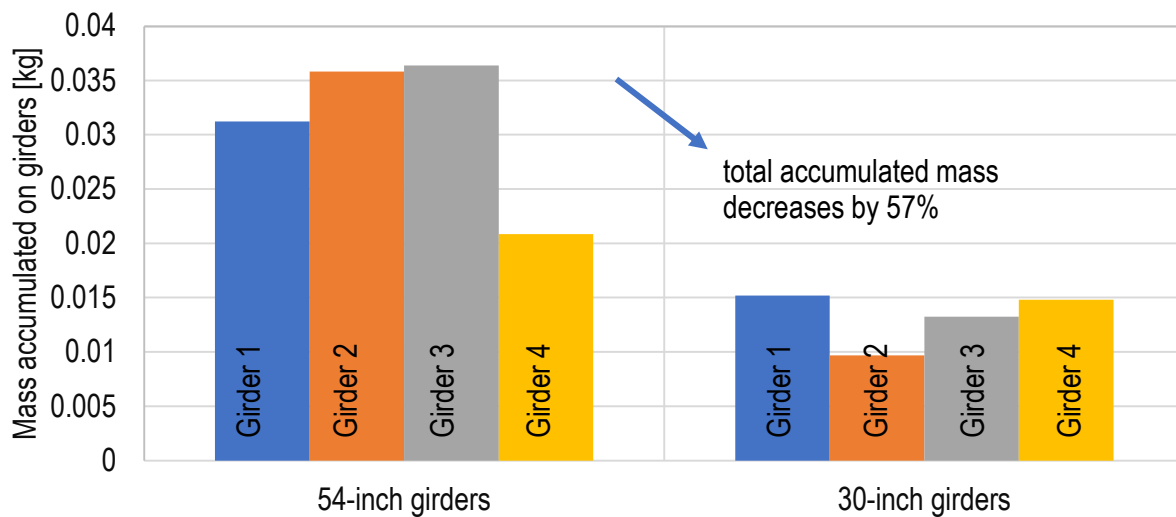


Figure 6-19: Droplet accumulation for 54-inch and 30-inch girder heights.

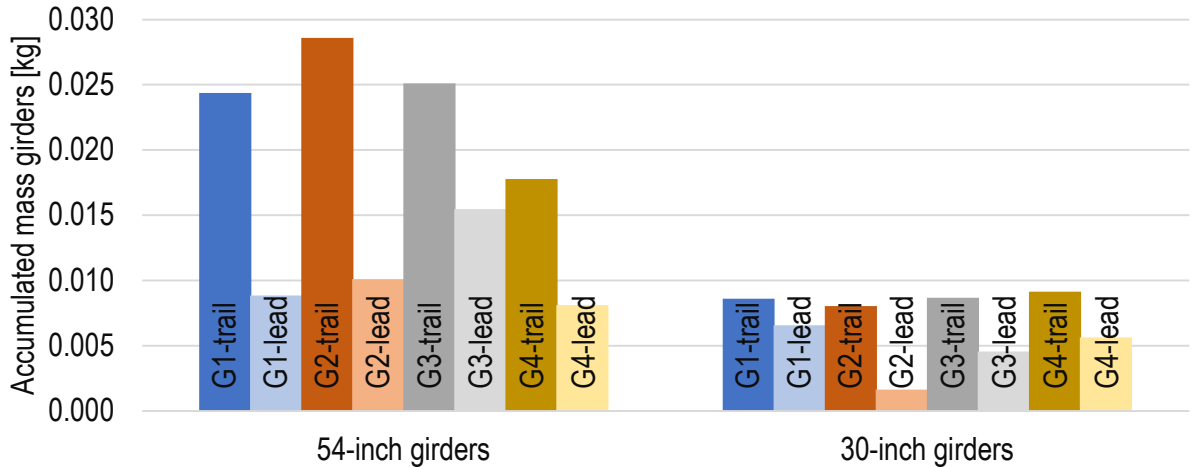


Figure 6-20: Droplet accumulation on leading vs trailing sides of girders.

### 6.6 Varying Width of Overhang

The base case had 3 ft (0.9 m) of bridge deck overhang beyond the leading side of the 1<sup>st</sup> girder and the trailing side of the last girder. To test the sensitivity of droplet accumulation to the amount of overhang, a case with 5 ft (1.5 m) of overhang, an extra 2 ft (0.6 m) on each side, was tested. A schematic of the two deck overhangs is shown in Figure 6-21.

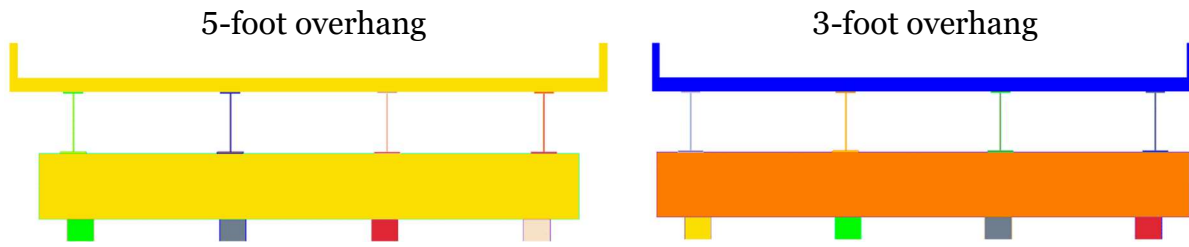


Figure 6-21: Schematic of 2 tested bridge deck overhangs.

Figure 6-22 shows the per girder accumulation of droplets for both the 5-foot and 3-foot overhang cases side by side for comparison. The increased overhang does reduce the total accumulation of droplets by about 20 percent, and this reduction affects all girders, not just the end girders that are below the overhang. This result indicates that the increased overhang reduces the total amount of droplet carrying eddies that are pulled under the bridge within the wake by the moving truck, which reduces deposition on each girder, as opposed to just shielding the outward facing surfaces of the end girders. There is also an effect on the girders at the ends, G1 and G4, and a shift between leading and trailing side deposition, as shown in Figure 6-23. For girder G1, on the side of the bridge facing the oncoming truck, the leading side has more deposition for the 5-foot overhang compared to the 3-foot overhang. The trailing side of G1, however, has more deposition on the 3-foot compared to the 5-foot overhang, resulting in the total deposition on G1 being greater in the 3-foot overhang case. Summing the deposition on the lower flanges yields 87% of 0.1 kg (0.22 lb) or 0.087 kg deposited on lower flanges for the 5-foot overhang compared to 85% of 0.12 kg (0.26 lb) or 0.105 kg that deposited on lower flanges for the 3-foot overhang.

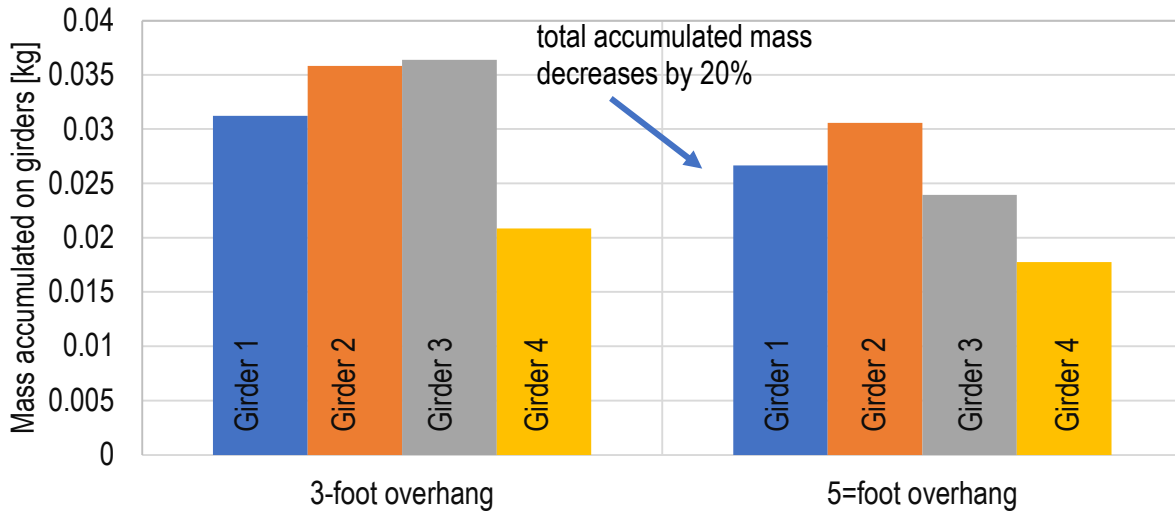


Figure 6-22: Droplet accumulation on girders for two deck overhangs.

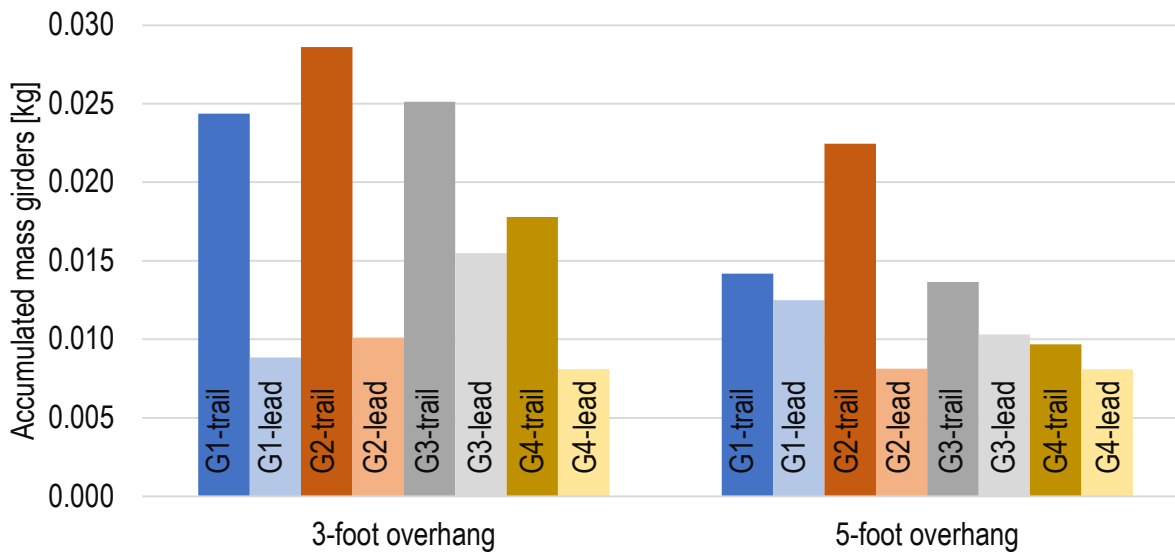


Figure 6-23: Droplet accumulation on girders showing leading and trailing side amounts.

## 6.7 Vertical Abutment versus Sloped Embankment

The presence of vertical abutment walls close to the roadway for a grade separated bridge configuration compared to a bridge with abutments with sloped embankments was thought to be a configuration that might have higher droplet deposition during snow and road salting events, see Figure 1-1 and Figure 1-2. To test this proposition, a geometry with a vertical wall abutment was built as shown in Figure 6-24. A significant difference in these two geometries is an additional triangular cross-section space in the sloped embankment case for the droplet laden truck wake to enter under the bridge and additional girder length where the girders extend over the embankment.

As shown in the upper frame of Figure 6-25, the additional space in the wedge over the embankment and the additional girder length over the embankment result in a greater total droplet accumulation on the girders for the sloped embankment case. Note however, that the additional space present over the sloped embankment also provides more space for the droplets in the eddies carried under the bridge to spread out. The extra frontal area for the droplets in the wake to enter under the bridge and the additional space for the droplets in the wake to spread out are competing effects. Apparently, the additional spreading has more impact on the concentration of the droplet deposition than the additional frontal area allowing more of the wake to enter under the bridge. The droplet deposition per unit length of girder is less for the sloped abutment than for the vertical abutment wall starting at about 22 seconds into a truck passage event. At 130 seconds into the event, deposition on girders for the sloped abutment is less by a factor of 0.82. This result does indicate that if corrosion risk is a function of droplet concentration, then the vertical wall is somewhat worse than the sloped embankment by around 20 percent.

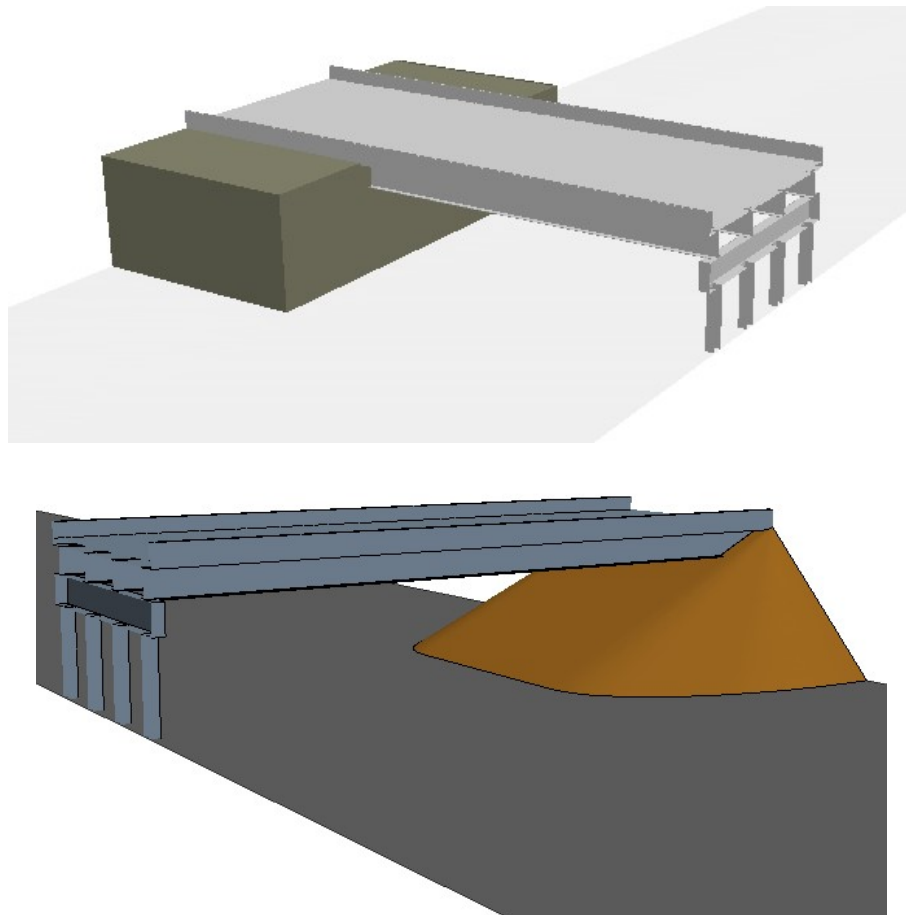
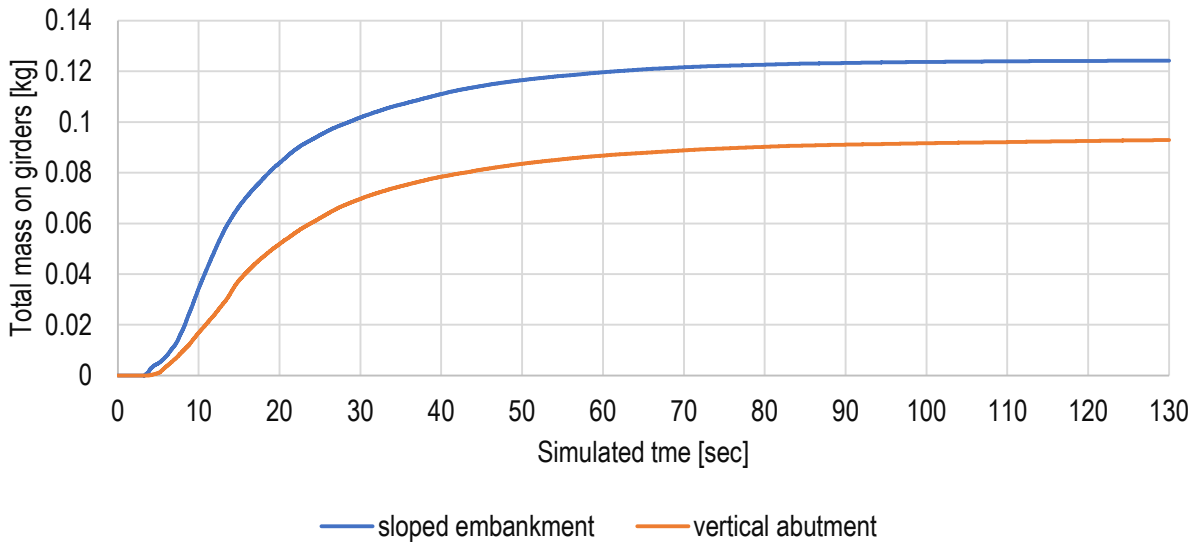
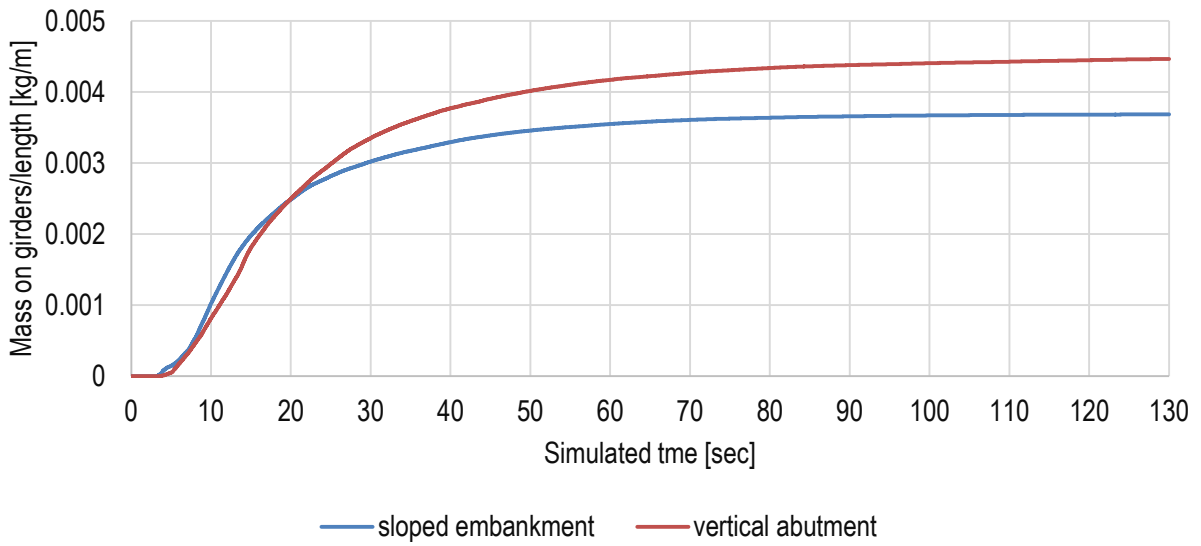


Figure 6-24: Vertical wall abutment (top) versus sloped embankment (bottom).



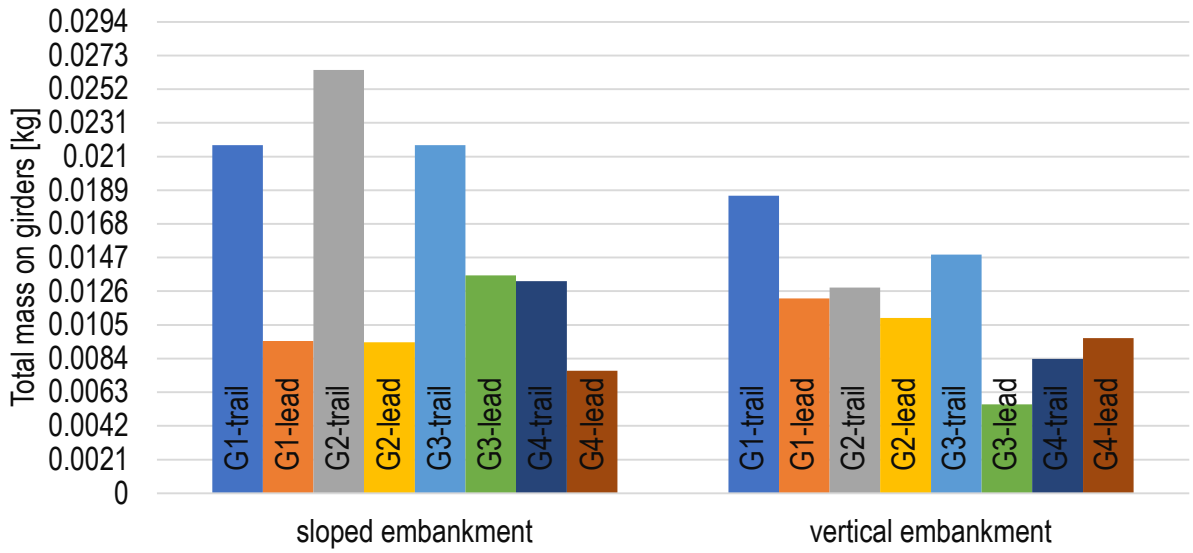
(a) Evolution of total droplet mass deposited on girders



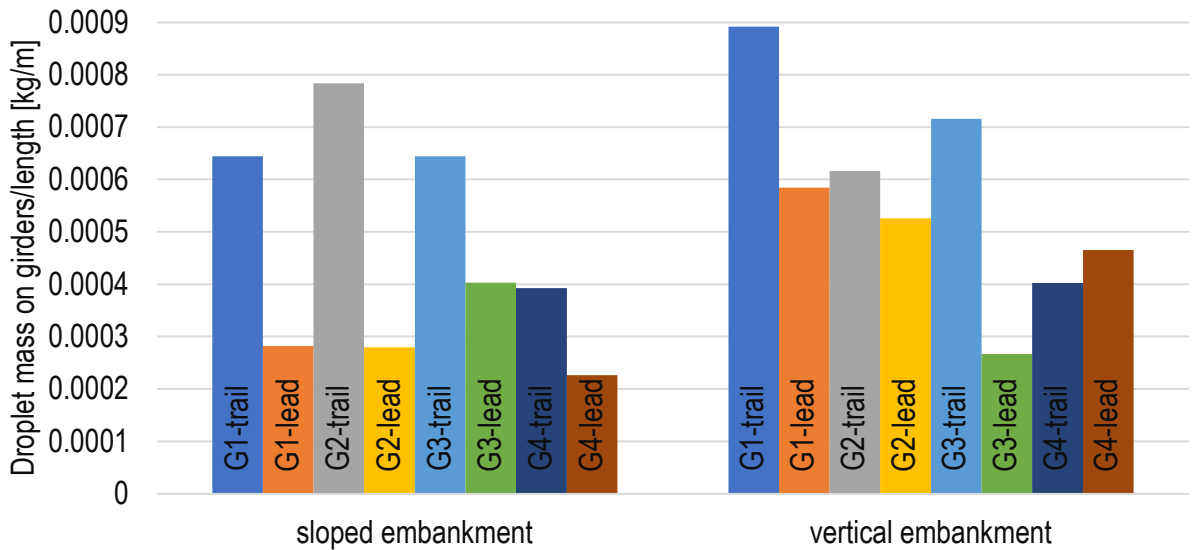
(b) Evolution of droplet mass per unit length deposited on girders

Figure 6-25: Droplet accumulation for vertical wall abutment vs sloped embankment.

Droplet accumulation on each girder separated into leading and trailing sides is shown in Figure 6-26, with side-by-side comparison of vertical wall and sloped embankment. These results indicate that the flow pattern in the vertical wall case changes enough to reduce the difference between droplet accumulation on the leading and trailing sides of the girders of the lead girders.



(a) Total droplet mass deposited on girders



(b) Droplet mass per unit length deposited on girders

Figure 6-26: Droplet accumulation on leading and trailing sides of girders compared for sloped embankment and vertical abutment.

## 6.8 Varying Wind Speed at Zero Angle of Attack

The droplets in the truck wake are small enough that they react very quickly to changes in the speed and direction of the surrounding air. The larger droplets shed from tires that have enough inertia, so they are not so easily turned, primarily collide with surfaces in the wheel well or trailer undercarriage, and they never make it into the wake, as noted previously. Consequently, droplets in the wake tend to stay within the turbulent eddies of the wake and travel with them. The effect of wind on droplet transport is of interest because even low velocity wind around 2 mph (3 kph) is sufficient to quickly change the direction of droplet travel. The situation is complex because the impact of wind on droplet transport in the truck wake ultimately depends on the impact of wind on the turbulent eddies that are transporting droplets within the wake. A few cases were run to see how large the effect of wind on droplet transport may be. Cases were run for wind speeds of 2, 10, and 25 mph (3, 16, and 40 kph) with wind angles with respect to the direction of the truck of 0, 45, 90, 135, and 180 degrees with 0 degrees being a headwind as shown in Figure 6-27.

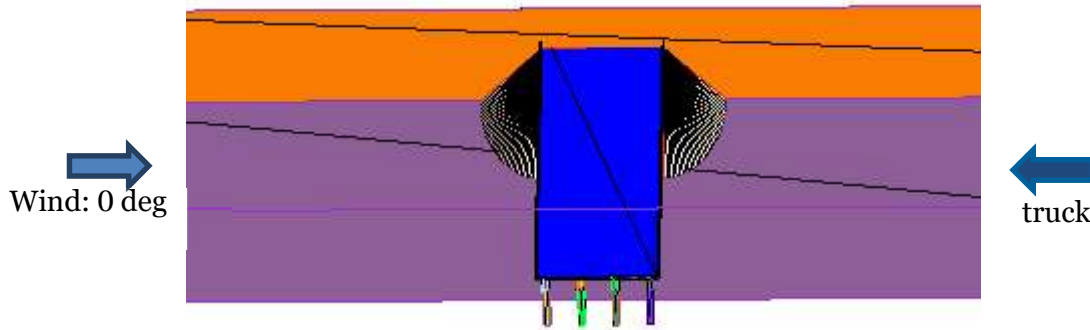
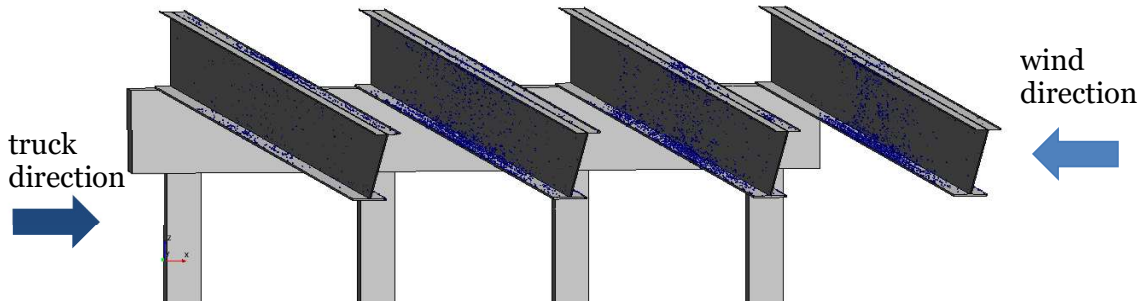


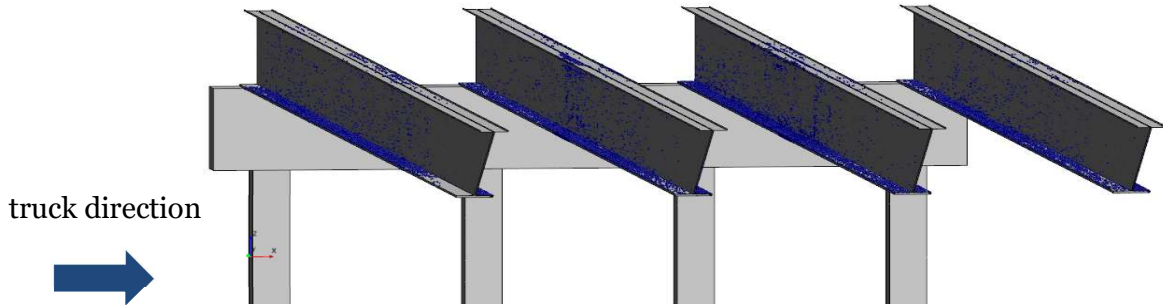
Figure 6-27: Schematic showing bridge with truck and wind direction.

The highest wind velocity tested was 25 mph (40 kph).

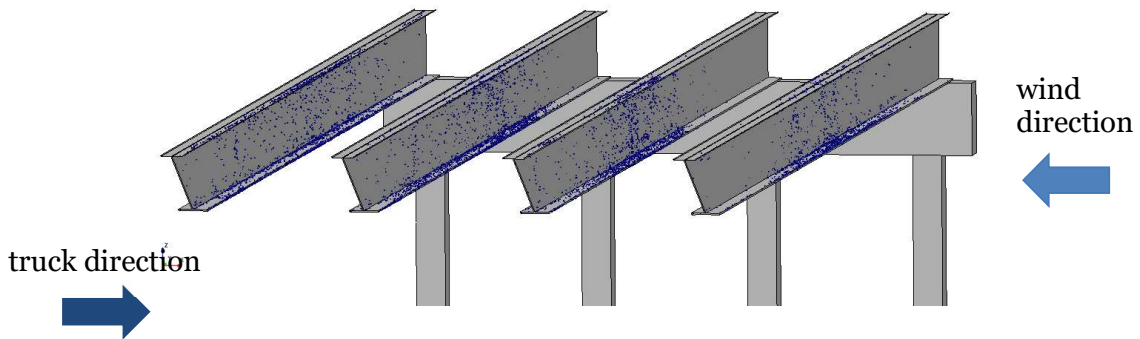
Figure 6-28 and Figure 6-29 compare droplet accumulations on the leading and trailing sides of girders to show the differences for the highest wind speed case. The Droplet distributions on the leading sides (a) and (b) and trailing sides (c) and (d) of girders for a 25-mph headwind and no headwind respectively are visualized in Figure 6-28. Droplet deposits appear to be heavier in the case of no headwind, especially on the bottom flanges.



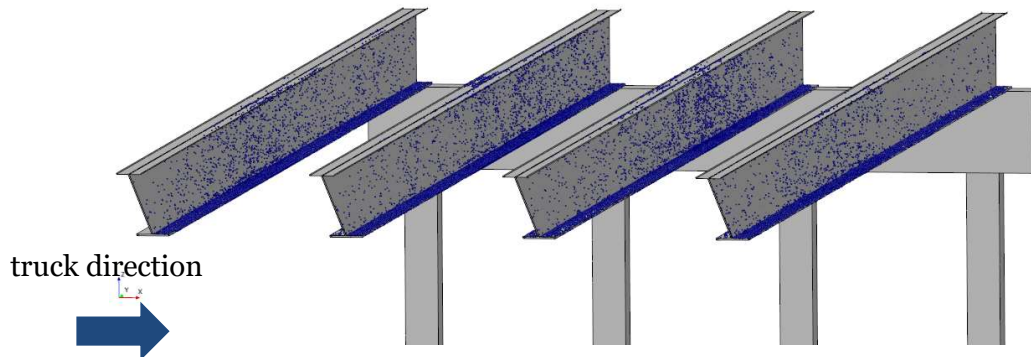
Droplet distribution on leading sides of girders; 25 mph headwind



Droplet distribution on leading sides of girders; no headwind



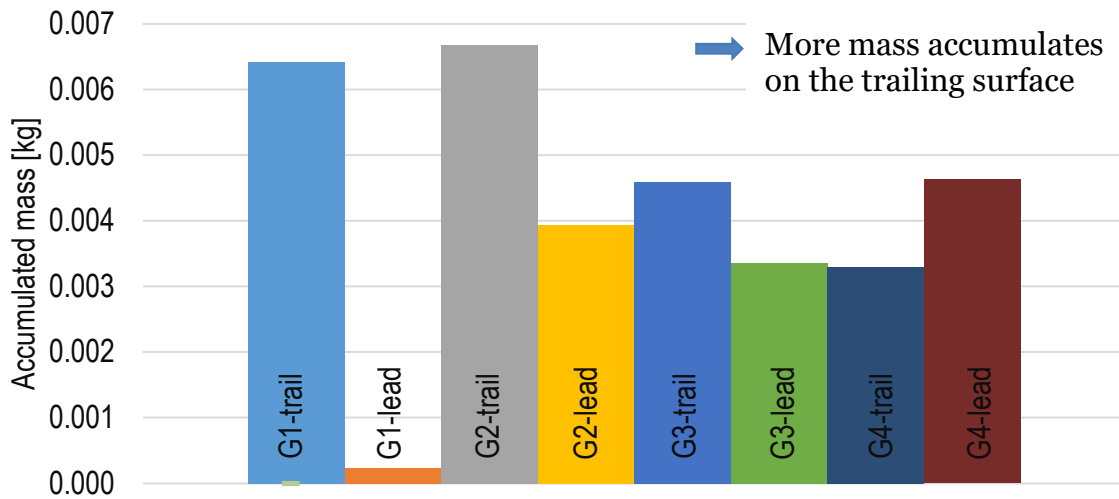
Droplet distribution on trailing side of girders; 25 mph headwind



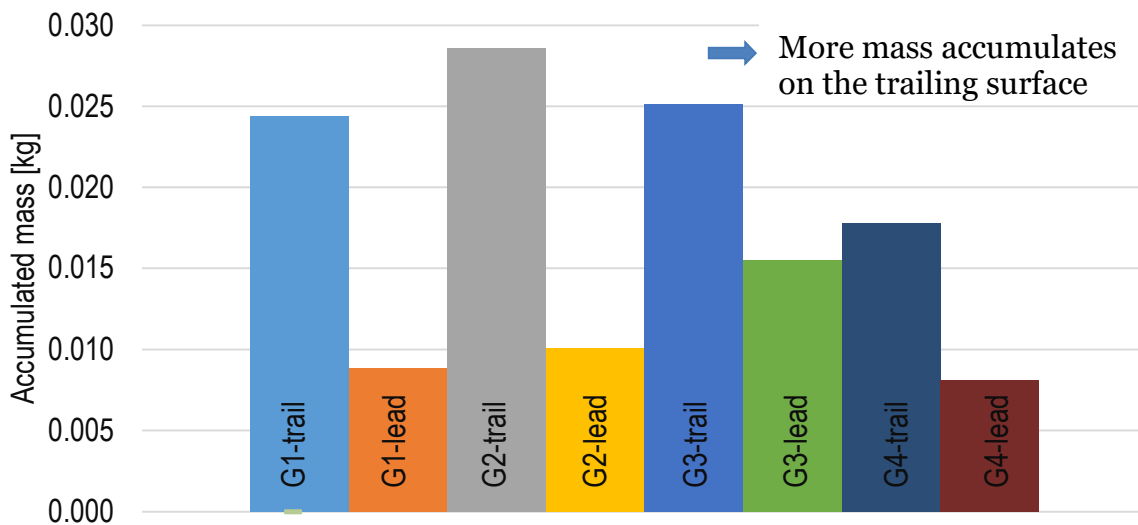
Droplet distribution on trailing side of girders; no headwind

Figure 6-28: Visualization of droplet accumulation on girders for 25 MPH headwind.

Figure 6-29 shows droplet accumulation on the leading and trailing sides of each girder for the 25-mph headwind case, in the upper panel, compared to the no headwind case, in the lower panel. Note that the scales of the vertical axis differ by a factor of nearly four. This scale difference was used to better show the differences in deposition on the various girders for the 25-mph headwind case, which had a far lower total deposition than in the no headwind case. For the leading side of the first girder, droplet deposition is less for the 25-mph headwind case by a factor of about 40. For the trailing side of the first girder, the deposition is about 3.4 times more in the no wind case compared to the 25-mph headwind case. Similar differences are observed for the other girders.



(a) 25 mph headwind



(b) No headwind

Figure 6-29: Droplet accumulation of leading and trailing sides of girders for 25 MPH headwind and no headwind.

The percentage of droplet deposition on the bottom flange versus the other girder surfaces for leading and trailing sides of the girders is shown in Figure 6-30 for a 25-mph headwind. As in other cases, most of the droplet deposition was on the bottom flanges for the case of truck passage

with a 25-mph headwind. However, in this case, the percentage deposited on the lower flange drops to the lowest of all cases tested, 68%, indicating that if the wind is strong enough it may affect the distribution of droplet deposition on the girders.

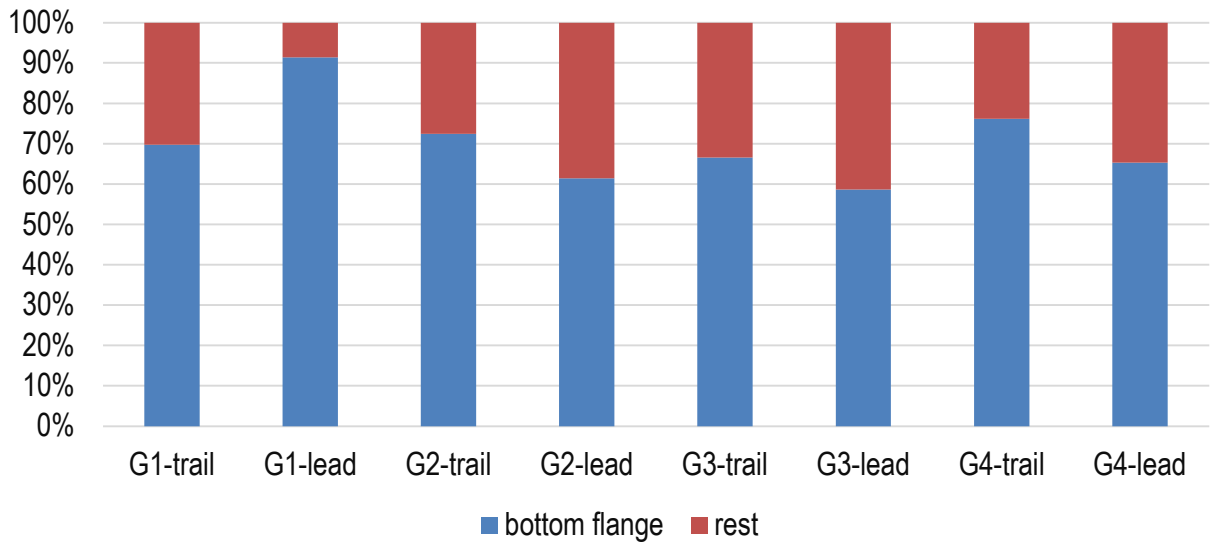


Figure 6-30: Percentage of droplet deposition on bottom flange by girder and side for 25-mph headwind.

The individual girder and total droplet deposition for the various headwind speeds is shown in Figure 6-31. A big difference in deposition occurs as a decrease by nearly a factor of 4 with a headwind as little as 2 mph (3 kph). For higher velocity headwinds of 10 and 25 mph (16 and 40 kph), the deposition is close to and even a little greater than for the 2-mph (3-kph) wind case.

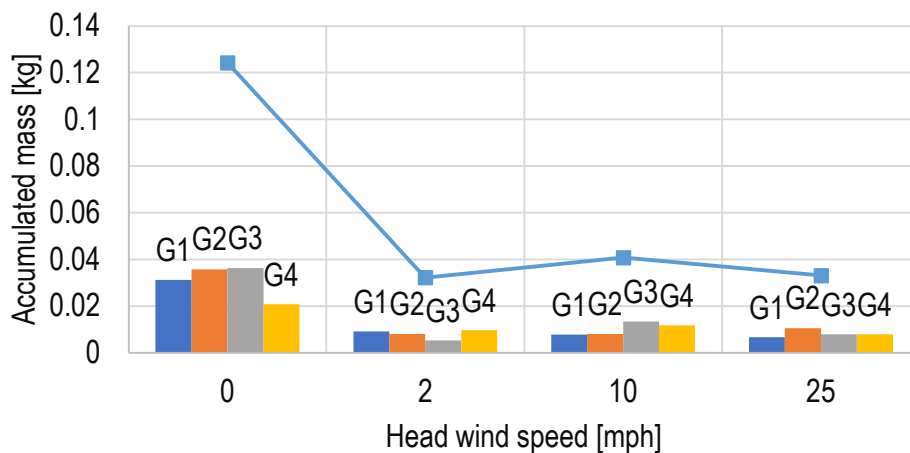


Figure 6-31: Variation of droplet accumulation of girders with wind speed for head wind. The percentage of droplet mass accumulation on the lower flange as a function of windspeed for the case with a headwind is shown in Figure 6-32. While total droplet deposition drops significantly in going from no wind to a 2-mph headwind, as shown in Figure 6-31, the percentage accumulation on the lower flange increases from 85% to 96%. With increasing headwind speed, the percentage of droplet accumulation on the lower flange decreases to 68%. While the effect of

wind on the eddy flow pattern carrying droplets between girders is complex, it appears likely that greater momentum transferred to droplets at higher wind speeds causes more of them to collide with the web and upper flange as opposed to settling out on the lower flange.

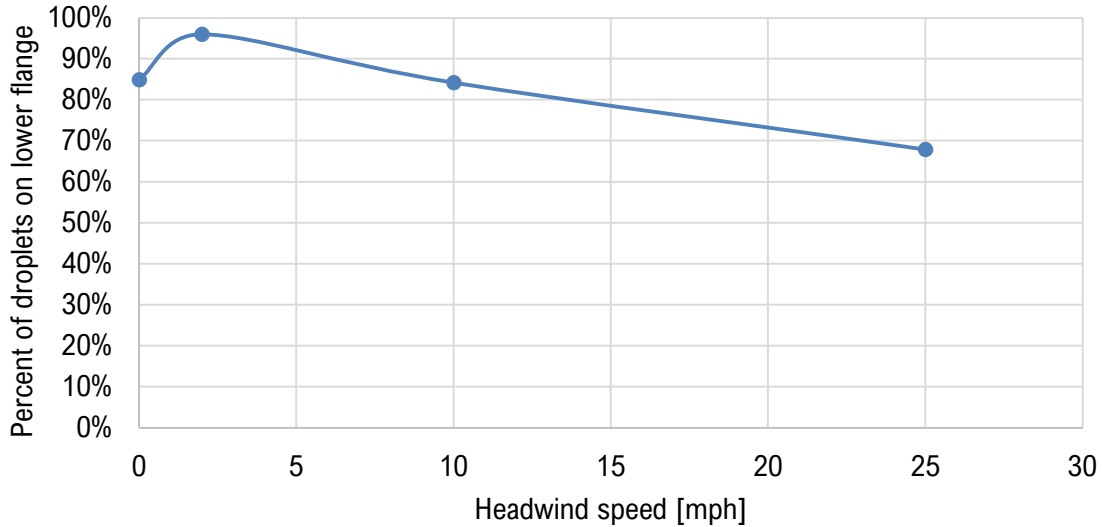


Figure 6-32: Percentage of droplet mass depositing on lower flange as a function of headwind speed.

## 6.9 Varying Wind Angle of Attack

Cases were run to test the effect of wind angle of attack with respect to the front of the truck for a wind speed of 25 mph (40 kph). A diagram showing direction of the truck and orientation of the 0-degree angle of attack is shown in Figure 6-33. For 25-mph (40-kph) wind, the worst-case deposition was for a headwind, and deposition drops off by about a factor of 5 as the wind direction shifts to a tailwind as shown in Figure 6-34. Also note that as the direction of the winds shifts from headwind to tailwind that the girder getting the most deposition shifts from G2 the 2<sup>nd</sup> girder back from the side where the truck enters under to bridge to G4, the back girder where the truck exits from under the bridge.

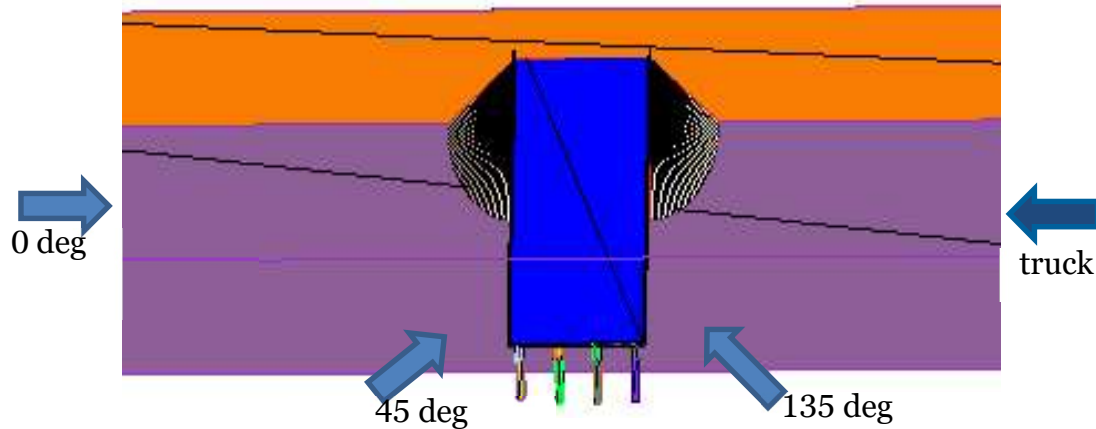


Figure 6-33: Diagram showing wind directions.

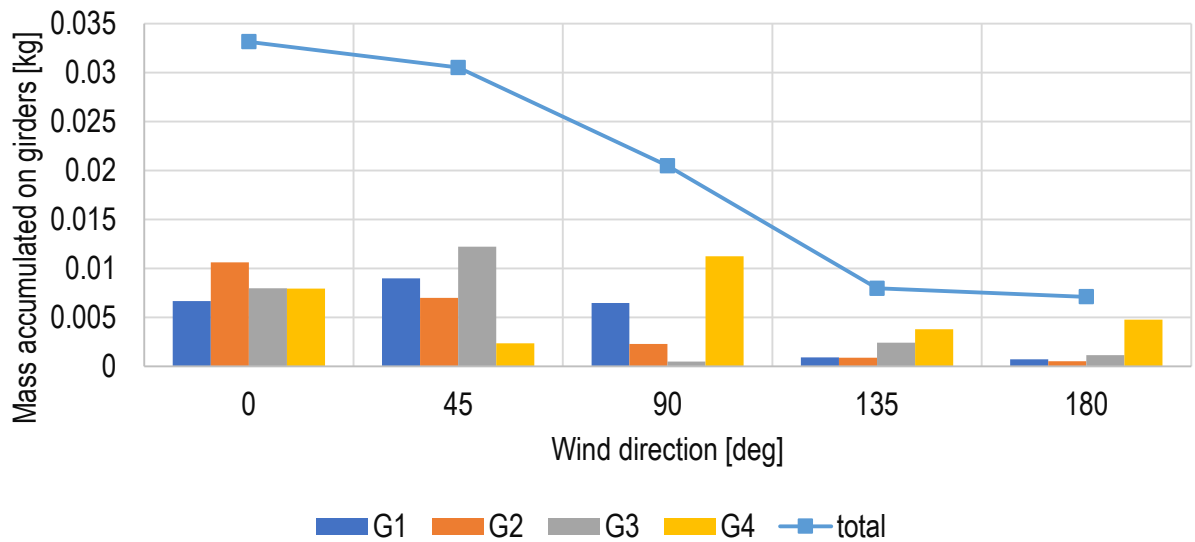


Figure 6-34: Per girder and total droplet accumulation on girders for wind directions between 0 and 180 degrees at a wind speed of 25 mph.

The variation with wind direction of the percentage of droplet deposition on the lower flange as opposed to the web and upper flange is shown in Figure 6-35 for the lowest nonzero wind speed of 2 mph (3 kph) and the highest wind speed of 25 mph (40 kph). At the low wind speed of 2 mph, the variation of the percentage of droplet deposition is between 85% and 96%, which is nearly all of the deposition. As noted previously, as wind speed increases imparting more momentum to droplets, a greater percentage of droplets collide with and deposit on the web and upper flange. At the highest wind speed tested of 25 mph, the variation of percentage of droplet deposition on the lower flange with wind angle is between 59% and 77%.

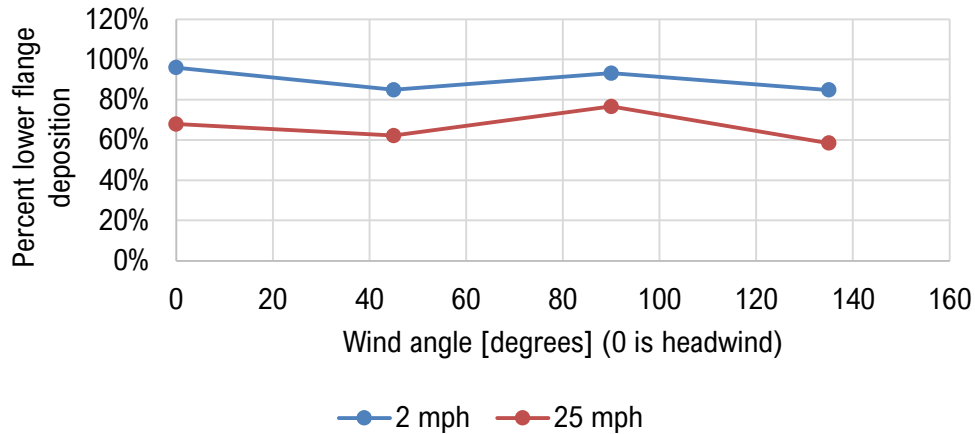


Figure 6-35: Percent of droplet deposition on lower flange as a function of wind angle for wind speeds of 2 mph and 25 mph.

Figure 6-36 shows the suspended droplet mass between girders versus time for the headwind and tailwind cases with a 25-mph wind. Those plots show that there is significantly more suspended droplet mass between girders for the headwind case. This condition is likely due to the tailwind dispersing the droplets in the truck wake better than in the headwind case where the bridge partially shields the oncoming truck from the wind as it gets close to the bridge.

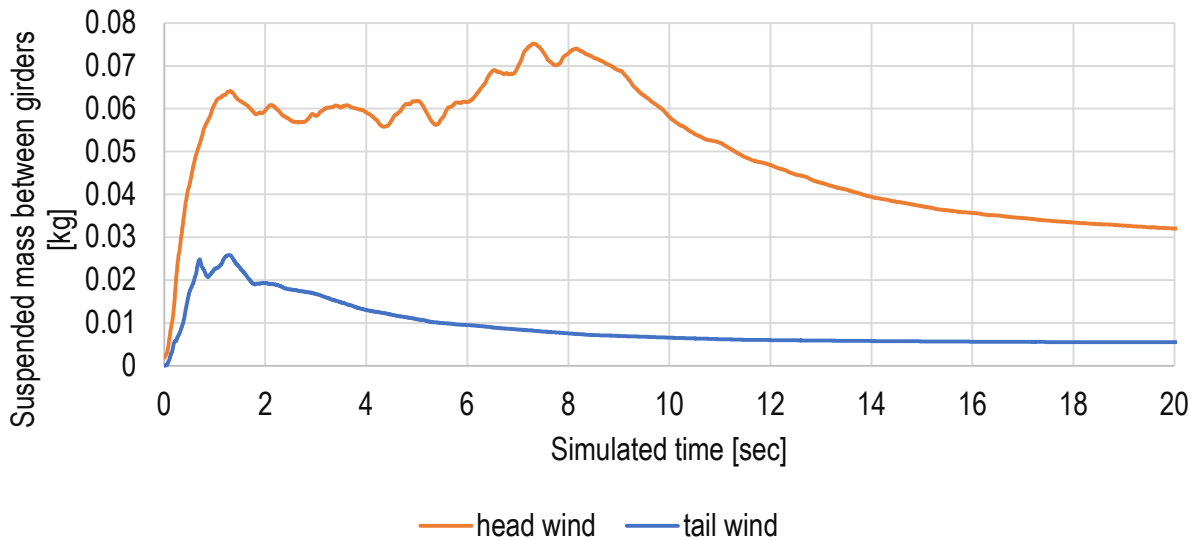


Figure 6-36: Suspended droplet mass between girders as a function of time for headwind and tailwind cases at a wind speed of 25 mph.

## 6.10 Constant Wind versus Wind Gust

Several cases were run to test the effect of wind gusts starting at 8 seconds after the truck has already moved from under the bridge at 4.5 seconds. The diagram in Figure 6-37 shows tested wind directions, 45 and 135 degrees and truck direction of travel. The upper plot of Figure 6-38, (a), shows droplet deposition for a steady 2-mph (3-kph) wind at various angles of attack for comparison with the wind gust cases, which are shown in Figure 6-38, (b), which shows droplet deposition for the no wind and 2-mph (3-kph) wind gusts at 45 and 135 degrees angle of attack.

That plot shows that the gust cases bring the droplet deposition up to near the level of the no wind case, at 0.138 kg for no wind, compared to 0.115 kg at 45-degree angle of attack and 0.122 kg deposition at 135-degree angle of attack, while steady 2-mph (3-kph) wind has deposition ranging from 0.032 kg at 0 angle of attack down to 0.018 at a 135-degree angle of attack. The direction of the wind and its steadiness and duration may influence the droplet deposition on the girders by quite a bit, but that variation does not appear to exceed deposition in the cases of no wind. The cases with wind that were run demonstrate the effects that wind may have on droplet deposition on the bridge girders, however, a large number of additional cases would have to be run to draw more reliable conclusions about the effects of wind on droplet deposition. The most important observation from the cases that were run, however, is that the addition of wind appears to enhance dispersion of droplets in the truck wake, and that effect tends to reduce droplet deposition on girders.

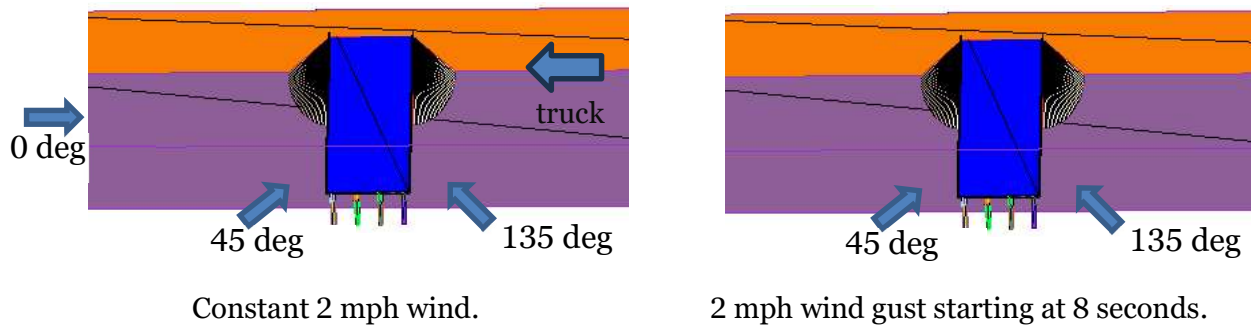
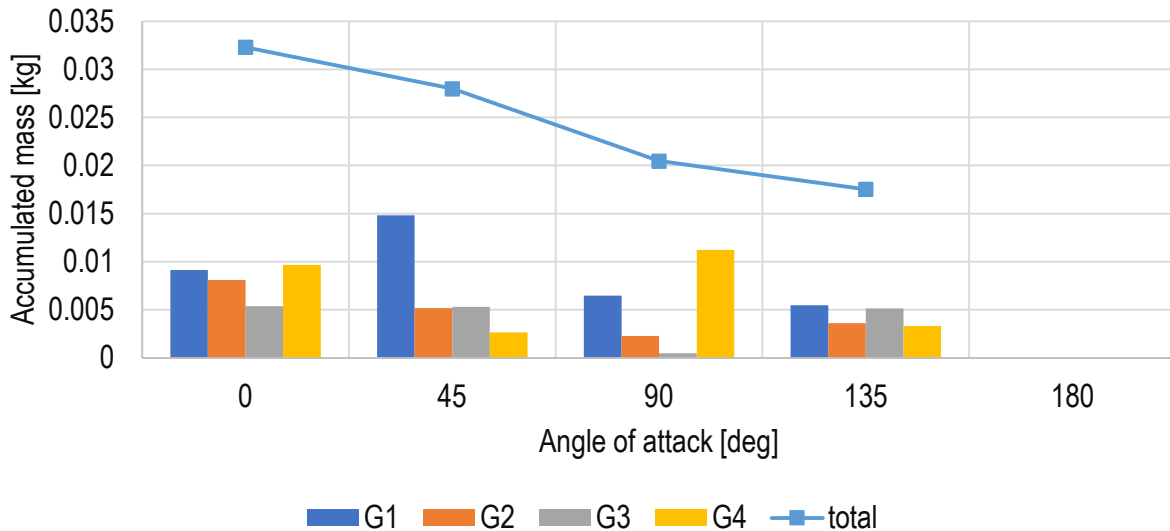
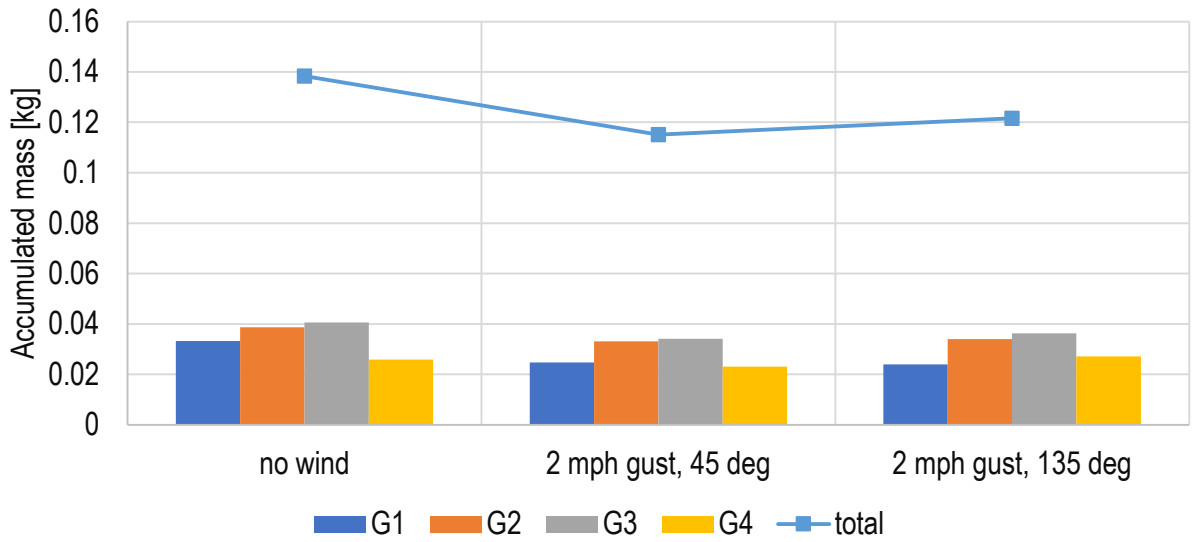


Figure 6-37: Diagram for cases of constant 2 mph wind versus 2 mph wind gusts at 45 and 135 degrees with respect to the front of the truck starting at 8 seconds.



(a) Droplet deposition for 2 mph constant wind at 0-, 45-, 90-, and 135-degree angle of attack.



(b) Droplet deposition for 2 mph wind gust starting at 8 seconds for 45- and 135-degree angle of attack compared to the no wind case.

Figure 6-38: Droplet deposition for a 2-mph wind gust at an angle of attack of 45- and 135-degrees in (b) compared to no wind also in (b) and constant 2 mph wind in (a).

## 7 Conclusions

Computational fluid dynamics was used to study the transport of droplets from tire spray from large trucks up to and deposition on the girders of an uncoated weathering steel bridge. The study focused on analyzing the effects of underclearance, girder spacing, girder height, deck overhang distance, vehicle speed, and wind on the deposition of truck tire spray from wet roads on overhead bridge girders. Large turbulent eddies in a truck wake are the primary transporters of tire spray droplets through aerodynamic drag upward and outward from the truck. This motion brings the droplets up into the space between bridge girders. The additional force of gravity acts to ultimately cause droplets to settle onto horizontal surfaces. Normally, two equation turbulence models such as the k-epsilon turbulence models using the Reynolds averaged Navier-Stokes equations allows for the largest number of cases in a parametric matrix due to the computational efficiency of that model. Large eddy simulation (LES) is much more computationally intensive requiring five to ten times the computer resources and time. LES was used in this study because it was necessary to accurately track the transport of droplets in the wake up to the space between girders and to track the deposition on girders. The use of LES limited the size of the case matrix. The fairly large number of parameters tested was achieved by using a base case that represented the likely geometry and conditions under most circumstances and then analyzing variation of each parameter from the base case in a reduced set of cases. Truck wakes at moderate speeds of 30 mph and above are broad and fully turbulent, characterized by the shedding of large turbulent eddies from the rear of the truck trailer that grow and move outward and upward from the path of the truck as it moves down the road. Droplets enter the truck wake from the wheel wells and other surfaces surrounding the wheels. To enter the wake, droplets thrown off from tires must be small enough to turn with the air flow moving out from the wheel wells, trailer undercarriage, and other surroundings, as opposed to colliding with and depositing on those surfaces. This requirement limits the size of droplets in the wake to less than about 100  $\mu\text{m}$  in diameter. Once droplets enter the wake, they are transported by the turbulent eddies in the wake. Droplet deposition on bridge girders is greatly influenced by shed eddy motion up to and interaction with the bridge girders and the space between bridge girders. The passage of the flat top of the truck trailer parallel to the bottom opening of the space between girders tends to induce a rotating cavity flow vortex in the space between with the direction of rotation in the direction of the truck motion at the bottom of the girders. This cavity flow is an average because the flow is highly turbulent and chaotic and particular patterns of flow between girders are easily broken up as eddies from the truck wake enter that space.

The effects of the various parameters tested can be summarized as follows:

- Effect of varying the number of girders while keeping bridge deck width constant:

As the number of girders increases, the total girder surface area increases but the width of cavity space between girders decreases. These are competing conditions; more surface area to intercept droplets leads to more deposition, with 6 girders having 1.3 times the droplet deposition of 4, while a smaller gap between girders makes it more difficult for eddies to enter the space between girders. With the addition of a 7<sup>th</sup> girder, the total droplet deposition decreases to about the amount for 4 girders.

- Effect of underclearance:

As the distance between the top of the trailer and the bridge deck increases, more of the droplet laden eddies in the wake can enter under the bridge, but the concentration of droplets decreases with height; these are competing influences. At 60 mph, with a 14-foot-high trailer, droplet accumulation on girders does not begin to decrease until the underclearance reaches 20 ft. From an underclearance of 20 to 30 ft, the droplet

deposition drops by a factor of 4, and from 30 to 40 ft, it drops by another factor of 2. At the lower truck speeds of 45 and 30 mph, droplet accumulation on girders drops monotonically with increasing underclearance from 16 to 40 ft.

- Effect of truck speed:

Droplet deposition on girders increases rapidly with truck speed. Going from 30 mph to 60 mph, at 16 ft of underclearance, droplet deposition on girders increases by a factor of 6.7. Therefore, at slower speeds, the rate of droplet accumulation is greatly reduced; however, it is still occurring, and at best the time until the accumulation on a new bridge becomes problematic may be extended by a factor up to 7 with slow moving traffic.

- Effect of varying height of girders:

Reducing the web height reduces the droplet deposition by somewhat more than the reduction in volume of the space between girders, likely due to weaker circulation of droplet laden eddies in the smaller space between girders. In the scenario investigated, reducing the girder height by 45% reduced the mass of accumulated droplets by 58%.

- Effect of width of overhang:

Increasing the width of the overhang from 3 to 5 ft, a factor of 1.7, does reduce deposition on the first couple of girders via a shielding effect, but only reduces total droplet deposition on girders by about 20% in a truck passage event.

- Effect of vertical abutment versus sloped embankment abutment:

The sloped embankment has a wedge of open space next to the travel lanes allowing more of the droplet cloud in the wake to enter under the bridge and consequently more total droplet deposition occurs in a truck passage event. However, the girders are longer in the sloped embankment case and the open wedge next to the travel lanes allows more space for droplets to spread out. These competing effects result in the droplet concentration in terms of droplet mass per unit length on girders directly over the travel lanes to be higher for the vertical wall case than the sloped embanked case by about 20 percent.

- Effect of wind considering direction and speed:

Studying the effects of wind in detail would require a much larger number of cases where both the wind speed and angles of the wind with respect to the truck are varied. Due to time limitations, cases in this study were limited to wind speeds of 2, 10, and 25 mph varied from 0 mph of the base case at a 0 angle of attack, which constituted a headwind. Angles of attack were limited to 0, 45, 90, 135, and 180, where 0 is a headwind, and the angles greater than zero blow across the road from the driver side to the passenger side of the truck. Although wind moving upward in the direction of bridge girders will easily move droplets in the wake toward the girders, the primary effect of the wind appears to be that wind disperses droplets faster than no wind cases and consequently lower droplet concentrations are transported up between girders with wind reducing deposition compared to no wind cases by a factor up to about four.

- Percentage droplet deposition on the lower flange:

In the absence of wind for the cases studied, more than 80% of droplets deposit on the lower flange for the highest truck speed of 60 mph at an underclearance of 16 ft. Lower

truck speeds and higher underclearances that result in droplets circulating at lower speeds between girders shift the percentage of droplets depositing on the lower flange even higher to 90% or more. In addition, both the direction of droplet circulation (downward for the trailing flange) and gravity favor droplet deposition on the trailing flange. Wind tends to disperse droplets in the truck wake and lower overall droplet deposition, but the addition of droplet momentum from wind does shift the droplet deposition to the web and upper flange. For a 25-mph wind, the percentage deposited on the lower flange varies with wind direction between 59% and 77%. Overall, results indicate that if corrosion develops, it is most likely to develop first on the trailing lower flange.

- Shielding effect of girders on the truck entry side of the bridge:

The truck drags droplets with it under the bridge from the entry side as well as throws up droplets in eddies during travel under the bridge. In general, girders on the side of the bridge that truck enters tend to catch much of the droplet flow dragged under the bridge with the truck, thus girders on the entry side shield girders closer to the side of the bridge that the truck exits. As noted above, the trailing lower flange gets upwards of 80% of the deposition in most cases. This effect of decreasing deposition on girders toward the exit side of the bridge is most apparent for bridges with more than 4 girders.

To summarize, truck motion on wet salted roads after snow events is characterized by fully turbulent wakes shedding energetic eddies that spread out from the truck in all directions normal to the direction of travel. The eddies easily transport droplets in the size range 10 to 100  $\mu\text{m}$  thrown off from the tires. When a truck passes under a bridge, the eddies carrying droplets have their upward flow blocked by the cavity space between girders, and they circulate in that space until they collide with a surface or their energy dissipates, depositing some of the droplet mass on the girders, primarily on the trailing lower flange, with each truck passage event. While the droplet deposition on girders with each truck passage event may be small, the droplets may accumulate over a long period of time, extending years, until the droplet accumulation and the salt left behind when droplets evaporate becomes problematic for uncoated weathering steel girders. The effects of girder spacing, underclearance, truck speed, girder height, width of overhang, vertical versus sloped embankment, and a limited set of cases with wind were tested in comparison to droplet deposition for a base case. For all of these parameters related to droplet deposition on girders, only the truck speed and underclearance change droplet deposition from a truck passage event by more than a factor of two. Underclearance has to be very large before increased underclearance begins to have a large effect on deposition exceeding a factor of two. Reducing truck speed from 60 mph to 30 mph can reduce deposition by a factor of about six. The rate of accumulation of truck passage events when the road is wet and has been salted may have the largest influence on the rate of droplet accumulation on girders and the time until the droplet accumulation on a bridge becomes problematic. The 2013 study [8] also showed that multiple trucks following each other closely keep droplets from tire spray circulating at girder level for a significantly longer time. These results indicate that the overall deposition of salt would increase with average daily traffic (ADT) volume or average annual daily traffic (AADT) volume. Thus, uncoated weathering steel bridges over (1) high ADT/AADT routes, and (2) routes with higher speed limits may be at higher risk of accelerated corrosion rates.

This study was limited to the mechanisms and related parameters that affect the rate of droplet accumulation on the girders of uncoated weathering steel bridges and was conducted in a laboratory using computational fluid dynamics, CFD. Results of this study indicate that a field study of the state of uncoated weathering steel bridges that focuses on correlating the rate of truck traffic and truck speed with accumulation and corrosion may be useful in developing better guidelines for identifying locations where the use of uncoated weathering steel in bridges is appropriate.

## 8 Acknowledgements

The funding for this project came from the Federal Highway Administration's (FHWA's) steel bridge research program, and through the Turner-Fairbank Highway Research Center's, Hydraulics Laboratory, Interagency Agency Agreement DTFH61-14-X-300002 between the United States Department of Transportation and Department of Energy (DOE). The work was performed under DOE's contract with UChicago Argonne, LLC contract number DE-AC02-06-CH11357. Justin Ocel of the FHWA secured the funding and provided technical direction in terms of defining bridge geometric parameters that may contribute to the "tunnel effect" leading to accelerated corrosion of uncoated weathering steel bridges.

## 9 References

- [1] ASTM. (1905). Standard Specifications for Structural Steel for Bridges, ASTM A 7, Proceedings of the Eighth Annual Meeting, Atlantic City, NJ, American Society for Testing and Materials, Philadelphia, PA.
- [2] ASTM. (1941). Tentative Specification for Low-Alloy Structural Steel, ASTM A 242, ASTM Standards – Part I Metals, American Society for Testing and Materials, Philadelphia, PA.
- [3] ASTM. (1968). Standard Specification for High-Strength Low-Alloy Structural Steel, up to 50 ksi [345 MPa] Minimum Yield Point, with Atmospheric Corrosion Resistance, ASTM A 588, Annual Book of ASTM Standards, Part 4, American Society for Testing and Materials, Philadelphia, PA
- [4] Nickerson, R. L. (1995). "Performance of Weathering Steel in Highway Bridges - A Third Phase Report." American Iron and Steel Institute. Washington D.C.
- [5] Congress, N., Forum on Weathering Steel for Highway Structures – Summary Report, Report No. FHWA-TS-89-016, Federal Highway Administration, Washington, D.C. (1989).
- [6] Zoccola, J. C. (1976). "Eight Year Corrosion Test Report - 8 Mile Road Interchange." Report Number RR-444. Michigan Department of State Highways and Transportation. Lansing, MI.
- [7] FHWA. "Uncoated Weathering Steel in Structures." Technical Advisory (TA) 5140.22. Federal Highway Administration. Washington D.C. <https://www.fhwa.dot.gov/bridge/t514022.cfm> last accessed Dec. 23, 2021.
- [8] Lottes, S. A., and Bojanowski, C. (2013). "Computer Modeling and Analysis of Truck Generated Salt-Spray Transport Near Bridges." Argonne National Laboratory (ANL), July 16, 2013. <http://www.osti.gov/scitech/biblio/1087817>.
- [9] SIEMENS, "Simcenter STAR-CCM+ Documentation Version 2020.2." 2020.



**Nuclear Science and Engineering Division**

Argonne National Laboratory

9700 South Cass Avenue

Lemont, IL 60439

[www.anl.gov](http://www.anl.gov)



Argonne National Laboratory is a U.S. Department of Energy  
laboratory managed by UChicago Argonne, LLC



U.S. Department  
of Transportation

**Federal Highway  
Administration**